CHALMERS

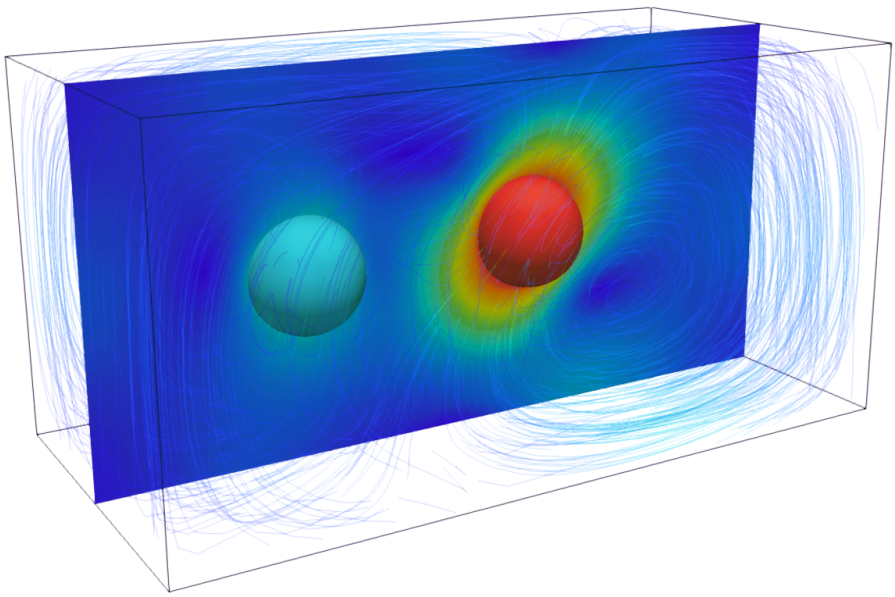

Hindered diffusion of nanoparticles

Investigations at molecular and continuum scales

ANANDA SUBRAMANI KANNAN

Department of Mechanics and Maritime Sciences
CHALMERS UNIVERSITY OF TECHNOLOGY
Göteborg, Sweden 2020

THESIS FOR THE DEGREE OF DOCTOR OF PHILOSOPHY IN THERMO AND FLUID DYNAMICS

Hindered diffusion of nanoparticles

Investigations at molecular and continuum scales

ANANDA SUBRAMANI KANNAN

Department of Mechanics and Maritime Sciences

Division of Fluid Dynamics

CHALMERS UNIVERSITY OF TECHNOLOGY

Göteborg, Sweden 2020

Hindered diffusion of nanoparticles
Investigations at molecular and continuum scales
ANANDA SUBRAMANI KANNAN
ISBN 978-91-7905-427-4

Doktorsavhandlingar vid Chalmers tekniska högskola
Ny serie nr. 2020:4894
ISSN 0346-718X
Department of Mechanics and Maritime Sciences
Division of Fluid Dynamics
Chalmers University of Technology
SE-412 96 Göteborg
Sweden
Telephone: +46 (0)31-772 1000

Cover:
Streamlines of velocity magnitude around two spherical Brownian particles (400 nm in diameter) diffusing in a square micro-channel.

Chalmers Reproservice
Göteborg, Sweden 2020

Hindered diffusion of nanoparticles
Investigations at molecular and continuum scales
ANANDA SUBRAMANI KANNAN
Department of Mechanics and Maritime Sciences
Division of Fluid Dynamics
Chalmers University of Technology

Abstract

Brownian theory provides us with a powerful tool which can be used to delve into a microscopic world of molecules, cells and nanoparticles, that was originally presumed to be beyond our reach. Consequently, modeling the inherent dynamics of a system through a Brownian transport equation is of relevance to several real-word problems that involve nanoparticles including, the transport and mitigation of particulate matter (PM) generated though fossil fuel combustion and nanocarrier mediated drug delivery. Experimentally forecasting these systems is challenging due to the simultaneous prevalence of disparate length and time scales in them. Correspondingly, an *in-silico* driven assessment at such nanoscales can complement existing experimental techniques.

Hence, in this thesis, a novel multiphase direct numerical simulation (DNS) framework is proposed to address the transport at these nanoscales. A coupled Langevin-immersed boundary method ($LaIBM$), that solves the fluid as an Eulerian field and the particle in a Lagrangian basis, is developed in this thesis. This framework is unique in its capability to include the resolved instantaneous hydrodynamics around the Brownian nanoparticle (without the need for an *a priori* determination of the relevant mobility tensors) into the particle (Langevin) equation of motion. The performance of this technique is established and validated using well-established theoretical bases including the well-known theories for unbounded and hindered diffusion (wherein hydrodynamic interactions mediated by the fluid such as particle-particle or particle-wall influence the governing dynamics) of Brownian particles in a liquid. Correspondingly, it is shown that directional variations in mean-squared displacements, velocity auto-correlation functions and diffusivities of the Brownian nanoparticle correspond well with these standard theoretical bases. Moreover, since the resolved flow around the particle is inherently available in the proposed DNS method, the nature of the hydrodynamic resistances (on the particle) including the inherent anisotropies and correlated inter-particle interactions (mediated by the fluid) are further identified and shown to influence particle mobility. Furthermore, this framework is also extended towards Brownian transport in a rarefied gas using first order models to account for the non-continuum effects. Thus, the utility of this novel method is established in both colloids and aerosols, thereby aiding in modeling the transport of a fractal shaped PM (in the latter) and a spherical nanocarrier in a micro-channel (in the former).

Keywords: Aerosols; Brownian motion; Colloids; Hydrodynamic interactions; Langevin-immersed boundary method; Mobility; Multiphase DNS; Nanoscale and Rarefied gas.

To my son... My lucky charm...

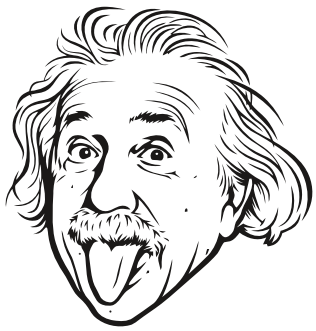

"Logical thinking cannot yield us any knowledge of the empirical world; all knowledge of reality starts from experience and ends in it."

- Albert Einstein, 1933

Acknowledgements

I am sure this is the first page which will be read to its entirety. Well, the irony is that I have reserved writing this one for the end. This is because it is the most important page in this thesis and it deserves as much deliberation (if not more).

So, I will begin by thanking my supervision/mentoring team who have expertly navigated this thesis to a successful completion. The first person I would like to thank (in my long list) is my main supervisor and mentor/confidant – *Henrik Ström*. I can safely say that he has toiled as much as I have (if not more) to bring this research effort to fruition. Thank you *Henrik* for supporting me throughout this entire journey (and for being available 24/7). Our slack conversations alone are such a rich resource of material for a series of journal papers. Next, I would like to thank my examiner/friend/mentor – *Srdjan Sasic*. I am here at this professional milestone primarily due to him. Thanks *Srdjan* for motivating, supporting and most importantly guiding me throughout the 8+ years we have worked together. I next would like to thank Fraunhofer-Chalmers Centre (FCC), Sweden and in particular my co-supervisor/mentor *Andreas Mark* for the never-ending support. Thank you *Andreas* for stepping into this project at a very critical juncture and helping us deliver on the research objectives. The biggest contributions from this thesis have resulted from the in-house FCC solver: *IPS IBOFlow*® and the ensuing developments. I would next like to thank my co-supervisor/mentor – *Gaetano Sardina*. Thanks *Gaetano* for your relentless support. Your keen sense of observation and critical thinking has significantly contributed to this research effort. Next in line is my co-supervisor/mentor – *Dario Maggiolo*. From being office-mates to collaborators, I have a learnt a lot from your way of working and your ideas. Post-processing statistical data would never be the same without your critical insights. Finally, I would like to thank my co-supervisor/mentor *Jonas Sjöblom* for his encouraging insights and support with building our experimental test rig. A word of appreciation also goes out to *Vasilis Naserentin* who provided me with GPU resources. I would also like to thank the center for scientific and technical computing at Chalmers University of Technology (*C3SE*), for providing the necessary computational resources and the Swedish Research Council (*Vetenskapsrådet*, Dnr 2015-04809) for financing this research.

'*All work and no play makes Ananda a dull boy!*' Thankfully this was not the case due to my comrades *Marco, Adam, Elias, Gonzalo, Niklas, Sudarshan, Mohsen, Magnus* and many more people at the division of fluid dynamics. Thanks for being such wonderful co-workers and more crucially friends. Coming to work everyday has been a sheer pleasure thanks to you guys! I would next like to thank my parents for supporting and believing in me. The foundation that you have provided is the sole reason why I am here in Sweden, writing a PhD thesis. Finally and most importantly, I would like to thank the *'Wonderwoman'* in my life – my wife. Thanks for always being available even when I was not. Your love, support and belief (in me) has dragged me to this professional milestone. I owe everything I accomplish to you!

I can go on writing this, but alas it has to end somewhere. So, I will conclude by acknowledging my gratitude towards everyone who has been a significant part of my 32 years of existence (you know who you are!). Tack så mycket alla!!

Ananda Subramani Kannan

Göteborg, December 2020

ABBREVIATIONS

AmgX	–	Algebraic Multi-Grid solvers
BGK	–	BhatnagarGrossKrook
CFD	–	Computational fluid dynamics
DNS	–	Direct numerical simulation
DPD	–	Dissipative particle dynamics
DSMC	–	Direct simulation Monte-Carlo
DPF	–	Diesel particulate filters
EC	–	European commission
FLBM	–	Fluctuating lattice Boltzmann method
GLE	–	Generalized Langevin Equation
IBM	–	Immersed boundary method
IBOFlow	–	Immersed Boundary Octree Flow Solver
LaIBM	–	Langevin immersed boundary method
LBM	–	Lattice Boltzmann method
LLNS	–	Landau and Lifshitz Navier-Stokes
OpenFOAM	–	Open-source Field Operation And Manipulation
FH	–	Fluctuating hydrodynamics
FLBM	–	Fluctuating lattice Boltzmann method
LGA	–	Lattice gas automata
LTI	–	Linear time invariant
MD	–	Molecular dynamics
MSD	–	Mean squared displacement
NS	–	Navier-Stokes equations
ODE	–	Ordinary differential equation
PDF	–	Probability distribution function
PM	–	Particulate matter
SDE	–	Stochastic differential equation
TIRFM	–	Total internal reflection fluorescence microscopy
VACF	–	Velocity auto-correlation function

NOMENCLATURE

Greek letters

α	Friction coefficient at the solid-fluid interface	
β_{St}^{corr}	Corrected Stokes mobility for hindered diffusion	$\mathrm{s\,kg^{-1}}$
β_{St}	Stokes mobility	$\mathrm{s\,kg^{-1}}$
$\delta(x)$	Dirac delta function	
$\Delta x(t)$	is the displacement $x(t) - x(0)$	m
Δt	Time step in the numerical simulation	
γ_{St}	Stokes friction factor	$\mathrm{kg\,s^{-1}}$
λ	Reduction in particle mobility	
λ_{gas}	mean free path of the gas	m
μ_f	Dynamic fluid viscosity	$\mathrm{kg\,m^{-1}\,s^{-1}}$
ν_f	Kinematic fluid viscosity	$\mathrm{m^2\,s^{-1}}$
ρ_f	Fluid density	$\mathrm{kg\,m^{-3}}$
$\boldsymbol{\omega_p^i}$	Angular velocity of the particle	
$\boldsymbol{\sigma}$	Total fluid stress tensor	
τ_B	Ballistic time scale of a Brownian particle	s
τ_D	Smoluchowski or diffusion time scale of a Brownian particle	s
τ_p	Particle response time	s
$\upsilon(r,t)$	Standard Gaussian white noise tensor field with uncorrelated components δ-correlated in space and time	
ζ	Magnitude of Brownian fluctuations	

Roman letters

A	Function of Kn that is determined based on empirical data	
b	Slip length in liquids	m
C_c	Cunningham correction	
$C(t)$	Auto-correlation function	
ΔV	Volume of a control element	$\mathrm{m^3}$
D_∞	Diffusivity of a free particle	$\mathrm{m^2\,s^{-1}}$
d_p	Particle diameter	m
F_f	Fluid force on a single Brownian particle in the control volume	N
$\mathbf{F_{IB}}$	Total force on the IB	
F_p	Pressure force on a single Brownian particle in the control volume	N
$f(x,t)$	Probability density function of a free Brownian particle	
h	Distance from the particle center to the wall surface	m
$\mathbf{I}$	Moment of inertia of the particle	
$\mathbf{J}$	Identity tensor	

k_B	Boltzmann constant	$\mathrm{m^2\,kg\,s^{-2}\,K^{-1}}$
Kn	Knudsen number	
L	Characteristic system scale	m
m_p	Particle mass	kg
$\mathbf{n}$	Normal at the surface over which the fluid stress is computed	
n	Number of moles of fluid in the equation of state	mol
N_1	Number of Brownian particles in a control volume	
N_{av}	Avogadro's number	$\mathrm{mol^{-1}}$
p	Pressure on a Brownian particle	$\mathrm{kg\,m^{-1}\,s^{-2}}$
Q	Mass-flow rate of a molecular gas in micro-channels	$\mathrm{kg\,s^{-1}}$
R	Universal gas constant	$\mathrm{J\,K^{-1}\,mol^{-1}}$
$r(x, y, z)$	Particle position vector	
r_p	Particle radius	m
R_f	Stochastic forcing of the fluid stress tensor FH	
$r(t)$	Impulse response of a stationary stochastic process	
$R(\omega)$	Fourier transform of the impulse response of a stationary stochastic process	
S	Surface over which the fluid stress is computed	
S_1, S_2	Cross-sectional surface area of a control volume	$\mathrm{m^2}$
Sc	Schmidt number	
$S(t)$	Stochastic forcing term in the Langevin equation	N
$S(\omega)$	Fourier transform of the stochastic forcing	
$\tilde{S}_{uu}(\omega)$	Velocity power spectral density	
T	Temperature	K
t	Time	s
$\mathbf{F_{IB}}$	Total torque on the IB	
$\mathbf{u_p}$	Particle velocity vector	
u_{rms}	Particle root mean squared velocity	$\mathrm{m\,s^{-1}}$
v	Fluid velocity vector	
x	Particle x-position	m
$\mathbf{x_p}(t)$	Particle position	m
$x(t), y(t)$	Linear signals in time domain	
$X(\omega), Y(\omega)$	Linear signals in frequency domain	

Superscripts and subscripts

$\langle\square\rangle^2$	Mean squared value
$\langle\square\rangle_\perp$	Wall-normal component
$\langle\square\rangle_\infty$	Free-diffusion
$\langle\square\rangle_\parallel$	Co-axial component

List of publications

This thesis is based on the following appended papers:

Paper A A. S. Kannan, V. Naserentin, A. Mark, D. Maggiolo, G. Sardina, S. Sasic, and H. Ström. A continuum-based multiphase DNS method for studying the Brownian dynamics of soot particles in a rarefied gas. *Chemical Engineering Science* **210** (2019), 115229. ISSN: 0009-2509. DOI: 10.1016/j.ces.2019.115229

Paper B A. S. Kannan, A. Mark, D. Maggiolo, G. Sardina, S. Sasic, and H. Ström. Assessment of hindered diffusion in arbitrary geometries using a multiphase DNS framework. *Chemical Engineering Science* **230** (2021), 116074. ISSN: 0009-2509. DOI: 10.1016/j.ces.2020.116074

Paper C A. S. Kannan, A. Mark, D. Maggiolo, G. Sardina, S. Sasic, and H. Ström. A hydrodynamic basis for off-axis Brownian diffusion under intermediate confinements in micro-channels. *International Journal of Multiphase Flow* (Submitted December 2020)

Paper D A. S. Kannan, A. Mark, D. Maggiolo, G. Sardina, S. Sasic, and H. Ström. Hindered diffusion of nanoparticles in a liquid re-visited with a continuum based direct numerical simulation framework. *To be submitted to a journal* (2021)

Paper E A. S. Kannan, T. S. B. Narahari, Y. Bharadhwaj, A. Mark, D. Maggiolo, G. Sardina, S. Sasic, and H. Ström. The Knudsen paradox in micro-channel Poiseuille flows with a symmetric particle. *Applied sciences* (Submitted November 2020)

ADDITIONAL RELEVANT PUBLICATIONS

Paper 1 A. S. Kannan, A. Mark, D. Maggiolo, G. Sardina, S. Sasic, and H. Ström. "A novel multiphase DNS method for the resolution of Brownian motion in a weakly rarefied gas using a continuum framework". *Proceedings of the 10th International Conference on Multiphase Flow (ICMF19).* Rio de Janeiro, Brazil, May 2019

Paper 2 H. Ström, J. Sjöblom, A. S. Kannan, H. Ojagh, O. Sundborg, and J. Koegler. Near-wall dispersion, deposition and transformation of particles in automotive exhaust gas aftertreatment systems. *International Journal of Heat and Fluid Flow* **70** (2018), 171–180. ISSN: 0142-727X. DOI: 10.1016/j.ijheatfluidflow.2018.02.013

Paper 3 A. S. Kannan, A. Mark, D. Maggiolo, G. Sardina, S. Sasic, and H. Ström. "Assessment of pore diffusion in a micro-channel using an immersed boundary method". *Proceedings of the 14th International Conference on Multiphase Flow in Industrial Plant (MFIP17).* Desenzano del Garda, Italy, 2017

Paper 4 A. S. Kannan, K. Jareteg, N. C. K. Lassen, J. M. Carstensen, M. A. E. Hansen, F. Dam, and S. Sasic. Design and performance optimization of gravity tables using a combined CFD-DEM framework. *Powder Technology* **318** (2017), 423–440. ISSN: 0032-5910. DOI: 10.1016/j.powtec.2017.05.046

Paper 5 A. S. Kannan, N. C. K. Lassen, J. M. Carstensen, J. Lund, and S. Sasic. Segregation phenomena in gravity separators: A combined numerical and experimental study. *Powder Technology* **301** (2016), 679–693. ISSN: 0032-5910. DOI: 10.1016/j.powtec.2016.07.003

Paper 6 J. Sjöblom, H. Ström, A. S. Kannan, and H. Ojagh. Experimental Validation of Particulate Matter (PM) Capture in Open Substrates. *Industrial & Engineering Chemistry Research* **53**.9 (2014), 3749–3752. DOI: 10.1021/ie404046y

Paper 7 J. Sjöblom, A. S. Kannan, H. Ojagh, and H. Ström. Modelling of particulate matter transformations and capture efficiency. *The Canadian Journal of Chemical Engineering* **92**.9 (2014), 1542–1551. DOI: 10.1002/cjce.22004

Contents

Part I

Extended Summary

1

Introduction

Brownian motion: a macroscopic window to the microscopic world

"These motions were such as to satisfy me, after frequently repeated observation, that they arose neither from currents in the fluid, nor from its gradual evaporation, but belonged to the particle itself."

- Robert Brown, 1828

Brownian motion, or the chaotic dance of molecules/nanoparticles due to incessant collisions with the constituent elements of a fluid, has been an integral part of modern day science ever since it was serendipitously noticed by Dutch scientist Jan Ingenhousz (in 1785) while observing finely ground charcoal under a microscope. This characteristic random behavior, named after Robert Brown (a British botanist) who noticed these irregular motions in a great variety of materials suspended in a liquid ranging from pollen to fragments of an Egyptian sphinx [13], has been the subject of extensive research since the 17^{th} century. From understanding the complex behavior of micro-organisms, to forecasting the next stock market crash, to studying the dynamics of super-massive black holes and to modern day artificial intelligence – understanding chaos through the lens of Brownian theory has been the approach of choice for a generation's worth of research. In fact, the significance of Brownian theory in modern day science is unmistakable, as this core idea is the subject of Einstein's famed dissertation [14] and many would argue that it is his biggest contribution (to science) along with the theory of relativity. Thus, Brownian theory is touted to be that elusive window into a microscopic world of molecules, cells and nanoparticles that was presumed to be beyond our reach.

The simplistic representation of systematic chaos as a mathematical abstraction of a random process, in a scale independent framework (i.e. applicable in the same form to both micro-organisms as well as spinning galaxies), has been the unique feature of modern day Brownian theory that makes it an appealing modeling technique across several research fronts. To limit the scope of the ensuing discussions, the developed ideas in this thesis are positioned with two potential overarching applications:

1. Cleaner emissions from combustion processes

2. Nanocarrier mediated drug delivery

These are explained in this chapter in order to establish the necessary context for the theoretical and numerical developments presented in this thesis.

1.1 Clean air: a basic requirement for society?

Urban air quality has been on the decline since the industrial revolution particularly due to the increasing energy demands from the modernization of our society. With the increasing dependence on energy from fossil fuels, the corresponding levels of particulate matter (PM) such as PM10 (less than 10 microns in diameter) and PM2.5 (less than 2.5 microns in diameter), that contain pollutants such as sulfates and nitrates rise [15]. These PM aerosols, which are usually formed due to incomplete combustion of hydrocarbon-based fuels during a variety of common combustion processes in power generation, vehicular propulsion etc., are hazardous to human health. This is due to their widespread dispersion in the atmosphere, particularly PM2.5, as its microscopic size allows the pollutant particles to enter the blood stream via the respiratory tract and travel throughout the body. Such an intravenous transport of PM can cause far-reaching health effects including asthma, lung cancer and heart disease [15]. This chronic issue with poor air quality is highlighted in Fig. 1.1, indicating that a significant portion of the global population breathes PM2.5 contaminated air at concentrations* exceeding the limits set by the World Health Organization (WHO).

A more local survey in Europe, further, identified that emissions from households, industrial plants and road transport accounted for a majority of the fine aerosols (PM2.5 and PM10) emitted in the region [16]. Hence, the European commission (EC) has implemented a series of directives that establishes the health based standards and objectives for these pollutants (Directive 2008/50/EC of the European Parliament [17]). Stringent PM emission control needs to be adopted if these demands from the EC are to be met, indicating a palpable need for novel strategies to mitigate the same. The most generic mitigation strategy is some form of after-treatment of the gases emitted as a result of the combustion of hydrocarbon-based fuels using a particulate filter. For vehicular emissions, which account for 10-15 % of the total PM emissions in Europe, a combination of the diesel oxidation catalyst (DOC), diesel particulate filter (DPF) and diesel NOx reduction catalyst (DeNOx) are employed downstream from the tail pipe to regulate the exhaust. Among these, the DPF (see Fig. 1.2), a dedicated unit that is commonly made from cordierite or silicon carbide extruded monoliths, is used to purge the exhaust gas of PM by trapping them in its constituent monolith channels. In a typical DPF, every second channel is plugged at either end, creating a chessboard-like appearance of the

*The US AQI is among the most widely recognized index for communicating air quality. This index converts pollutant concentrations into a color-coded scale between 0-500, where higher values indicate increased health risk.

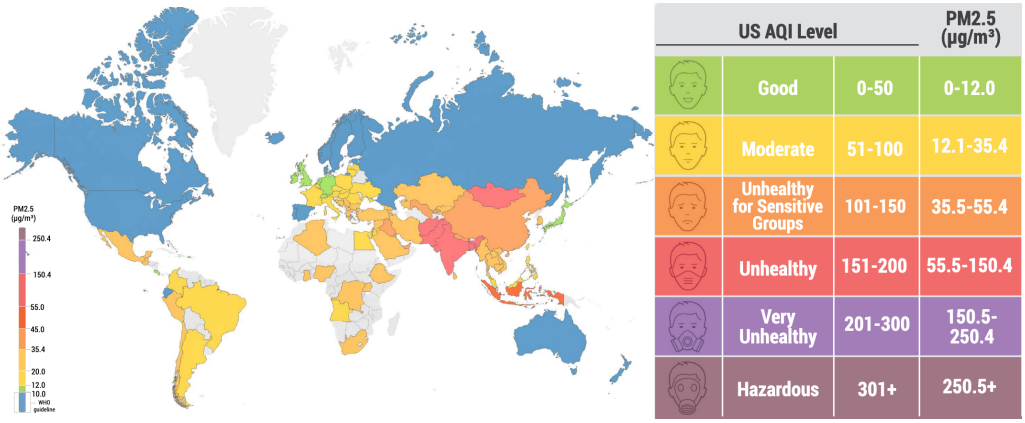

Figure 1.1: *This map presents average PM2.5 exposure by country for 2019, as calculated from available city data and weighted by population. Grey countries and regions indicate that these locations had insufficient data available. This figure is adapted from the report published by IQAir, a Swiss air quality technology company [15].*

monolith front and back. Further, the flow in these channels is laminar, meaning that PM accumulates in the channel through Brownian or molecular deposition/diffusion and interception. Although effective at PM capture, these DPF's are associated with a significant fuel penalty, mainly because of the pressure build up due to deposition. Hence, smarter technologies to circumvent the deficiencies of these traditional monolith filters are desirable, consequently, creating a niche requirement for advanced experimental and modeling techniques to better design and further improve these existing systems.

1.2 Nanocarriers: a new tool to combat cancer?

While the industrial revolution has had a detrimental impact on the environment, it has simultaneously benefited mankind by improving the overall standard of living, catering to better hygiene and sanitation. These improved conditions for living coupled with the modern advancements in medical science have brought about dramatic declines in the mortality rate from infectious diseases. These improvements, however, come at the cost of changing demographics and exposure to a wider class of risk factors, increasing the incidence of another dangerous disease, i.e. cancer, in the human population (with more than 10 million new cases reported every year) [20]. Current cancer treatments include surgical intervention, radiation and chemotherapeutic drugs, which often also kill healthy cells and generate a toxic response in the patient. It would, therefore, be desirable to develop strategies that can either passively or actively target cancerous cells [21]. The aim of such smart drug-delivery systems is to administer smaller drug doses to patients while offering improved therapeutic efficiency and fewer side effects when compared with conventional drug delivery methods [22].

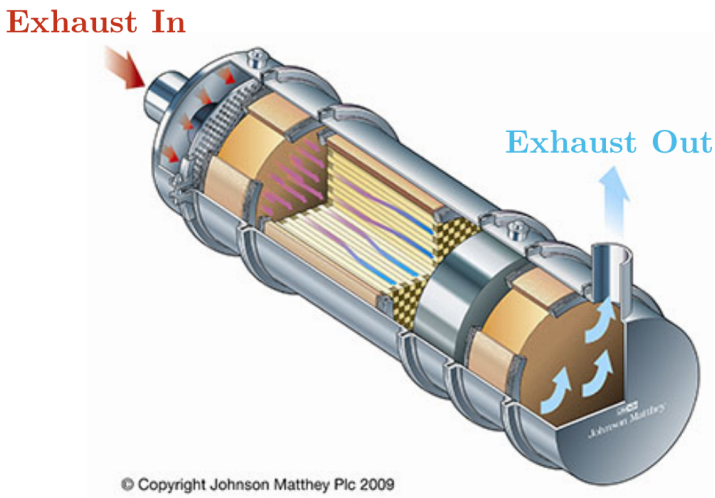

Figure 1.2: *An example of a PM emission mitigation device: diesel particulate filter (DPF) employed in diesel powered drives. This figure is adapted from [18].*

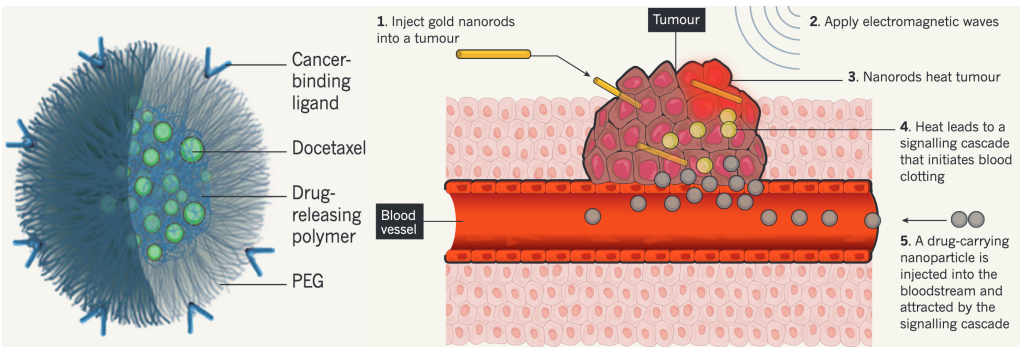

Figure 1.3: *An example of nanocarrier mediated drug delivery targeting tumor cells. The carrier is a 100 nm polymer sphere (poly-ethylene glycol or PEG) loaded with docetaxel, a drug that kills malignant cells. This figure has been adapted from Bourzac [19].*

Recent research in nanomedicine [22, 23], or the application of nanotechnology to achieve innovation in healthcare, has catapulted the technological advancements in both active and passive targeting of a cancerous cells to new heights. These recent advances are also resulting in therapies that were previously thought impossible, such as drugs that change their properties depending on where they are in the body or targeting tumor cells at inaccessible regions. Some labs are even testing ideas inspired by robotics, such as nanoparticles that communicate with each other to increase accumulation at a tumor site [19]. Correspondingly, Fig. 1.3 depicts a plausible way to actively target cancerous cells. The tumor site is injected with gold nanoparticles and is subsequently heated to warm the site up, thereby bringing about a signaling cascade that initiates blood clotting. The drug carrying nanoparticle (termed as a nanocarrier), which is injected in the blood, is attracted to this signaling cascade due to the unique markers it possesses, binding selectively only with the tumor cells. In this case, the nanocarrier (which is 100 nm in diameter) consists of a hydrophobic biodegradable polymeric core (made of polyethylene glycol or PEG) that encapsulates the active substance (the drug docetaxel) and enables its controlled release. Moreover, this coating also provides the needed mobility to transport the nanocarrier in the blood stream. It follows that the targeted delivery of a nanocarrier is governed by a complex interplay of hydrodynamic and multivalent interactions with the biomolecules (such as red blood corpuscles) in blood. Hence, novel insights into the dynamics of a nanocarrier in such a system can enable advanced, personalized and targeted nanomedical services by delivering the next level of cancer treatments to clinicians and patients. A numerical model of this system would definitely accelerate such a development as experimental assessments are both cumbersome and time-consuming.

1.3 Brownian behavior: the connecting link

Two disparate applications that target some of the most pressing concerns of today are introduced in this chapter. Although these use cases seem uncorrelated, they are united by a common thread that correlates behavior at the smallest scales to the observed system-wide phenomena. This brings us back to the title of this chapter - 'Brownian motion: a macroscopic window to the microscopic world', meaning, the Brownian perspective can provide the missing link in these challenging problems. This is particularly relevant here as we deal with nanoparticle (with a size range 1 nm to 1 μm) transport in a fluid, where multiple effects (both molecular and hydrodynamic in nature) compete for dominance in governing the inherent particle dynamics. Moreover, in these cases, the particles diffuse in the vicinity of a wall and/or other particles, thereby increasing the complexity of the transport process. Thus, a comprehensive insight into the complex interplay between the micro- and macro scale phenomena mediated (in-part) by the hydrodynamic fields developed (in the surrounding fluid) is crucial to improving our understanding of the underlying transport phenomena in these systems. Moreover, as the aforementioned systems involve fine particles, experimentally forecasting the hydrodynamics is challenging due to the simultaneous prevalence of disparate length and time scales. This necessitates the parallel development of numerical approaches that complement existing experimental

techniques. Hence, the development of a general numerical technique that can handle both the complex hydrodynamics as well as the accompanying Brownian behavior in such systems, is the overarching objective of this thesis. The corresponding developments in this regard are detailed in the subsequent chapters and in the appended papers.

1.4 Document structure

This thesis is organized as follows. In Chapter 2 the aims and objectives of this work are established. Next, in Chapter 3 the relevant theoretical background on Brownian theory in a fluid (i.e. both unbounded and bounded flows) is presented. This chapter establishes the basis that is needed to interpret the results presented in the appended papers. This is followed by Chapter 4 which provides an overview of the numerical methods typically used in Brownian modeling, including a detailed account of a novel continuum based direct numerical simulation (DNS) framework (which is one of the primary contributions of this thesis) and positions its relevance with respect to the available methods. In Chapter 5 some essential highlights from this thesis are listed within the context of the appended papers. Finally, Chapter 6 consists of the concluding remarks within the context of the overarching goals of this thesis (as established in Chapter 2) along with a brief description on the future scope of this research effort.

2 Aim

The transport of nanoparticles (in the size range 1 nm to 1 μm) in a fluid presents a challenging problem that couples both molecular and hydrodynamic (or continuum) phenomena. Consequently, it is governed by disparate length and time scales. Thus, the main objective of the current work is to develop various strategies to numerically resolve phenomena at these relevant scales within the context of the applications introduced in Chapter 1. These overarching objectives are listed as follows:

1. To develop a general numerical method that can handle nanoparticle dynamics in a fluid, including the accompanying macro-scale and micro-scale effects, using a continuum based framework (multiphase DNS) i.e. projecting down from the continuum to the molecular scales.
    - Extend the ideas from traditional Langevin based treatments to include the fully resolved hydrodynamics around the particle.
    - Derive a generalized method that extends the applicability of well established resolved-surface multiphase DNS techniques (such as the immersed boundary method, for instance).
    - Demonstrate the capability of this method by validating it against existing analytical theories for Brownian motion in both unbounded as well as bounded domains (i.e. for both free and hindered diffusion.)
2. Establish a hydrodynamic basis, using numerical simulations for diffusive transport of nanoparticles, within the context of the two use cases briefly described in Chapter 1 (i.e. hindered diffusion).
    - Probe the hydrodynamic fields around a Brownian particle (uniform and fractal shaped) in a rarefied gas (i.e. micro-channel flows).
    - Identify the relevant nature of the hydrodynamic stresses on the particle, i.e. the directional bias of the hydrodynamic resistance (along the wall-normal and co-axial directions) on a particle transported along the co-axial centerline of a micro-channel and the corresponding implications on its diffusive behavior.
    - Identify anomalies in the directional bias of the hydrodynamic resistance in non-symmetric scenarios such as off-axis (i.e. a position that is displaced from the co-axial centerline of the channel) diffusion in micro-channels.

3

Nanoparticle dynamics

Brownian transport in a fluid

In the context of this thesis, *nanoparticle dynamics* predominantly refers to the incessant and irregular motion of a nanoparticle in a liquid or gas. The surrounding fluid mediates the complex interactions between the nanoparticles and the surrounding environment (for instance bounding walls or other particles). The physical Brownian motion of nanoparticles (investigated in this thesis) is undertaken in a Newtonian fluid with a non-porous and inert nanoparticle. These investigations are carried out numerically in a dilute fluid (whose density is much lower than that of a particle) using theory and methods that probe both the short and long time-scale aspects of the Brownian behavior. A continuum based hydrodynamic approach to describing Brownian systems is adopted in this thesis. Correspondingly, a brief survey of Brownian theory along with the necessary theoretical basis required to interpret the reported results (appended in the papers) is elaborated in this chapter.

3.1 Overview of Brownian theory

The fundamentals of modern Brownian theory were established in the 1900's by Albert Einstein [14], William Sutherland [24], Marian von Smoluchowski [25] and Paul Langevin [26]. It is surprising that this Brownian perspective played almost no role in physics until 1905 and was generally ignored even by the physicists who developed the kinetic theory of gases, though it is now frequently remarked that Brownian movement is the best illustration of the existence of random molecular motion [27]. It was Einstein who first attempted to establish the relevance of Brownian behavior by combining statistical mechanics and Stokes' result [28] for the friction around a spherical particle due to a steady flow [14]. Einstein's theory neglects the inertia of the particle, implying that an infinite force is required to change its velocity to achieve a random displacement at each step. Von Smoluchowski, shortly afterwards, published a more comprehensible derivation of a similar result (in terms of a random walk – or discrete straight trajectories), using a theoretical model taken over from gas theory [25]. He clarified that each (apparently) straight segment of the Brownian trajectory is a consequence of multiple collisions with

the fluid particles which gives rise to a net displacement along that direction. Langevin used this random walk theory and coupled it with a continuum assumption of the fluid to recover Einstein's result through the use of a stochastic differential equation: the Langevin equation* [26]. The particle inertia was inherently accounted for within this description. Although Langevin employed a continuum description of the fluid (at the scale of the particle), the fluid is perceived through its constituent molecules. These constantly collide with the Brownian particle, accelerating and decelerating it perpetually. Thus, the random displacements can be estimated from the balance between the viscous damping from the fluid and thermal fluctuations due to molecular collisions. This molecular basis of Brownian theory was confirmed by Jean Baptiste Perrin consequently proving the existence of molecules [30]. A chronological account of these early developments in Brownian theory is available in the review by Brush [27].

Langevin's theory neglected fluid inertia as it used the steady state Stokes' drag for damping the thermal fluctuations from molecular collisions (i.e. the Brownian particle is significantly heavier than the molecules it is interacting with). Consequently, Ornstein and Uhlenbeck generalized the original Langevin description to include non-Stokes behavior (i.e. fluid inertia) as well [31]. They achieved this by deriving the frequency distribution function for the velocity and displacement of a free (unbounded) particle undergoing Brownian motion [31]. The resulting random process is commonly referred to as the Ornstein-Uhlenbeck process. Using this treatment, they showed that the velocity auto-correlation function (VACF) of the particle decays exponentially. However, Kubo [32] (another prominent name in the field) noted that this description is not valid at the shortest time-scales, in which the Brownian particle suffers only a few or no impacts (i.e. the particle has a well-defined velocity). These observations are also applicable in systems where the Brownian particle is not necessarily heavier than the molecules interacting with it. Computer simulations of the atoms in liquid argon by Rahman [33], further, corroborated these observations by demonstrating a power law dependence for the VACF at long time-scales (as opposed to the exponential decay). Thus, a generalized form of the Langevin equation (GLE) was proposed by Kubo [32] to account for dynamical coherence in Brownian displacements at short times. Additionally, hydrodynamic models for the fluid (to generalize Stokes' law for the frictional force), can also be used to describe Brownian motion inclusive of fluid inertia, as shown by Alder and Wainwright [34], Zwanzig and Bixon [35], Widom [36] and Hinch [37], to name a few. All these developments culminated into the modern hydrodynamic theory of Brownian motion for a free particle, which has been further validated with exhaustive experimental evidence, recently, by Blum et al. [38], Huang et al. [39] and Kheifets et al. [40]. A more detailed overview of these theories is also available in the reviews by Chandrasekhar [41], Bian et al. [42], Radhakrishnan et al. [43] and Mo and Raizen [44].

Correspondingly, the rest of this chapter establishes the needed mathematical bases which are derived from these popular hydrodynamic theories for both bounded and unbounded Brownian diffusion in a fluid (either liquid or gas). Note that the continuum assumption

*A translation of Langevin's original work is available at [29]

§§ needs to be satisfied for these bases to hold since, it is assumed that the momentum of a Brownian particle relaxes to an equilibrium through its interaction with the immediately surrounding fluid (i.e. the system is strongly overdamped by the viscous friction forces). This limit in a fluid, where the Brownian particle interacts through continuum-level forces, permits these macro-scale abstractions of molecular level phenomena.

3.2 Mathematical basis for free diffusion

In this thesis, we are concerned with the transport of nanoparticles in the size range 1 nm to 1 μm, which would mean that both macro- and molecular scale effects compete for dominance. Physically, this results in two primary consequences – firstly, the molecular effects manifest as a random driving force on the particle maintaining its incessant irregular motion and secondly, the ensuing hydrodynamic effects give rise to a frictional force (or drag) for a forced motion. Thus, in mathematical terms, a superposition of these two opposing effects gives rise to the meandering Brownian displacements, which when averaged over long times yields a net diffusivity (a measure of the rate at which particles diffuse) for the Brownian particle. Such a Brownian behavior is typically represented within the Stokes-Einstein or (alternately) Langevin bases for a freely (unbounded) diffusing particle. These representations are followed in this thesis as well and are described below.

3.2.1 Stokes-Einstein description

Einstein's seminal work [14] provided two major contributions: (i) it relates the mass diffusion to the mean squared dispacement (MSD) of the particle and (ii) connects two transport processes – the mass diffusion of the particle and the momentum diffusion of the fluid. These contributions are contained in the equations that describe the long-term statistical behavior of a Brownian particle. Correspondingly, the MSD of a particle with position vector $r(x, y, z)$ is given as:

$$< \Delta r(t)^2 >= 6D_\infty t. \tag{3.1}$$

Eq. (3.1) can be used for directly estimating diffusivity from a measurement of the particle MSD (in a general random-walk like process). Further, the diffusivity, D_∞, of a freely diffusing particle is given by the Stokes-Einstein relation as:

§§The continuum assumption considers the fluid as a continuous collection of macroscopic volumes (which are orders of magnitude greater than the distance between two adjacent molecules of fluid) within which the molecular details of the system are smoothed out. This concept of a continuous medium permits the definition of averaged quantities that reflect the underlying molecular nature such as temperature, density, pressure, velocity etc. at each point in the fluid domain (these quantities are assumed to have a continuous distribution in space and time) [45, 46]

$$D_\infty = \beta_{St} k_B T, \tag{3.2}$$

where, β_{St} is the Stokes' mobility (reciprocal of the friction coefficient γ_{St} [47]) of the particle, which for a sphere in an incompressible fluid at steady state is:

$$\beta_{St} = \gamma_{St}^{-1} = \frac{1}{6\pi\mu_f r_p}, \tag{3.3}$$

with, μ_f as the dynamic viscosity of the fluid and r_p as the particle radius, respectively. Note that Eq. (3.3) is applicable when the no-slip (i.e. fluid velocity at the particle surface is zero) condition is valid at the particle. The particle response time, τ_p, or the time scale of a particle slowing down owing to friction from the fluid (after an initial impulse) is estimated from the mobility as:

$$\tau_p = m_p \beta_{St}. \tag{3.4}$$

The Eq. (3.2) balances the mass transport of the particle with the momentum transport of the fluid. Consequently, the drag on the particle is steady and the thermal kicks (due to collisions with the fluid molecules) average to zero over a long period, leaving the drag on the particle as that in a deterministic fluid. It follows that, the particle inertia is neglected in this description, meaning an infinite force is required to change the velocity of the particle at each instance in the trajectory. Thus, the particle velocities cannot be defined, leading to a fractal trajectory or random walk as shown in Fig. 3.1. A mathematical model corresponding to this case is a Gaussian white noise process for the velocity. Meaning, the instantaneous position $x_p(t)$ corresponds to a Wiener process[¶¶], which is continuous but nowhere differentiable in time. Note that the velocity can still be determined from consecutive positions along the random walk, if the observations are time-resolved sufficiently. Consequently, the chosen temporal resolution should capture the relevant mass-diffusion process as given by the diffusion or Smoluchowski time-scale:

$$\tau_D = \frac{r_P^2}{D_\infty}, \tag{3.5}$$

Another inherent assumption in the Stokes-Einstein treatment is that the Schmidt number (Sc), given as the ratio ν_f/D_∞, is $\ll 1$, where ν_f is the kinematic viscosity (μ_f/ρ_f) of the fluid. Physically, this means that momentum diffuses much faster than does the particle and this motion is viscous-dominated. In particular, the fluid velocity quickly relaxes to the solution of the steady Stokes' equation as the particle barely moves [49].

[¶¶]A continuous-time stochastic process $W(t)$ for $t \geq 0$ with $W(0) = 0$ and such that the increment $W(t) - W(s)$ is Gaussian with mean 0 and variance $t - s$ for any $0 \leq s < t$, and increments for non-overlapping time intervals are independent [48].

Thus, the Eq. (3.2) captures the long term behavior of a free Brownian particle in a viscous fluid well, however it disallows a definition of an instantaneous particle velocity. This is particularly relevant at the shortest time scales of motion ($\ll \tau_D$), when the Brownian particle moves in a straight line with a constant velocity before collisions with fluid molecules slow it down and randomize its motion (as shown in experiments by Huang et al. [50]). At this scale, known as the ballistic regime, the particle's inertia becomes significant and its motion is highly correlated. The ballistic time-scale (τ_B) can be deduced from the collisional time scale of the molecules (i.e. the duration between successive random bombardments). This is resolved using Langevin's treatment [26]. Finally, and most importantly, the Brownian process is assumed to be a Markovian, i.e. the future states of the system are independent of the present and past states. This assumption is usually valid, when it is assumed that the fluid is inertia-less (as is the case in the Stokes-Einstein description).

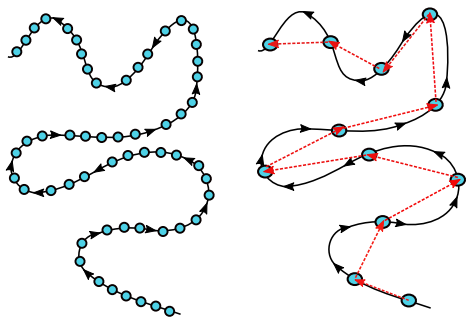

Figure 3.1: *Concept of random-walk: On the left is the actual trajectory of a Brownian particle, while on the right are the observed locations of the particle as extracted from a Stokes-Einstein description (Eq.* (3.2)*) at the diffusive time scale (τ_D in Eq.* (3.5)*). The red arrows indicate the fractal trajectory (random walk) that is usually identified from this description.*

3.2.2 Langevin description

The fundamental theory of Einstein and Smoluchowski is restricted to time scales at which the decay of the velocity of the Brownian particle is negligible (i.e much larger than the particle response time). Hence, a more complete description of the Brownian motion of a free particle was proposed by Langevin [26, 41]. Although Langevin's approach, like Einstein's, is from a mathematical point-of-view rather simple, there is a very subtle conceptual point at the basis of his theory for Brownian motion. This is the validity of Stokes' law (which has a macroscopic nature) together with the assumption that the Brownian particle is in statistical equilibrium with the molecules in the liquid. In other words, despite the mass of the colloidal particle being (exceedingly) larger than the mass of the molecules, energy equipartition is assumed to hold. This equation of motion[†] for

[†]Brownian motion occurs in 3D and Eq. (3.6) applies only to the x-component of this motion.

the Brownian particle, with mass m_p, is formally based on Newton's second law as:

$$m_p \frac{\mathrm{d}u_p}{\mathrm{d}t} = -\gamma_{St} u_p + \chi(t), \tag{3.6}$$

where, u_p denotes the velocity of the particle and $\chi(t)$ is the stochastic forcing (in the attached papers this is referred to as $\mathbf{F_{Brownian}}$) that denotes the fluctuating part of the Brownian motion. It should be noted that both these parts are related as they are a result of the same fundamental phenomenon, i.e. random collisions with the surrounding molecules. The frictional term γ_{St} is given by Eq. (3.3). Hence, the Langevin equation (3.6) is the momentum equation for the particle with a random forcing for the non-equilibrium behavior and with a friction force that is linear in instantaneous velocity. The fluctuating component $\chi(t)$ is assumed to be independent of the velocity u_p and further fluctuate rapidly in comparison with variations in velocity. Consequently, in this description, the particle velocity is well defined and is subject to both the viscous dissipation (friction force) from the fluid and the random stochastic forcing. Uhlenbeck [31] further showed that Eq. (3.6) is constrained by certain restrictions on the fluctuating component $\chi(t)$, i.e. it follows a Markovian Gaussian white noise process. Hence, the stochastic forcing satisfies:

$$\begin{gathered} \langle \chi(t) \rangle = 0, \quad \langle \chi(t) \chi(t') \rangle = \tilde{S}_{uu} \delta(t - t') \\ \langle \chi(t) x(t') \rangle = 0, \quad \langle \chi(t) u_p(t') \rangle = 0. \end{gathered} \tag{3.7}$$

Here, $\langle ... \rangle$ denotes an ensemble average in thermal equilibrium and $\tilde{S}_{uu}$ is the strength of the Gaussian noise (which will be determined below). In the Langevin Eq. (3.6), u_p is continuous and differentiable under the constraints of a stochastic differential equation (provided $\chi(t)$ is an additive and independent noise). Thus, the MSD and velocity auto-correlation function (VACF) can be extracted from this equation as shown below.

MSD and VACF

The MSD can be derived by re-writing Eq. (3.6) in terms of the position $x(t)$ and averaging the same using the $\langle ... \rangle$ operator under the constraints presented in Eq. (3.7), followed by the application of the equipartition theorem $m_p \langle u_p^2 \rangle = k_B T$[‡]. Correspondingly, we obtain the expression for the MSD at all time scales as:

$$\langle \Delta x^2(t) \rangle = \frac{2 k_B T}{\gamma_{St}} \left(t - \frac{m_p}{\gamma_{St}} + \frac{m_p}{\gamma_{St}} \mathrm{e}^{\frac{-\gamma_{St} t}{m_p}} \right). \tag{3.8}$$

[‡]A colloidal particle suspended in a liquid at temperature T is assimilated to a particle of the liquid, so that it possesses an average kinetic energy $\frac{2RT}{N_{av}}$. Accordingly we get: $\frac{1}{2} m_p \langle u_p^2 \rangle = \frac{2RT}{N_{av}}$

In Eq. (3.8), when $t \gg \tau_B$, the exponential term is negligible, leading to the Einstein's result for long-term or over-damped behavior i.e. Eq. (3.1) (in 1D). However, when $t \ll \tau_B$ or as $t \to 0$, the ballistic or under-damped result can be obtained:

$$< \Delta x(t)^2 >= \frac{k_B T}{m_p} t^2 = u_{rms}^2 t^2. \tag{3.9}$$

Here, u_{rms} is the root-mean-squared velocity of the particle. The corresponding time scale (i.e. the relaxation time for the Brownian particle) in the ballistic regime, τ_B, is given as:

$$\tau_B = \frac{m_p}{\gamma_{St}}. \tag{3.10}$$

The VACF of the Brownian particle can be derived by evaluating the solution of the first-order inhomogeneous stochastic differential equation i.e. Eq. (3.6). Ornstein-Uhlenbeck showed that the VACF of a freely diffusing Brownian particle is:

$$C(t) \equiv \langle u_p(0) u_p(t) \rangle = \left\langle u_p^2(0) \right\rangle \mathrm{e}^{\frac{-\gamma_{St} t}{m_p}} = \frac{k_B T}{m_p} \mathrm{e}^{\frac{-\gamma_{St} t}{m_p}}. \tag{3.11}$$

The detailed derivation of both the MSD and VACF is available in Appendix 7.2.

3.2.3 Linear response theory and the Langevin equation

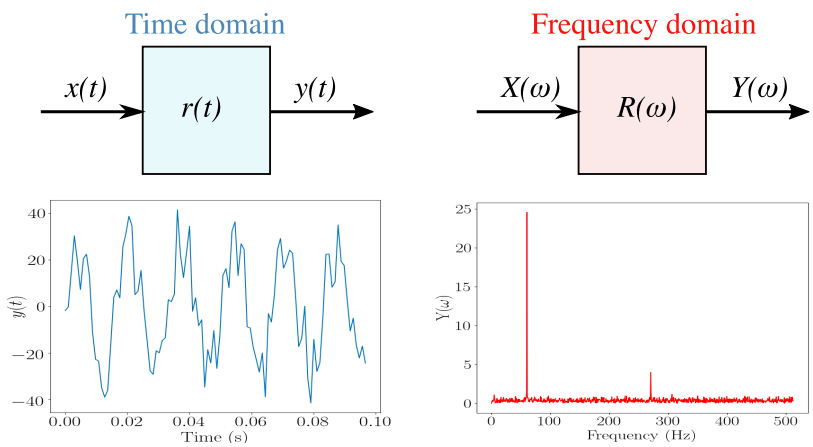

Figure 3.2: *Schematic of an output from a linear time invariant (LTI) system in the time (left) and frequency (right) domains.*

Linear response theory describes how an (small) external perturbation affects the macroscopic properties of a system. In this context, a Brownian process can be regarded as a system which is regularly perturbed by thermal kicks (from the fluid molecules) and can correspondingly be modeled using linear response theory (as shown by Ounis and Ahmadi [51–53]). Since the magnitude of these applied stochastic forces are small, the response of the system has a linear dependence on it. Moreover, this response does not depend on the time when the stochastic forcing is applied, meaning it is a linear time-invariant (LTI) system. Consequently, the Brownian system is perturbed by a Gaussian white noise with zero mean ($\mathbb{E}[\chi(t)] = 0$) and a co-variance given by the Dirac-delta function ($\mathbb{E}[\chi(t)\chi(\tau)] = \delta(t-\tau)$). This forcing appears at a time-scale lesser than the particle response time (τ_p). Consequently, such a strategy is adopted to model Brownian behavior in this thesis.

The correlation functions, derived previously (see Eq. (3.11)) represents a stationary[¶] stochastic process in the time domain, which satisfies the Wiener-Khinchin theorem[‖]. It follows that, such time signals can be represented in the frequency space using the corresponding Fourier transforms. Correspondingly, the power spectral density, $\tilde{S}_{uu}(\omega)$, of the random process (based on the velocity), which is needed in order to describe the Gaussian white noise signal, can be deduced as:

$$\tilde{S}_{uu}(\omega) = \frac{k_B T \gamma_{St}}{\pi m_p} = \frac{2{\gamma_{St}}^2}{\pi} D_\infty, \tag{3.12}$$

Thus, the stochastic forcing term, $\chi(t)$, is modeled as a Gaussian white noise process with the vector of spectral intensity S^n_{ij} given as:

$$S^n_{ij} = \tilde{S}_{uu}(\omega)\delta_{ij}. \tag{3.13}$$

A detailed derivation of this power spectrum (i.e. Eq. (3.13)) is provided in Appendix 7.3.

To summarize, in this thesis, the Langevin behavior is studied as an LTI system, i.e. a Gaussian white noise perturbed Brownian particle that is immersed in a fluid is studied. This approach is chosen as it is easy to implement in a Lagrangian form within the numerical framework developed in this thesis. Moreover, this approach accurately reproduces the necessary dynamics of the system (see Fig. 3.3) as well. Additionally, hindered diffusion can easily be included in such a Langevin description by accounting

[¶]A continuous-time random process, $X(t), t \in \mathbb{R}$ is wide sense stationary if:

1. $\mu_X(t) = \mu_X$, for all $t \in \mathbb{R}$, where μ_X is the mean.
2. $C_X(t_1, t_2) = C_X(t_1 - t_2)$, for all $t_1, t_2 \in \mathbb{R}$, where C_X is the correlation function.

[‖]The power spectrum $S(\omega)$ of a stationary random process and its auto-correlation function are Fourier transform pairs

for the relevant particle mobility in Eq. (3.3), as will be elaborated in the subsequent section.

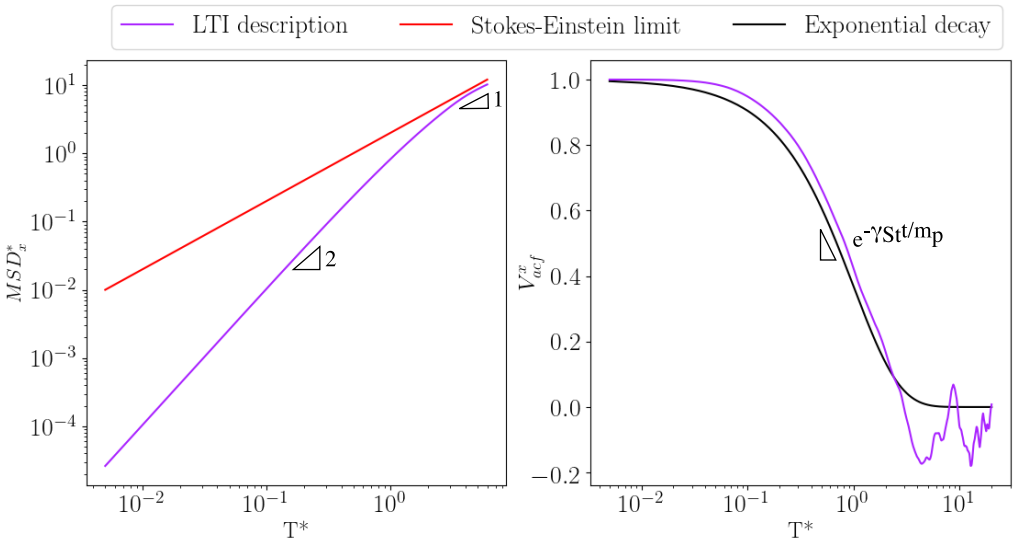

Figure 3.3: *1D Brownian behavior modeled as an LTI system (stochastic forcing done using a Gaussian white noise signal): Particle mean-squared behavior (represented as* $MSD_x^* = MSD_x/D_\infty\tau_p$*) in the left panel and VACF in the right panel. Note that the Langevin Eq.* (3.6) *is integrated using a forward Euler explicit time marching scheme. The mean-squared behavior shows the clear transition from the correlated ballistic regime (indicated with slope 2) to an un-correlated and linear Stokes-Einstein regime. Further,* V_{acf}^x *decays exponentially.*

Note, however, that this approach is valid only under the following conditions:

1. The random forcing appears as a white noise at a scale lesser than the particle response (or ballistic) time scale τ_p.
2. The hydrodynamic coupling between the particle and the fluid (i.e. the fluid friction) is given by the steady Stokes' drag [47].
3. There is equipartition of kinetic energy among the degrees of freedom of the system, i.e. between the molecules of the fluid and the particle performing Brownian motion.

The white-noise assumption is satisfied when the particles are much larger than the surrounding fluid molecules without being much less dense [37]. The validity of the steady drag has been a source of debate for several applications of the Langevin treatment, especially when the particle-fluid density ratios are lower (i.e unsteady effects such as Basset history and added mass forces begin to play a role) [33, 34, 37]. However, for

the typical cases studied in this thesis, the particle-fluid density ratios are significantly higher, meaning that the hydrodynamic coupling can be given by steady hydrodynamic forces. Moreover, the particle Reynolds number[††] is $\ll 1$, for the nanoparticles studied in this thesis, meaning, the fluid inertia is negligible.

3.3 Hindered diffusion

In the previous section, a detailed mathematical basis for describing free (or unbounded) diffusion is established. In particular, the Langevin approach, which is central to this thesis, has been described in detail. However, not all real systems are so ideally behaved. In many cases, the Brownian particle diffuses in an environment where other interactions mediated by the fluid (such as particle-particle, particle-wall or non-continuum effects), assume a governing role in dictating the dynamics of the system. Within the context of this thesis, nanoparticle transport in such altered environments is referred to as hindered diffusion (i.e. the free diffusion of a Brownian particle is 'hindered' by additional effects mediated by the fluid). It is well established that the mobility of the particle is altered and in most cases reduced when diffusing in the vicinity of a wall or another particle. This was confirmed by direct measurements in Brownian systems, first by MacKay and Mason [54] and later by others [50, 55–70] using advanced particle tracking techniques. This reduction in particle mobility is attributed to the associated increase in the hydrodynamic resistance on the particle when diffusing in the vicinity of a wall or another particle. A detailed account of related hindered diffusion theories for Brownian motion is available in the reviews by Deen [71], Burada et al. [72] and Mo and Raizen [44]. The details on these theoretical developments are omitted from this section for brevity (but are briefly discussed in the appended papers, see Papers *B* and *D*).

A similar reduction in the hydrodynamic resistance is also noticed for a particle suspended in a rarefied gas, as first reported by Epstein [73] and later by Cercignani and Pagani [74, 75]. The reduction in this case is, however, due to the existence of non-continuum effects in the gas. These are attributed to the longer mean free paths (or distance between successive molecular collisions) in air when compared with a corresponding liquid (where the molecules are more tightly packed). Thus, a new transport scale defined by the Knudsen number (Kn):

$$Kn = \frac{\lambda_{gas}}{L}, \tag{3.14}$$

with λ_{gas} as the mean free path of the gas and L as a characteristic system length scale, is introduced in these systems. This scale identifies the relative importance between (microscopic) molecular and (macroscopic) hydrodynamic interactions (or the degree of

[††]Ratio between inertial and viscous forces given as $\frac{d_p \rho_f u_p}{\mu_f}$

rarefaction). When $Kn > 0.001$, the particle does not perceive the gas as a continuum any longer and begins directly interacting with its constituent molecules, particularly as the particle sizes are very close to the mean free path (molecular length scales) of the surrounding gas. Thus, the overall resistance to motion is also reduced.

In this thesis, hindered diffusion is modeled by correcting the Stokes' mobility (in Eq. (3.3)) used in the Langevin basis to adequately represent the actual mobility of the particle. Correspondingly, the respective treatments adopted for this mobility correction (in liquids and gases) are described in this section.

3.3.1 Wall-bounded diffusion

The dynamics of Brownian particles close to a rigid wall are significantly affected by wall interactions. When a rigid particle approaches within a few radii from the wall, its mobility is altered. Usually, this mobility is discussed along two principal directions relative to the motion between the particle and the wall, a co-axial (or parallel) and wall normal (or perpendicular) mobility, respectively. Independent measurements of the mobility and diffusion coefficient (D) of Brownian particles diffusing near a wall have indicated that they are each to be corrected by the same factor [50, 57, 61, 63–65, 76, 77]. This implies that these quantities are functions of the radial position of the Brownian particle in relation to the boundary walls. This is due to the increased hydrodynamic resistances in the vicinity of a wall, leading to a reduction in particle mobility. Further, the wall-normal motion is impeded more strongly than the co-axial one. This is expected as, for wall-normal motion, the fluid between the particle and the wall needs to be squeezed out, correspondingly, increasing the resistance. This basis was first established by Faxén and later improved upon by the analytical theories of Brenner [78, 79] for longitudinally bounded flows.

The correction to the particle mobility in a liquid is represented as λ throughout this thesis. This is done by multiplying the Stokes' mobility (see Eq. (3.3)) for a free particle with this factor as:

$$\beta_{St}^{corr} = \frac{1}{6\pi\mu_f r_p \lambda}, \tag{3.15}$$

where β_{St}^{corr} is the corrected Stokes' mobility. Most recently, Kihm and co-workers [63, 80] further validated with experiments that the reduction in mobility (by the factor λ) is indeed described by the analytical theories of Brenner [78, 79]. Moreover, λ can represent any other effect such as a slip-wall [81, 82] or even other neighboring particles (multi-particle diffusion) [60, 78, 83, 84], provided the appropriate correlation is used. An overview of most analytical/theoretical developments including the appropriate expressions for λ can be found in the classical books of Happel and Brenner [85] and Kim and Karilla [86].

3.3.2 Diffusion in a rarefied gas

Diffusion of a nanoparticle in a rarefied gas is usually not classified under hindered diffusion, however, within the context of this thesis, this is also included within this broad classification. The motivation behind this inclusion is that these systems are also modeled in a similar way as hindered diffusion in liquids, i.e. the particle mobility is corrected to incorporate the necessary deviations from the Stokes' mobility (Eq. (3.3)). For rarefied gases, these deviations are due to the breakdown of the continuum assumption when the characteristic dimensions of the flow are comparable to the mean free path of the gas (in this case air has a mean free path of approximately 67 nm at 20°C and standard atmospheric pressure). Thus, for the range of Brownian particles considered in this thesis (1 nm to 1 μm), rarefaction effects of the gas are also relevant. Under such conditions, the fluid can no longer be regarded as being in thermodynamic equilibrium (with the particle) and a variety of non-continuum or rarefaction effects are likely to be exhibited [87]. This necessitates an additional correction factor in the Langevin equation, Eq. (3.6) (in a similar manner as that of λ) while modeling the relevant Brownian behavior. Note that in a rarefied gas the no-slip boundary condition, traditionally employed at the particle surface, is no longer applicable and a sub-layer (known as the Knudsen layer) of the order of one mean free path starts to affect the fluid interaction between the bulk flow and the particle.

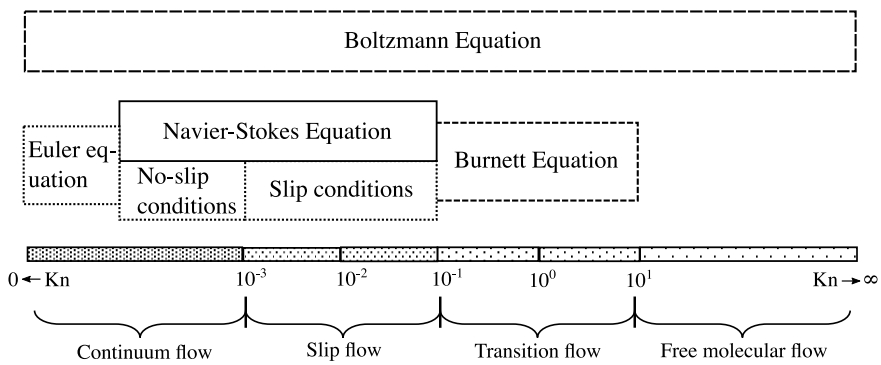

Figure 3.4: *Flow regimes classified based on the Knudsen number (figure adapted from Bird [88]).*

Rarefied flows are characterized by Kn into the following four regimes: continuum flows ($Kn < 0.001$), slip flows ($0.001 \leq Kn < 0.1$), transition flows ($0.1 \leq Kn < 10$), and free-molecular flows ($Kn \geq 10$) [87, 89–94]. The applicability of the continuum hypothesis is determined on the basis of these regimes, as shown in Fig. 3.4. Systems which are strongly rarefied or at the limit of free molecular flow are characterized by a Kn greater than unity while those which are at the continuum flow limit are characterized by a Kn much lower than unity. As Kn increases, the rarefaction effects become more pronounced and eventually the continuum assumption breaks down. Hence, the particle-fluid interaction has to be resolved by solving the Boltzmann equation (will be discussed

in Section 4.1.2). Nevertheless, conventional continuum descriptions of the forces can be extended to describe weakly rarefied or slip flows ($10^{-3} < Kn < 10^{-1}$) by imposing the appropriate slip and temperature jump boundary conditions on the surface [87].

Early attempts at understanding such rarefied flow regimes at low densities began with Maxwell [95], when he derived a slip boundary condition for a dilute gas using kinetic theory. This idea was extended by Cunningham [96], who derived an empirical first-order slip velocity correction factor from hydrodynamic theory for small *Kn*. Further, Millikan [97] confirmed that the drag reduction (due to hindered momentum transfer between the particle and fluid) at higher *Kn* can be deduced using the Cunningham correction (C_c) when formulated as a function of *Kn* as:

$$C_c(Kn) = 1 + AKn, \tag{3.16}$$

where, A is a function of *Kn* that is determined based on empirical data. The Cunningham correction produces results that are in excellent agreement with the available experimental data as shown by Alan and Raabe [98]. Mosfegh et al. [99] summarize the Cunningham-based slip correction factors (and corresponding A values) that have been proposed and commonly used (based on extensive experimental trials) for air with mean free path of 67.3 nm at 101.3 kPa and 23°C. Among these, the most commonly used correlation is the one proposed by Davis [100] and is given as -

$$C_c = 1 + Kn\left(1.257 + \mathrm{e}^{\frac{-1.1}{Kn}}\right). \tag{3.17}$$

Correspondingly, the correction to Stokes' mobility (i.e. Eq. (3.3)) for diffusion in rarefied gases is given as:

$$\beta_{St}^{corr} = \frac{1}{6\pi\mu_f r_p(\frac{1}{C_c})}. \tag{3.18}$$

The Eq. (3.18) shows that C_c is always used in conjunction with the steady Stokes' drag, which is by definition obtained using a no-slip condition at the particle surface. The continuum hypothesis could also be extended for moderate *Kn* by exchanging the no-slip condition for a slip condition (at the particle surface) [101]. This approach can be used with some success in the slip flow regime (up to $Kn \approx 0.15$). Nevertheless, in this thesis, we limit ourselves only to the empirical first-order Cunningham slip correction due–in–part to its relative ease of implementation (within the developed framework) and demonstrated capability to adequately represent non-continuum effects in weakly rarefied gases [98]. Moreover, these higher-order slip conditions are highly geometry dependent [102], further adding to the complexity of the problem. Consequently, there is not yet a consensus in open literature neither on the best choice for a higher-order slip formulation, nor on their advantages in complex geometries [103].

4

Numerical modeling approaches

Molecular and continuum based methods

The primary objective of this thesis is to present a novel continuum based framework to assess the (Brownian) dynamics of a nanoparticle under any given condition (either free or hindered diffusion). Traditionally, the modeling of Brownian behavior has been approached from two perspectives – building up from micro-scales or projecting down from the macro-scale. This dichotomy consequently leads towards assessments at varying levels of detail. The former are generally at a high level of detail but at a microscopic scale of abstraction, while the latter are lacking in the molecular details but are, however, at a relevant macroscopic scale. In this thesis, a continuum based abstraction is preferred (as elaborated in Chapter 3). Furthermore, these continuum based projections are additionally improved by consistently incorporating the missing molecular details, thereby extending their applicability. Note also that molecular methods are used as well in order to investigate certain complex dynamics in rarefied particulate flows where a continuum based abstraction fails. Thus, in this chapter, these numerical treatments are described in relation to the theoretical bases introduced in the previous chapter. Furthermore, a brief review of the current state-of-the art in the numerical modeling of Brownian motion is also presented here.

4.1 Current state-of-the-art

Early analytical developments within Brownian theory were derived with both first principles based approaches using kinetic theory (i.e. Langevin, Fokker-Planck[§§] and

[§§]The Fokker-Planck equation for the distribution function f of the Brownian particles (derived from the Langevin Eq. (3.6)) is given as:

$$\frac{\partial f}{\partial t} = \frac{\partial}{\partial u_p} \cdot (\gamma_{St} u_p f) + q \frac{\partial^2 f}{\partial u_p^2},$$

Boltzmann equations [31, 41]) and hydrodynamic approaches using the linearized Stokes' equations¶¶ [86, 104]. Most modern techniques heavily borrow from these classical approaches and further improve upon them. Correspondingly, these modeling techniques are classified into three overarching categories based on the corresponding level of computational abstraction (as shown in Fig. 4.1). These are: micro-scale, meso-scale and macro-scale methods, in decreasing level of spatial resolution (i.e. moving from meter-scales to pico/nano-scales), respectively. Due to the large scale-separations, the dynamics of the Brownian particles are largely dependent on the detailed mechanics of the suspending fluid. Thus, the wide spectrum of available methods are generally applicable (efficiently) based on the governing length scales of the system as represented in terms of Kn. Correspondingly, micro-scale methods are more relevant when directly describing molecular-scale interactions ($Kn \geq 10$) and macro-scale methods when the continuum theory holds ($Kn \to 0$). The meso-scale methods are applicable when the continuum theory begins to fail and when micro-scale methods are too expensive. The relevant developments within these three categories of numerical methods are described below.

4.1.1 Micro-scale methods

Dynamic simulations of Brownian systems at a molecular level of abstraction (using kinetic theory) were pioneered by Alder and Wainwright [105]. The aim of such a method was to obtain the spatial and temporal evolution of the relevant macroscopic properties of the system on the basis of the mechanical laws governing the molecular motion. This method, referred to as molecular dynamics (MD), solves the Newton's equation of motion for the simulated molecules/particles interacting through Lennard-Jones, hard-sphere, electrostatic, etc. types of inter-particle forces. This was first successfully used by Rahman [33] to demonstrate the non-exponential decay of the VACF in liquids and has since been used for several applications, including studying bio-molecules [106]. The MD technique evaluates the time-dependent behavior and evolution of a molecular system, from which the thermodynamic and kinetic properties are evaluated. Although such an approach works reasonably efficiently in liquids (where the molecules directly interact with only a few neighboring molecules), it gets computationally expensive in dilute gases where a molecule could have potentially thousands of collision partners. This could make the problem completely intractable for certain applications, as the computational burden of the method scales with the square of the number of simulated molecules. This is because the computation for any single molecule requires the consideration that all other molecules are possible collision partners [88]. This inherent limitation of the MD method, led to the development of the most widely used molecular method for dilute gas flows, the direct simulation Monte Carlo (DSMC). This method, pioneered by Bird [88, 107], is also similar to the MD approach with one crucial difference: the inter-molecular collisions are dealt with on a probabilistic rather than a deterministic basis (hence the

where $q = \frac{k_B T \gamma_{St}}{m_p}$

¶¶The continuum Navier-Stokes equations can be linearized by neglecting the non-linear convective terms, meaning the Brownian particle is diffusing in a quiescent fluid.

name Monte-Carlo). DSMC has been shown in principle to be an exact solution of the Boltzmann equation*** [108], meaning the necessary molecular nature of the system can be obtained without the need for any additional models or fitting. The DSMC method can in principle be used across the regimes indicated in Fig. 3.4. However, it is best applicable to describe flows with $Kn \geq 10$, as it can get computationally expensive when $Kn \to 0$. Moreover, Michaelides recently used this method to assess nanoparticle diffusivity in an isothermal fluid within narrow cylindrical pores [109], further demonstrating the usefulness of the method in assessing the micro-scale dynamics of a Brownian system. Thus, Bird's DSMC framework is used in this thesis to describe rarefied gas dynamics in the transition regime. More specifically, the effect of a symmetric nanoparticle in rarefied micro-channel flows is investigated using a DSMC solver (*dsmcFoamPlus*), details of which are discussed in the succeeding sections.

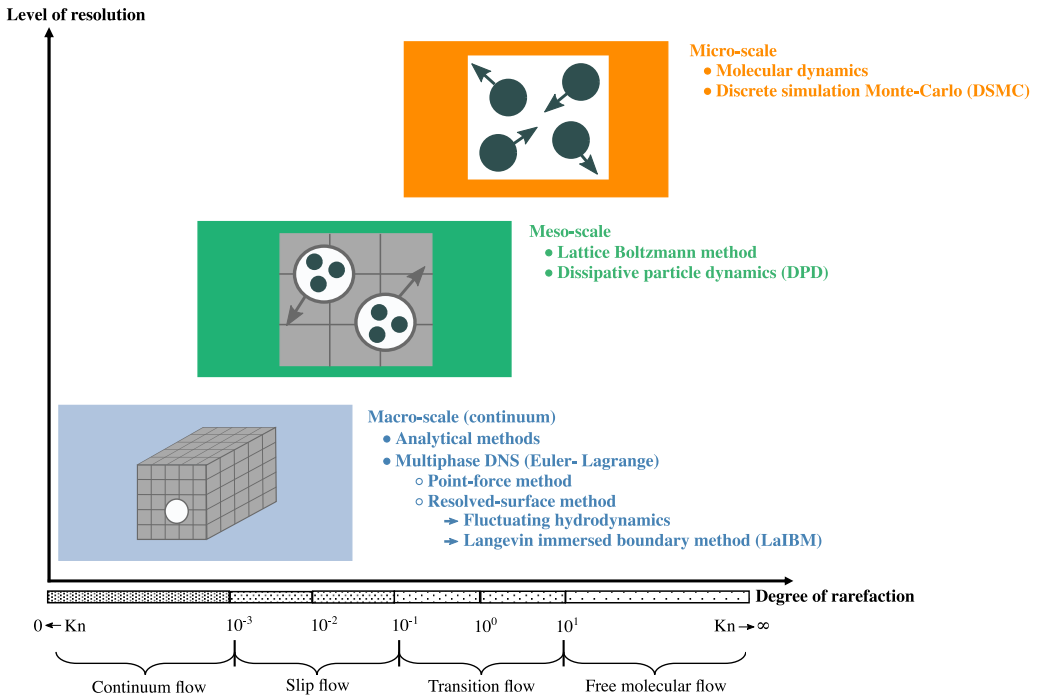

Figure 4.1: *Classification of numerical methods based on their corresponding scales of abstraction in terms of level of detail.*

***The Boltzmann transport equation is given as:

$$\frac{\partial f}{\partial t} + u_p^i \frac{\partial f}{\partial x^i} + a_p^i \frac{\partial f}{\partial v_p^i} = \left(\frac{Df}{Dt}\right)_{\text{coll}} ,$$

where, u_p^i and a_p^i represents the velocity and acceleration of a distribution of molecules/particles. Note that f is a one-particle distribution function, i.e. it is assumed that the probability of finding a particle at a particular point in phase space is independent of the coordinates of all other particles in that phase space. Such a description is only valid for a dilute gas.

4.1.2 Meso-scale methods

Simulating every aspect of a system at a molecular level of detail can not only be very expensive but also unnecessary. Under conditions where Kn is sufficiently low that a detailed molecular basis is intractable, while still being sufficiently high enough that the continuum based approaches are reaching their limit (i.e. usually in the slip and transition flow regimes), a meso-scale approach is more preferred. Methods at this level of abstraction are based on microscopic models and meso-scopic kinetic equations. The basic premise for using these simplified kinetic-type methods for macroscopic fluid flows is that the macroscopic dynamics of a fluid is the result of the collective behavior of many microscopic particles in the system and that the macroscopic dynamics is not sensitive to the underlying details in the microscopic physics [110]. Consequently, in mesoscopic kinetic theory, the distribution of particles in a gas is the quantity which evolves on timescales around the mean collision time between the molecules (i.e. at a scale where the system relaxes to local equilibrium through collision events).

Some of the most widely used mesoscopic methods for modeling Brownian behavior are the lattice Boltzmann method (LBM) and dissipative particle dynamics (DPD). These are briefly described below.

Lattice Boltzmann method

The LBM framework originated from lattice gas automata (LGA), which was proposed as a new technique to solve the continuum averaged Navier-Stokes equations (described later in Eq. (4.1)). Consequently, these equations were solved using a simulation where particles of the same mass are allowed to move on a regular lattice and local collision rules are introduced at the nodes which conserve the number of particles and momentum (discrete particle kinetics utilizing a discrete lattice over discrete time) [111–113]. The lattice gas automata was extended to solve the Boltzmann equation (for a distribution of particles/molecules) with a linear BGK collision operator, that directly captures the relaxation of the distribution function towards the equilibrium Maxwellian distribution. This is achieved by discretising the Boltzmann equation in velocity space, physical space and time[†††]. Thus, the particles in the LGA method are replaced by distribution functions in the LBM approach. A more detailed account of the LBM framework is beyond the scope of this thesis and the reader is referred to detailed reviews on the same by Chen and Doolen [114] and the book by Kruger et al. [115].

[†††]Discretized Boltzmann equation:

$$f_i\left(x + c_i\Delta t, t + \Delta t\right) = f_i(x,t) - \frac{\Delta t}{\tau}\left(f_i(x,t) - f_i^{eq}(x,t)\right),$$

where, $f_i(x,t)$ moves with velocity c_i to a neighboring point on the lattice $x + c_i\Delta t$ at the time step $t+\Delta t$ and τ is a velocity-dependent collision time that relaxes the system to the equilibrium distribution f_i^{eq}.

LBM has been used in conjunction with existing MD methods, for studying Brownian behavior in finite size suspensions. Ladd [116, 117] proposed one such hybrid method that solved the particle dynamics using Newton's equations of motion (MD) and the surrounding fluid using the LBM framework. Since the molecular fluctuations are inherently absent in the Boltzmann equation, these are additionally included in the fluid description using the fluctuating hydrodynamics approach of Landau and Lifshitz [118], leading to a stochastic term in the the time evolution of the velocity distribution function. This approach, also known as the fluctuating lattice Boltzmann method (FLBM), was extended to polymer solutions by coupling it to a Langevin evolution of the particle dynamics, by Ahlrichs and Dunweg [119] and later by Mynam et al. [120]. Despite being highly paralellizable, LBM is memory-intensive. Consequently, propagating populations requires a large number of memory access events. Moreover, FLBM has a few bottlenecks associated with the choice of the discretization scheme for the stochastic differential equation, primarily due to the correlation between the form of the required fluctuation-dissipation relations and the choice of scheme [121].

Dissipative particle dynamics

DPD, on the other hand, can be considered as a coarse-grained MD method that allows for the simulation of larger length and time scales than molecular dynamics and avoids the lattice-related artefacts of LBM. This model consists of a set of point particles that move off-lattice, interacting with each other through three types of forces: a conservative force derived from a potential, a dissipative force that tries to reduce radial velocity differences between the particles and a stochastic force directed along the line joining the center of the particles. The last two forces can be termed as a pair-wise Brownian dashpot which represents the viscous forces and thermal noise between the groups of atoms represented by the dissipative particles. All these forces describe additive pair-interactions between particles (obeying Newton's third law). Hence, DPD conserves momentum. Due to this, the behavior of the system is hydrodynamic at sufficiently large scales [122]. Note that all interactions have a finite radial range. For a more detailed description of this method, the reader is referred to the review by Espanol [122].

DPD is particularly suited for evaluating the hydrodynamics of complex fluids at the mesoscale with finite Kn. Typical applications are suspensions of polymers. This method has also been used in conjunction with the Langevin equation to assess Brownian systems. Gubbioti and co-workers used DPD to account for a spatially dependent mobility field determined *a priori*. This field was solved in conjunction with a rigid body Langevin equation [123] to assess hindered diffusion in micro-channels. This method is perfectly suited for studying pore scale diffusion in symmetric channels, however, the *a priori* determination of the mobility field gets progressively harder in heterogeneous pores, thereby limiting its applicability. Another disadvantage of DPD is that it contains a large number of parameters that have to be selected carefully. For instance, the choice of the radial cut-off limits is delicate and affects the emergent hydrodynamic behavior. Finally, as with other mesocale methods, these can also be memory intensive as the dynamics of

individual particles have time scales significantly shorter than the hydrodynamic time scales.

4.1.3 Macroscopic methods

The Macroscopic or continuum based methods are in essence coarse-grained abstractions of micro- and meso-scale descriptions that rely on two fundamental assumptions: (i) the continuum limit, i.e. the point in space where the field is defined is a volume element containing a large number of atoms and (ii) the local equilibrium assumption, i.e. these volumes are large enough to reproduce the thermodynamic behavior of the whole system. This concept of a continuum fluid is fundamental to the viscous damping being described in the Langevin equation, which models the total fluid resistance (in the over damped limit) as the continuum Stokes' drag on the particle (as elaborated in Chapter 3). Hence, the original Langevin equation (i.e. Eq. (3.6)) can be considered to model Brownian behavior at a continuum level of abstraction, consequently requiring the molecular fluctuations to be added additionally (as these have been averaged out in a continuum description) through the stochastic forcing term.

This continuum assumption permits the governing equation system to be simplified into non-linear partial differential equations, i.e. the Navier-Stokes (NS) equations [28, 47, 124][***]. This equation, for an incompressible (divergence free) fluid is given by the following continuity and momentum equations:

$$\begin{aligned} \boldsymbol{\nabla} \cdot \boldsymbol{v} &= 0, \\ \rho_f \left(\frac{\partial}{\partial t} \boldsymbol{v} + \boldsymbol{v} \cdot \boldsymbol{\nabla} \boldsymbol{v} \right) &= -\boldsymbol{\nabla} P + \mu_f \boldsymbol{\nabla}^2 \boldsymbol{v}, \end{aligned} \tag{4.1}$$

where, $\mathbf{v}$ and P are the velocity vector and pressures in the fluid, respectively[‡‡].

The NS equations are strongly non-linear, meaning they require advanced iterative techniques such as computational fluid dynamics (CFD) for obtaining the desired solution. Alternately, these equations can also be linearized by neglecting the non-linear convective terms, giving an equation system that can be determined by semi-analytical solutions. This means that the solution to the governing hydrodynamic fields (obtained from the NS equations) coupled with the integration of the Langevin equation for the particle yields

[***]A concise history of the conceptual foundations of fluid mechanics from the time of Newton's Principia in 1687 up to the definitive work of Stokes in 1845, can be found in [125]

[‡‡]The operators are given as:

$$\boldsymbol{\nabla} = \left(\frac{\partial}{\partial x}, \frac{\partial}{\partial y}, \frac{\partial}{\partial z} \right), \boldsymbol{\nabla}^2 = \left(\frac{\partial^2}{\partial x^2} + \frac{\partial^2}{\partial y^2} + \frac{\partial^2}{\partial z^2} \right)$$

a reasonable description of Brownian behavior. Note that within the context of this thesis, the former CFD based approaches are grouped under multiphase direct numerical simulation or DNS methods while the latter are grouped as analytical methods. These are described below.

Analytical methods

Analytical approximations of the NS equations, obtained by linearizing Eq. (4.1) or neglecting the non-linear convective terms when $Re_p \ll 1$ (meaning the particle is diffusing in a quiescent fluid) is given as:

$$\begin{aligned} \boldsymbol{\nabla} \cdot \boldsymbol{v} &= 0, \\ \rho_f \frac{\partial}{\partial t} \boldsymbol{v} &= -\boldsymbol{\nabla} P + \mu_f \boldsymbol{\nabla}^2 \boldsymbol{v}, \end{aligned} \tag{4.2}$$

are used to estimate the hydrodynamic resistance γ_{St} used in the Langevin Eq. (3.6). A variety of methods have been reported in literature to solve the linearized (unsteady) Stokes' Eq. (4.2), as listed in the classical books by Happel and Brenner [85] and Kim and Karilla [86]. Among these, the method of reflections pioneered by Smoluchowski [25] and later extensively used by Brenner [78] has been popular in solving the steady Stokes' equations (i.e. without the time derivatives in Eq. (4.2)). This technique has since been extended to Brownian motion by Ermak and McCammon [126] through the Brownian dynamics (BD) approach. The BD approach was further extended towards a colloidal system of N-particles in a viscous, incompressible fluid under creeping flow conditions by Brady and Bossis [127] through the Stokesian dynamics (SD) approach. Despite being successful at simulating the rheology of spherical particles in a suspension, both BD and SD neglect unsteady particle inertia to accommodate for computational efficiency, thus, limiting their applicability to only particle-fluid systems at high density ratios.

In most real systems of interest, the net force on the particle from the fluid includes both reactive (e.g. added mass or Basset history forces) and resistive (e.g. viscous dissipation) components. These can be included by solving the unsteady Stokes' equation for the fluid given in Eq. (4.2). Consequently, the method of reflections for steady Stokes' flows was extended by Ardekani and Rangel [128] and later by Simha et al. [129] to account for these unsteady effects within the mobility estimates. Felderhof [130, 131] further simplified this problem using a point-particle approximation to determine the dynamics of sufficiently small spherical particles (i.e. approximating the spherical particle by a point force, reducing this to a Green's function problem). All these approaches may not be analytically tractable in a closed-form without approximations (despite the linearity) particularly in situations with reduced symmetry. Moreover, the solution procedure gets progressively elaborate (in a mathematical sense) when describing asymmetrical particles (such as nanofibers, nanorods, nanosheets, nanowires or nanotubes) and/or channels such

as an arbitrary pore. This is due to the direct dependence of the morphology (including shape, size and structure/composition) of the particle on its corresponding hydrodynamic interaction [85, 86]. Note that detailed descriptions of these aforementioned analytical methods are beyond the scope of this thesis. For a broader perspective on these methods, the reader is referred to the classical books by Happel and Brenner [85] and Kim and Karilla [86]. Additionally, papers on the subject by Felderhof [130], Simha et al. [129], Mo and Raizen [44] and Brady and Bossis [127], are also a relevant resource.

Multiphase direct numerical simulation (DNS)

The NS equations can also be solved numerically using computational fluid dynamics (CFD). This solution procedure discretizes the equation system both temporally and spatially in the domain of interest. The chosen discretization reduces the partial differential equations into a linear algebraic equation system that can be solved directly using efficient sparse-matrix solvers. In this thesis, a finite volume discretization is used to solve the NS equations [132]. Moreover, this solution is coupled to the Brownian description of the particle through the Langevin equation. Such a method that can simultaneously account for both the particle dynamics via a solution to the particle transport equation and the fluid hydrodynamics via a solution to the governing fluid equations (using CFD), along with the accompanying interactions is referred to as a multiphase CFD technique. Note that in this method the fluid and the particle are treated individually and the coupling is achieved through both the hydrodynamic drag and the fluctuation-dissipation relation in the Langevin description (see Appendix 7.1).

Within the context of multiphase CFD, direct numerical simulations (or DNS) refers to a class of methods that directly solve the coupled equation system describing the various phases [133]. Thus any macro-scale description of Brownian motion can inherently be considered a multiphase DNS method when, the Brownian particle and the surrounding fluid are accounted-for individually. Moreover, the two phases under consideration can be coupled with each other to varying degrees. These are given as 2-way and 4-way coupling, respectively. The 2-way coupled system represents both particle-fluid and fluid-particle coupling, implying that each phase is affected by the presence of the other. While, a 4-way coupled system is a 2-way coupled system with additional interaction between the constituent particulate phase entities (i.e. particle-particle interactions such as collisions) also included. The continuum based methods discussed in this thesis are 2-way coupled since we deal with single or (at the most) pairwise hydrodynamic behavior. It follows that, the two phases can be adequately represented as an Eulerian-Lagrangian combination. Consequently, in this thesis, the fluid is solved as an Eulerian field (using CFD) and the particle Langevin equation is solved in the Lagrangian frame of reference. This Lagrangian representation (or inertial frame of reference) is further classified as point-force (or point-particle) or surface-resolved treatments [133], based on how the particulate phase is resolved (see Fig. 4.2).

As the name suggests, the point-force approach (shown in the left panel of Fig. 4.2)

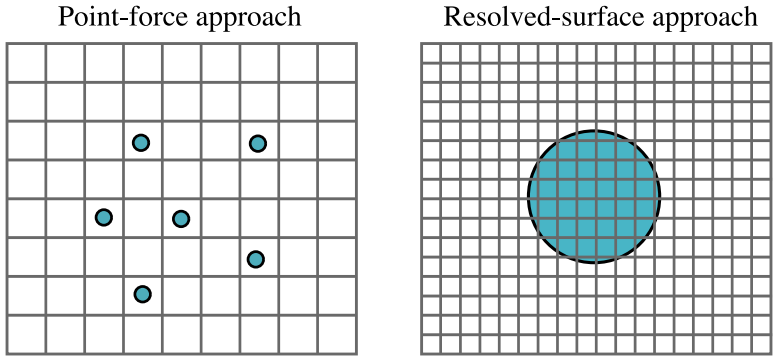

Figure 4.2: *Different types of Lagrangian representations where the shaded area represents the particle (with effective diameter d_p) and the grid represents the spatial resolution for the continuous phase solution (where Δx is the effective cell resolution): Left panel – point-force representation ($d_p < \Delta x$). Right panel – Resolved surface representation ($\Delta x \ll d_p$). This figure is adapted from Michaelides et al. [133].*

includes the Lagrangian particulate phase as point masses (or sources) i.e. the particles have negligible volume but a finite mass or inertia and move at their own (independent) velocity. Usually, this approach is referred to as a pseudo-DNS method, since the relevant hydrodynamic forces on the particle are modeled (and not resolved). Despite this, since the solution from the NS equations governing the fluid at the point where the particle is located is used in the hydrodynamic models, it is an improvement over the analytical methods listed earlier. The point-particle assumption is central to this Lagrangian representation with an ordinary differential equation (ODE) based on the changing particle position. Such an equation, which was provided by Maxey and Riley [134], also includes unsteady fluid effects such as the added mass (due to fluid acceleration caused by the particle acceleration) and Basset history forces (due to acceleration between the phases and the development of a boundary layer near the interfacial surface) [135]. The corresponding equation of motion for a Brownian particle is given as:

$$m_p \frac{\mathrm{d}\mathbf{u_p}}{\mathrm{d}t} = -\gamma \mathbf{v_{rel}} + F_{am} + F_{history} + \chi(t), \tag{4.3}$$

where, F_{am} and $F_{history}$ represent the added mass and Basset history forces, written as:

$$F_{\mathrm{am}} = -\frac{1}{2}\rho_f V_p \left(\frac{d\mathbf{u_p}}{dt} - \frac{D\mathbf{v_{rel}}}{Dt} \right), \tag{4.4}$$

$$F_{\mathrm{history}} = -\frac{3}{2} d_p^2 \sqrt{(\pi \rho_f \mu)} \int_0^t \frac{\frac{d\mathbf{v_{rel}}}{d\tau}}{\sqrt{t-\tau}} d\tau, \tag{4.5}$$

with, $\mathbf{v_{rel}}$ as the relative velocity between the particle and the fluid (at the location of the particle) i.e. $\mathbf{u_p} - \mathbf{v}$, τ as the time period for the integration and the material

derivative as $\frac{D}{Dt} \equiv \frac{\partial}{\partial t} + u_j \frac{\partial}{\partial x_j}$. This Eq. (4.3) is integrated over the duration of the simulation (i.e. t). Consequently, in this approach, the hydrodynamic interactions with the fluid are modeled as point forces (i.e. for e.g. the steady state Stokes' drag is used to describe the particle-fluid coupling). Thus, for this to work, these point-particles have to be sufficiently smaller than the spatial discretization or resolution (Δx) of the surrounding fluid ($d_p < \Delta x$). Note that the flow between the particles and the particle and flow boundaries is actually resolved and is further used within the particle equation of motion. Consequently, this approach has been widely used to study Brownian transport (including their turbulent dispersion) in a gas, as first shown by Ounis and Ahmadi [51, 52]. Despite being a popular method, these point-force based methods inherently fail when the particles have a definite volume (i.e. the point-particle assumption is not valid), as is the case during pore diffusion wherein the particles occupy a significant portion of the flow domain. Correspondingly, the applicability of these point-force methods is limited to studying dilute particulate flows in channels where the particles are significantly smaller than the characteristic channel dimension.

Thus, due to the inherent limitations of the point-force treatment, the resolved surface approach (shown in the right panel of Fig. 4.2) is the preferred choice in this thesis (since we deal with particles that are significant when compared with a relevant system length scale). In this approach, the detailed flow around each particle must be solved to a high degree of resolution. This permits the flow solution to be numerically integrated over the particle surface in order to obtain the net momentum exchange with the surrounding fluid [133]. Thus, the Lagrangian method updates the particle position based on this integrated interaction. If particle rotation is permitted, a torque equation can be used to determine its angular velocity. Consequently, the resolved surface approach has found increasing incidence in some of the most recent studies on Brownian hydrodynamics, overcoming some of the major drawbacks of the point-forcing approach. Note that in this approach, the spatial grid resolution Δx, in the vicinity of the particle, must be fine enough to allow for a detailed resolution of the fluid stresses around it ($\Delta x \ll d_p$). Thus, the resolved-surface approach is computationally intensive, such that simulation of many (e.g. hundreds or thousands of) particles will generally be impractical on even the most advanced computers [133].

It is reiterated that the continuum based multiphase DNS frameworks available do not contain the relevant molecular details (thermal fluctuations), as these have been averaged out during the derivation of the NS equations (Eq. (4.1)). Thus, when these methods are used in Brownian hydrodynamics simulations, the corresponding micro-scale effects have to be consistently incorporated within the continuum description of the system. Traditionally, this can be accomplished by either adding the relevant fluctuations to the fluid phase or on the Brownian particle (as in the Langevin description). While the Gaussian forcing of the particle has been well explored, since the original assessments of Langevin [26], the stochastic forcing of the fluid or the fluctuating hydrodynamics approach is a relatively newer idea. This is described in brief below.

Fluctuating hydrodynamics

The fundamental concept behind this approach is that at intermediate length and time scales between the molecular and the hydrodynamic levels of abstraction, thermally induced fluctuations can be reduced to random fluctuations in the fluxes of the conserved variables, i.e. the momentum, heat and mass fluxes. Correspondingly, the fluctuations are included only within the deterministic fluid description, thereby ensuring that the microscopic conservation laws and thermodynamic principles are obeyed, while also maintaining the fluctuation-dissipation balance. These constitute a group of methods referred to as the fluctuating hydrodynamics (*FH*) approach of Landau and Lifshitz [118] which is derived using the fluctuation-dissipation theorem of statistical mechanics applicable at mesoscopic scales [136, 137]. Correspondingly, the Landau and Lifshitz Navier-Stokes (LLNS) equations is given as:

$$\begin{aligned} \nabla \cdot \mathbf{v} &= 0, \\ \rho_f \left(\mathbf{v}_t + (\mathbf{v} \cdot \nabla)\mathbf{v}\right) &= \nabla \cdot \sigma, \\ \sigma &= -P\delta_{\mathbf{ij}} + \mu \left[\nabla \mathbf{v} + (\nabla \mathbf{v})^T\right] + R_f, \end{aligned} \tag{4.6}$$

where, $\delta_{\mathbf{ij}}$ is the identity tensor and R_f is the random fluctuations in the total fluid stress tensor σ, respectively. These non-equilibrium fluctuations, which are captured through the random stresses (stochastic momentum flux), are modeled as:

$$R_f = \sqrt{\mu_f k_B T}[\upsilon(r,t) + \upsilon(r,t)^T]. \tag{4.7}$$

Here, $\upsilon(r,t)$ is a standard Gaussian white noise tensor field with uncorrelated components, that is δ-correlated ¶¶¶ in space and time. The particle motion is solved using Newton's equation of motion (velocity u_p is directly estimated from the hydrodynamic force on the particle). Note that the LLNS equations are stochastic partial differential equations that reduce to the NS equations (Eq. (4.1)) in the limit of large volumes. The validity of the LLNS equations (see eq. (4.6)) for non-equilibrium systems has been extensively assessed by Espanol et al. [138] and verified using molecular dynamics simulations by Mansour et al. [139]. Further, the LLNS based methods have been used predominantly in liquid-solid systems, wherein the breakdown of continuity (i.e. the traditional NS equations) occurs at considerably smaller scales [140]. Hence, this approach has successfully been incorporated in several numerical methods that describe Brownian dynamics in dilute fluids and in modeling reactive multi-species fluid mixtures [141–145]. These numerical simulations have been carried out either using the finite volume method [142, 143, 146–148], finite difference method [149], finite element method [150] or the immersed boundary method [151–154] (an alternate approach to solving the NS equations). All these techniques represent a surface-resolved approach to solving Brownian diffusion using *FH*. A detailed insight into these *FH* based methods is beyond the scope of this thesis and the reader is

¶¶¶ $\langle \upsilon(r,t)\upsilon(r,\tau)\rangle = \delta(t-\tau)$. Thus, $\upsilon(r,t)$ is correlated with itself only when $t = \tau$.

referred to the papers by Donev et al. [143, 144] , Uma et al. [142], Atzberger et al. [151, 152], Balboa et al. [153] and to the reviews by Radhakrishnan et al. [43] and Griffith and Patankar [148] for the same.

Although the fluctuating hydrodynamic approach has found utility in Brownian particle dynamics studies, there are still some bottlenecks associated with its implementation in general finite volume or finite element based DNS frameworks. The main difficulty is in devising a discretization scheme for the stochastic differential equations primarily because of the correlation between the form of the required fluctuation-dissipation relations and the choice of scheme [121]. Further, finite-volume discretizations naturally impose a grid-scale regularization (smoothing) of the stochastic forcing. Moreover, the non-linear LLNS equations are ill-behaved stochastic partial differential equations that are challenging to integrate [155]. This is because, the stability properties of the available numerical schemes for the nonlinear LLNS system are not well understood and the whole notion of stability is different from those in regular deterministic schemes [144]. Finally, and most crucially, employing the LLNS equations to describe gas-solid flows is still heavily debated particularly due to the higher Kn encountered in these systems.

Since the overarching objective of this thesis is to develop a general numerical method (for Brownian transport) which is applicable in both liquids and gases, the FH based methods are not preferable. Consequently, an alternate approach is proposed where the particle motion is modeled using a stochastic differential equation (in the spirit of the Langevin Eq. (3.6)) while employing the resolved-surface Lagrangian treatment, thereby leaving the fluid equations unaltered. This idea is described in detail in the subsequent sections (see Section 4.3). However, prior to this discussion, some desirable features of such a framework are first listed in order to establish the minimum requirements for the ensuing numerical development.

4.2 Desired features of a DNS framework

The brief overview of the current state-of-the-art in the numerical modeling of Brownian systems identified a noticeable requirement for a general method that can easily be implemented within the confines of a multiphase DNS framework at a reasonable computational load. It is possible to envisage a DNS scheme where the NS equations for the fluid are solved coupled with the Langevin equation (which includes a random forcing term) for particle motion. Since the flow around the Brownian particle is fully resolved, hydrodynamic interactions mediated by the fluid (such as particle-particle or particle-wall effects) are inherently accounted for in such a description. The only noticeable challenge is to consistently account for the random forcing of the particle. Moreover, since the continuum formulation of the fluid is untouched in this approach, existing discretization schemes used in CFD can be applied effectively. The Langevin equation can also be integrated using elementary temporal integration strategies that obey the Itô interpretation [156]. In summary, the development of such a Langevin based resolved-surface

Euler-Lagrangian method seems feasible and is the primary objective of this thesis. Consequently, we can establish some desirable features for such a framework:

1. *General DNS methodology:* applicability is not restricted by the choice of the solver (i.e. can be applied across a variety of resolved-surface DNS frameworks such as the immersed boundary method, arbitrary-Lagrangian-Eulerian technique etc.)
2. *Sound theoretical basis:* the stochastic forcing is consistently incorporated within the validity of the fluctuation-dissipation theorem, so that the statistical behavior is accurately reproduced.
3. *Reasonable computational overhead:* effectively utilize the current generation of advanced sparse matrix GPU solvers to further make simulations tractable.
4. *Capability to handle both gas-particle and liquid-particle systems:* adequately resolve the varying particle diffusion dynamics in liquids and gases.
5. *Capability to handle hindered diffusion:* simulate challenging theoretical problems involving hydrodynamic interactions mediated by the fluid (such as particle-boundary, particle-particle interactions).
6. *Capability to handle asymmetric systems:* simulate non-symmetric particles and/or geometries with ease.

In the remainder of this chapter, the fundamental aspects of the numerical tools used and developed in this thesis are elaborated. First, a detailed account of the novel Langevin based multiphase DNS method developed is presented (used in **Papers A**, **B**, **C** and **D**) followed by a brief account of the utilized DSMC solver (in **Paper E**).

4.3 *Langevin* immersed boundary method (*LaIBM*)

One of the primary objectives of this thesis is to develop a multiphase DNS method that can overcome the limitations of the available continuum based multiphase CFD methods and further extend their applicability towards assessing nanoparticle transport in a fluid. Consequently, as motivated in the earlier sections, an Euler-Lagrange resolved surface approach is chosen as a basis for such a development. Such an approach is also favorable since it is simpler to formulate and easier to implement. However, the available methods need to be extended to also include both non-equilibrium (rarefied) as well as molecular-scale details, in order to accurately represent the Brownian diffusion of a nanoparticle. Hence, an improved multiphase DNS framework that can simultaneously handle particle-fluid and fluid-particle coupling (i.e. at least 2-way coupled) as well as the accompanying Brownian dispersion of the nanoparticle at high solid volume fractions would be ideally suited to describe the nanoparticle dynamics discussed in Chapter 3. Since this method

leverages both the Lagrangian Langevin description and an immersed boundary method, it is henceforth referred to as the Langevin-Immersed boundary method or $LaIBM$. Note that the immersed boundary method solves the Eulerian fluid field using discretizations of the governing NS equations similar to those applied in conventional CFD [132].

In this section, the necessary numerical details of the $LaIBM$ framework are provided within the context of the resolved-surface Euler-Lagrangian multiphase DNS class of methods discussed in Section 4.1.3. Further, a general overview of immersed boundary methods is also provided to establish the needed context.

4.3.1 Immersed boundary methods: A general overview

Immersed boundary methods are a class of numerical techniques employed in the CFD (i.e. numerical solutions to the NS equations Eq. (4.1) using for e.g. finite volume discretization) of complex flow systems that greatly simplify the spatial discretization demands. This method, originally proposed by Peskin [157] to simulate cardiac mechanics and the associated blood flow, solves the governing equations in a Cartesian grid that does not conform with the complex geometries of the simulated system. In essence, the object around which the flow is to be assessed is *immersed* in a standard Cartesian flow grid and its presence is accounted for by slightly modifying the governing NS equations. Note that a surface grid still has to be generated for the immersed body (IB), however, the volume grid on which the actual governing equations are solved for can be generated with no-regard to this surface grid [158] i.e. regular boxy domains can be used over which the IB object (included as an external *.stl* geometry file) is triangulated. The main advantages of such a treatment are as follows:

1. Using a Cartesian grid can significantly reduce the per-grid-point operation count due to the absence of additional terms associated with grid transformations.

2. On a non-body conforming grid, complexity and quality are not significantly affected by the complexity of the geometry.

3. Including body motion in IB methods is relatively simple due to the use of a stationary and non-deforming Cartesian grid.

4. Dynamic refinement around the immersed object is permissible, meaning, the accuracy is increased at a minimal computational overhead.

Incorporating the presence of the IB in the NS equations is the primary challenge in setting up this framework. Usually this modification takes the form of a source term (or forcing function) in the governing equations that reproduces the effect of the boundary. This is usually done in one of the following ways:

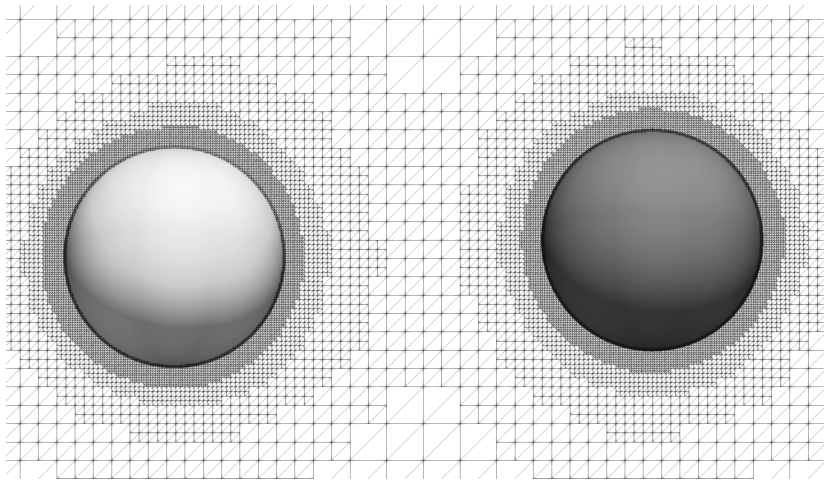

Figure 4.3: *Example of an immersed Cartesian octree grid around a pair of spherical Brownian particles with a diameter of 400 nm each (x-z plane): Note that there is no need for a body conforming mesh as the spheres cut through an adaptive Cartesian octree background grid on which the discretized NS equations are solved.*

1. Continuous forcing: the source term is introduced into the continuous equations (i.e. prior to the discretization) around the vicinity of the IB.
2. Discrete forcing: the source term is only introduced in the discretized equations around the vicinity of the IB (typically within the IB).
3. Implicit forcing: there is no source term introduced into the equations. Instead, a boundary condition is used to constrain the velocity at the IB surface so that the correct behavior is reproduced.

The continuous forcing approach is very attractive for flows with immersed elastic boundaries and was originally envisioned by Peskin for the coupled simulation of blood flow and muscle contraction [157]. In this method, the IB is represented as a set of elastic springs whose locations are tracked in a Lagrangian framework by a collection of mass-less points that move with the local fluid velocity. The effect of the IB on the surrounding fluid is essentially captured by transmitting the elastic stress (calculated using Hooke's law) to the fluid through a localized forcing term in the momentum equations [158]. This forcing is, however, distributed over a band of cells around each Lagrangian point (based on the discrete Dirac delta function). Consequently, this approach poses challenges for rigid bodies as the forcing terms are not easy to implement at the rigid limit. Moreover, due to the smoothing of the forcing term, a sharp representation of the IB is not available. Consequently, this method is explicit, first-order accurate and unstable.

Hence, for dealing with sharply defined rigid bodies (as we do in this thesis), a better forcing alternative is desired. This can be fulfilled by employing a discrete (or non-

distributive) direct forcing approach that adds the requisite source terms in the vicinity of the IB. Despite being second order accurate, this approach is only explicitly formulated and can be unstable for unsteady flows. Alternately, the implicit forcing approach can also be used to treat bodies with sharply defined edges. In this method, the velocity at the IB is constrained by an implicitly formulated immersed boundary condition (IBC) that is second-order accurate. This unique and stable treatment is central to the efficiency and accuracy of the multiphase DNS framework used in the thesis and is elaborated in the following section.

4.3.2 Immersed Boundary Octree Flow Solver: IPS IBOFlow®

In this thesis, we use the multiphase flow solver `IPS IBOFlow®`, developed by the Fraunhoffer-Chalmers Research Centre (FCC), Sweden [159]. This solver employs a unique mirroring immersed boundary method (MIBM) to efficiently handle the particle-fluid coupling (resolved-surface DNS). The MIBM discretizes the NS equations over a Cartesian octree grid[¶¶¶] that can be dynamically coarsened and refined. Further, it is coupled with a finite-element (FEM) rigid body solver to resolve the particle short range dynamics (i.e. handle the particle motion in a Lagrangian basis). This coupling between the Eulerian and Lagrangian descriptions is elucidated in Fig 4.4. Details on these two core-components of the solver are further presented below beginning with the MIBM used.

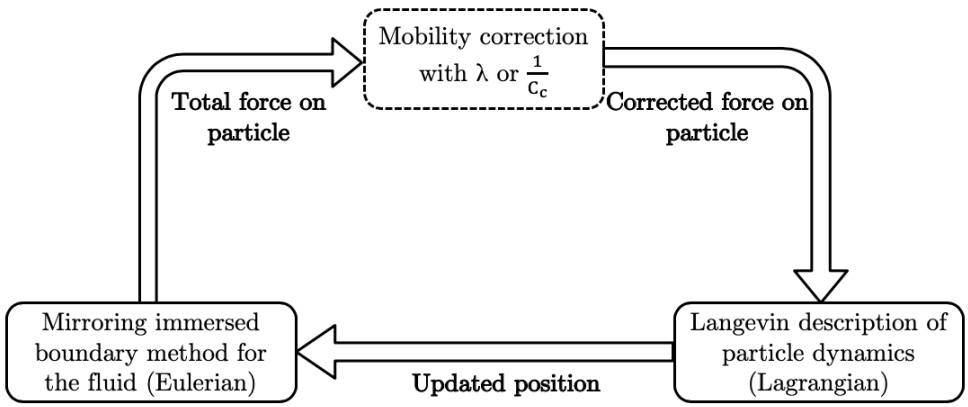

Figure 4.4: *Overview of the LaIBM framework: the particle dynamics are handled in a Lagrangian basis while the surrounding fluid is resolved in an Eulerian one. Note that the Lagrangian basis utilizes the resolved fluid stresses on the particle (from the Eulerian solution) to compute/correct the particle mobility. This framework is 2-way coupled. This figure is adapted from* ***Paper C*** *[3].*

[¶¶¶]This is a recursive decomposition of the spatial domain into blocks (not necessarily rectangular) in which each internal node has exactly eight children. Octrees are most often used to partition a three-dimensional space by recursively subdividing them it into eight octants.

Eulerian description of the fluid: mirroring immersed boundary method

The governing equations for the flow around the immersed boundaries are given by the continuity and momentum equations for incompressible flows i.e. the NS equations (see Eq. (4.1)). This set of equations are solved together with the implicit Dirichlet IB condition:

$$u_i = u_i^{ib}, \tag{4.8}$$

which sets the velocity of the fluid to the local IB velocity. In MIBM, the velocity is set by an implicitly formulated second-order accurate immersed boundary condition. In this method, the interior cells and the cells close to the surface are identified as shown in Fig. 4.5.

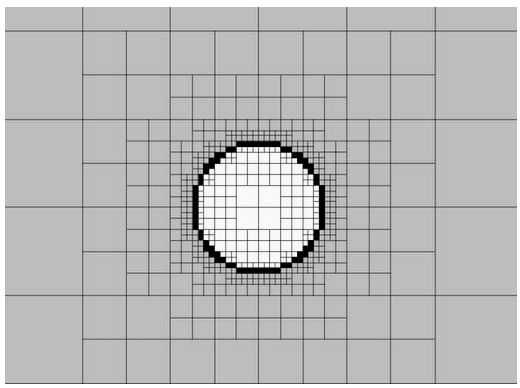

Figure 4.5: *2D view of the adaptive dynamic grid refinement around an immersed spherical particle (with diameter 400 nm). Cell types shown are exterior (grey), interior (white) and mirror or IB cells (black). This figure is adapted from* ***Paper A*** *[1].*

For the mirroring cells that lie close to the surface, their centers (mi) are geometrically mirrored over the local IB to the exterior points (e) as:

$$u_i^{ib} = \frac{u_{mi} + u_e}{2}. \tag{4.9}$$

By mirroring the velocity field over the IB second order accuracy is achieved. Typically, the exterior points do not coincide with a grid point, hence, implicit tri-linear interpolation is adopted to accomplish this. When the velocity is mirrored over the IB, a fictitious (velocity) field is generated within it. To fulfill the continuity equation, this field needs to be replaced by the IB velocity in all flux calculations (note that the velocity within the IB is not used). A more detailed description of this method is available in [160–162].

It should be noted that in the current method the total force acting on the IB is given by the surface integral of the total stress tensor over the IB as:

$$\mathbf{F^i_{IB}} = \int_{IB} \boldsymbol{\sigma} \cdot \mathbf{n} dS = \int_{IB} (-P\delta_{ij} + \tau) \cdot \mathbf{n} dS = \int_{IB} \left(-P\delta_{ij} + \mu_f \boldsymbol{\nabla}^2 \boldsymbol{v}\right) \cdot \mathbf{n} dS, \quad (4.10)$$

where, δ_{ij} is the Dirac delta and σ is the total fluid stress tensor with $P\delta_{ij}$ and τ as the pressure and viscous contributions for a surface S with normal $\boldsymbol{n}$, respectively. The index i represents the degrees of freedom for the IB in a Cartesian basis. The corresponding torque on the IB with a position vector $\mathbf{r}$ is calculated using:

$$\mathbf{T_{IB}} = \int_{IB} \mathbf{r} \times \boldsymbol{\sigma} \cdot \mathbf{n} dS. \quad (4.11)$$

The pressure-velocity coupling in Eq. (4.1) is handled using the segregated SIMPLEC method, [163] which first approximates the momentum equation with an estimated pressure field and then corrects the pressure by employing the continuity equation. All variables are stored in a co-located grid arrangement (meaning the variables such as pressure, velocity etc. are stored at the cell centers). Further, the Rhie-Chow [164] flux interpolation is used to suppress pressure oscillations. A partitioned approach is employed to solve the coupled problem. Correspondingly, the grid and assembly are fully parallelized on the CPU and the resulting large sparse-matrices are solved on the GPU with Algebraic Multi-Grid solvers (AmgX) [165]. The IB method described above has been extensively validated and used for the DNS of complex multiphase flow phenomena [162, 166–172]. More recently, it has also been extended towards non-Newtonian flows as well [173, 174].

Lagrangian Langevin description of the particle

The particulate phase in the $LaIBM$ framework is governed by the Lagrangian Langevin equation of motion (see Eq. (3.6)). This equation balances the macro-scale hydrodynamic drag on the particle with the molecular-scale Brownian fluctuations. For the diffusion of a particle (represented by an IB) with mass m_p, translational velocity $\mathbf{u^i_p}$, angular velocity $\boldsymbol{\omega^i_p}$ and moment of inertia $\boldsymbol{I}$, the corresponding Lagrangian Langevin basis is rewritten as:

$$m_p \frac{\mathrm{d}\mathbf{u^i_p}}{\mathrm{d}t} = \mathbf{F^i_{IB}} + \mathbf{F^i_{Brownian}}, \quad (4.12)$$

$$\mathbf{I} \frac{\mathrm{d}\omega^\mathbf{i}_\mathbf{p}}{\mathrm{d}t} = \mathbf{T^i_{IB}} - \boldsymbol{\omega^i_p} \times \mathbf{J} \cdot \boldsymbol{\omega^i_p}. \quad (4.13)$$

In Eqs. (4.12) and (4.13), note that the continuum resolved translational ($\mathbf{F^i_{IB}}$) and rotational ($\mathbf{T^i_{IB}}$) hydrodynamic fields are directly used in the Langevin equation, thus, enforcing a direct coupling of the Eulerian solution with the corresponding Langevin equation of motion (resolved-surface DNS). Thus, these Eqs. (4.12) and (4.13) are modeled as an LTI system as established in Section 3.2.2. Note that the hindered diffusion of the Brownian nanoparticle is included through the correction factors to the particle mobility used in the stochastic forcing term $\mathbf{F^i_{Brownian}}$ (synonymous with $\chi(t)$ used in Eq. (3.6)) i.e. either λ or $1/C_c$ based on if hindered diffusion or rarefied hydrodynamics are being evaluated, respectively. The essential descriptors of this representation in terms of the mobility correction λ (i.e. in a liquid) are given below.

The directional reduction in mobility, λ^i, which is required in the stochastic forcing term used in $\mathbf{F^i_{Brownian}}$, is estimated by normalizing the magnitude of the hydrodynamic force on the confined Brownian particle ($\mathbf{F^i_{IB}}$) with the corresponding Stokes' drag (along the i^{th} direction) on the same particle. This is given as:

$$\lambda^i = \frac{\mathbf{F^i_{IB}}}{\gamma_{St}\mathbf{u^i_p}}. \tag{4.14}$$

Here, the Stokes' friction factor γ_{St} has the form as defined in Eq. (3.3) and a representative particle time scale , τ_p, is given as:

$$\tau_p = \frac{m_p}{\gamma_{St}\|\lambda^i\|} \tag{4.15}$$

The force $\mathbf{F^i_{Brownian}}$, which represents the Brownian fluctuations in the particle motion, is modeled as a Gaussian white noise process (an LTI system as described in Section 3.2.3) as given by:

$$\mathbf{F^i_{Brownian}(t)} = m_p\mathbf{G}\sqrt{\frac{\pi\mathbf{S^i_{uu}}}{\Delta t}}. \tag{4.16}$$

Here, $\mathbf{G}$ is a vector of normally distributed independent random numbers of zero mean and unit variance (Gaussian distribution) and Δt is the time step length during which the Brownian force is active. The vector of spectral intensity $\mathbf{S^i_{uu}}$ (as given in Eq. (3.12)), is a function of the directional Brownian diffusivity D^i, which is in-turn given by the Stokes-Einstein relation with the corrected mobilities as:

$$D^i = \frac{D_\infty}{\lambda^i} = \frac{k_B T}{\gamma_{St}\lambda^i}, \tag{4.17}$$

where, D_∞ (or bulk diffusivity) is given by Eq. (3.2) with a further reduction by λ^i

(in accordance with [175–177]) to account for confinement effects. Note that unbounded Brownian diffusion is simulated by setting λ as unity. Moreover, a rarefied gas-solid system is modeled by using $1/C_c$ (as given in Eq. (3.17)) in place of λ.

These linear and angular momentum conservation equations (Eqs. (4.12) and (4.13)) are integrated using the Newmark time-marching scheme [178]. In this method, acceleration, velocity and displacement at time $t = t^{n+1}$ are obtained as functions of the values at $t = t^n$ by assuming a linear acceleration during that small time step. This one-step semi-implicit method can be represented by the following set of equations:

$$\dot{u_p}^{n+1} = \dot{u_p}^{n} + \frac{\Delta t}{2}\left(\ddot{u_p}^{n} + \ddot{u_p}^{n+1}\right) \tag{4.18}$$

$$u_p^{n+1} = u_p^n + \Delta t \dot{u_p}^{n} + \frac{1-2\kappa}{2}\Delta t^2 \ddot{u_p}^{n} + \kappa \Delta t^2 \ddot{u_p}^{n+1} \tag{4.19}$$

The scheme is unconditionally stable with κ as a tuning parameter that has a default value of 0.25 (the constant average acceleration method) [178]. It is stressed that this solution (or solution process) to Eq. (4.12), a stochastic differential equation (SDE), is not synonymous with the commonly encountered ordinary differential equations (ODE's). The integration of these SDE's are constrained by certain properties of the stochastic time integral as first defined by Itô [156]. To understand these constraints let us split the integral time interval into a number of small time steps which are then summed to give the final solution. This limit result is not independent of the choice of the intermediate time interval, which is used while splitting the solution into smaller time steps, as one would expect from classical Riemann integration laws [179][§§§]. This is because the solution would change depending on the time point at which the integration is started, as these are random time evolving systems (the trajectories have infinite variation). Hence, it is very important to decide on the sense (or form) of the integral which should be solved. The Itô sense, which has a clear probabilistic interpretation and is most often used to describe Brownian processes, assumes that the integral is solved from the beginning of the time interval. This interpretation is most convenient for numerical simulations because the increment of the stochastic process is uncorrelated with the variables at the same time. This would mean that, forward stepping explicit schemes are preferred while solving SDE's in an Itô sense. More generally, higher order schemes (such as higher order Runge-Kutta schemes) can introduce spurious drifts in the solution and should be avoided [180].

[§§§]A bounded function $f : [a, b] \to \mathbb{R}$, is said to be Riemann integrable over $[a, b]$ if there is a number $A \in \mathbb{R}$, such that for every $\varepsilon > 0$, there is a $\delta > 0$; implying that any partition $P = \{a = x_0 < x_1 < ... < x_n = b\}$ of the interval $[a, b]$, with lengths $|x_i - x_{i-1}| < \delta$ for all $i = 1, ..., n$. Further, if there exists $t_i \in [x_{i-1}, x_i]$, then:

$$\left| \sum_{i=1}^{n} f(t_i)(x_i - x_{i-1}) - A \right| < \varepsilon \implies \int_R^b f(x)dx = A$$

4.3.3 Some unique capabilities of *LaIBM*

LaIBM is developed with the ambition of satisfying the requirements listed in Section 4.2. Thus, this framework has some unique features which are derived from the existing capabilities of the resolved-surface multiphase DNS method (described in Section 4.3.2). These are:

1. *Contains the resolved hydrodynamics around the Brownian particle:* the framework leverages a resolved solution of the hydrodynamics around the Brownian particle to estimate the relevant reduction in mobility λ.

2. *Mobility estimation on-the-fly:* closely coupled with the previous point, since the resolved hydrodynamics are used to compute mobility, the instantaneous hydrodynamic fields around the particle are directly reflected in the estimated diffusive behavior.

3. *Multi-particle dynamics:* diffusion of several particles and the accompanying hydrodynamic interactions mediated by the fluid can be assessed simultaneously (each particle's motion is individually solved for and the accompanying inter-particle hydrodynamic interactions are included in the respective λ's).

4. *Not limited by symmetry considerations:* the framework is derived for any shape or form (singular or aggregates) of the particle and the accompanying domain (straight or arbitrary tortuous channels) and is, hence, not limited by the availability of uniform solutions to the hydrodynamic resistances nor symmetry considerations, such as other methods reported in literature [68, 104, 130, 175].

4.3.4 Some limitations of the framework

As with any method development, the over-arching objectives are made realizable (primarily to demonstrate a proof-of-concept) for the derived DNS method, by simplifying the system under investigation. The corresponding assumptions that currently limit the developed framework are:

1. *Validity of the Langevin equation:* the early iterations of this new DNS method are derived based on the fundamental assumption that the steady Langevin equation (i.e. Eq. (3.6)) is valid. This means that the framework is limited to handling high particle-fluid density ratios (where unsteady effects such as history and added mass forces are negligible). The main issue with handling lower density ratios is that the unsteady effects would be included in F_{IB} and T_{IB}, but not in the Brownian forcing modeled using Eq. (4.16). Hence, the stochastic forcing term would have to be re-derived.

2. *Gaussian white noise assumption:* closely coupled with the previous point, the Brownian fluctuations are assumed to be a Gaussian white noise that is delta correlated in time (i.e. Markovian in nature). This means that the VACF of the Brownian particle decays exponentially (as given in Eq. (3.11)), whereas in real liquids it is shown to have a long time tail [33, 34, 181]. This is attributed to the unsteady hydrodynamic effects on the particle (fluid inertia mediated).

3. *Negligible fluid inertia:* although, the framework can inherently handle the convective fields in the fluid, the numerical studies chosen in this thesis mimic low Reynolds number hydrodynamics i.e. primarily creeping flows ($Re_p \ll 1$), where the fluid inertia is negligible, are simulated. This choice is made to maintain the validity of the steady Langevin Eq. (3.6) and the analytical bases discussed in Chapter 3.

4. *Rarefaction effects are modeled and not resolved:* gas-particle systems modeled in this DNS framework are limited by the first-order Cunningham correction, which is based on a theoretical ansatz that is not necessarily always valid. Nevertheless, the corresponding parameters (in the expression for C_c) are fitted to experimental data and the agreement is good for all Kn. Thus, the non-continuum diffusion dynamics are being modeled and not resolved.

5. *Numerical instabilities in the IBM:* the inherent length and time scales in the Brownian transport problem (of a nanoparticle) are very close to the machine precision of most modern computing platforms, meaning, these problems push existing sparse matrix solvers to the limit. Thus, a scaling up of the problem (using the Reynolds and Schmidt number's) is needed in the current iteration of the DNS method to circumvent these issues without a loss of generality.

4.4 Direct simulation Monte-Carlo

The direct simulation Monte-Carlo (DSMC), developed by Bird [88, 107, 182], is a stochastic particle-based technique for modeling dilute real gases in which the molecular diameter is much smaller than the mean free path (λ_g). This method leverages three physical characteristics of a dilute gas:

1. Molecules move in free flight without interaction at time scales in the order of the local mean collision time.

2. The impact parameters and initial orientation of colliding molecules are random.

3. There are an enormous number of molecules per cubic mean free path and only a small fraction need be simulated to obtain an accurate molecular description of the flow.

These three assumptions are highly accurate for dilute gases and combined they enable the DSMC method to simulate macroscopic non-equilibrium flows [183]. It is reiterated that the defining characteristic of a non-equilibrium flow is the local departure (within a volume) from the Maxwell-Boltzmann equilibrium distribution functions for molecular velocity and internal energy. The continuum based methods (including the multiphase CFD techniques developed in this thesis) inherently assume only small departures from this equilibrium distribution, while the DSMC method is able to predict the distribution functions (within each small gas volume) with no such assumptions or restrictions on the shape of the distribution.

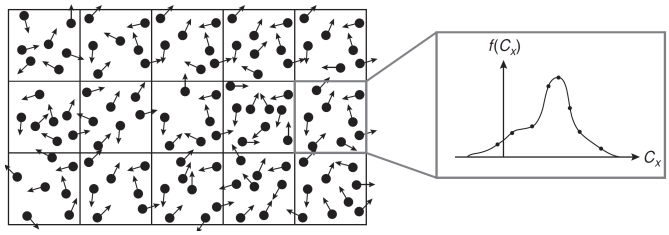

Figure 4.6: *Schematic of a DSMC simulation domain with simulator particles that represent a large number of identical real molecules within discretized collision cells. An example of a sampled distribution function from a single DSMC cell is also shown. This figure is adapted from Boyd and Schwartzentruber [183].*

The primary objective of the DSMC method is to decouple molecular motion (modeled deterministically) and inter-molecular collision (modeled probabilistically) over small time intervals. The time interval over which the solution is sought is subdivided into smaller sub-intervals over which the particle motion and collisions are decoupled. Consequently, the trajectories are computed over a time interval which is lesser than the mean collision time in discretized collision cells (see Fig. 4.6). Further, DSMC relies on discrete parcels, which each contain a collection of molecules, to represent the total molecular number density (N) of the real gas. This enables collisions between pairs of simulated particles to be modeled with precisely the same physical considerations as collisions between pairs of real molecules. Consequently, the deterministic nature of molecular movement and collisions (as simulated with MD, for example) is lost. A DSMC simulation cannot determine precisely which real molecules actually collide and what impact parameters characterize the initial conditions of such collisions. This loss of determinism is also a result of moving simulated particles in straight lines for a fraction of their mean collision time. In effect, although the distribution functions are accurately resolved at spatial and temporal scales of the mean free path and mean collision time, the precise locations of the real molecules comprising those distributions are no longer known below these scales (positions of simulated particles within a DSMC cell significantly below the mean free path is irrelevant to the method) [183].

In this thesis, the open-source solver *dsmcFoam+* developed by White and co-workers [184–186] is used for carrying out the relevant assessments. This code-base, which is built within the OpenFOAM (or Open-source Field Operation And Manipulation) suite

of libraries [187], is licensed under the GNU general public license with a publicly available software repository [188]. Further, it has been extensively validated against experimental and theoretical data across a wide variety of rarefied flows [184, 186, 189–194]. A brief overview of this solver is provided in Fig. 4.7. For a more comprehensive outlook of this method, the reader is referred to Bird's monograph [182] and to the papers by White et al. [184, 185].

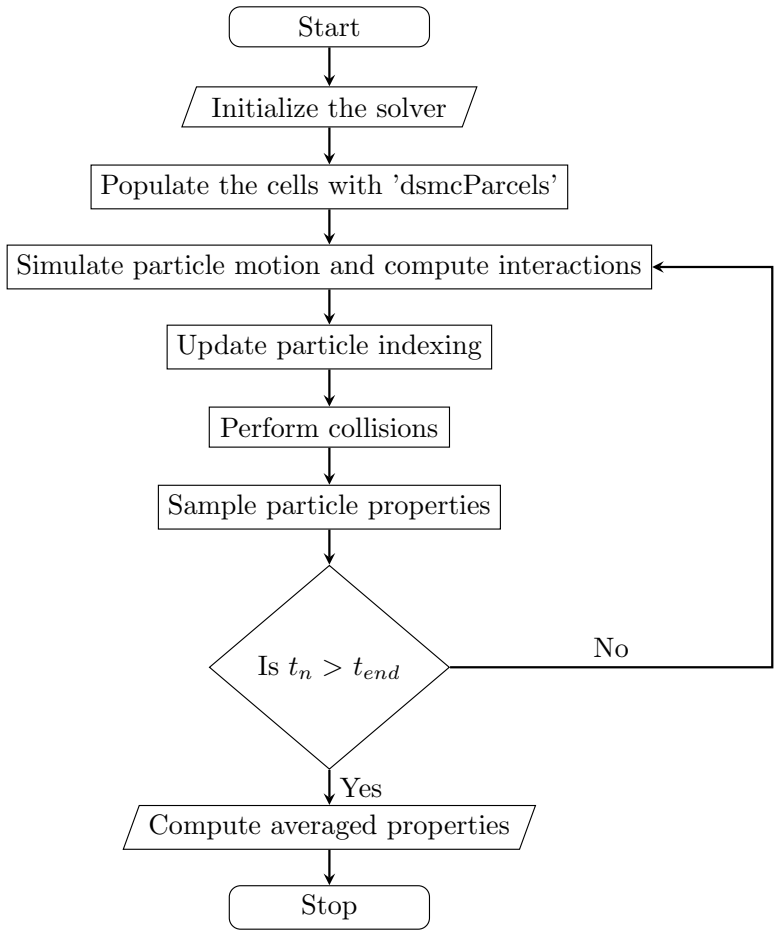

Figure 4.7: *Overview of the dsmcFoam+ solver (adapted from White et al. [185]).*

5

Highlights

Summary of the key scientific contributions and papers

The primary objective of this thesis is to develop an *in-silico* based evaluation strategy for the transport of Brownian nanoparticles in a fluid (a gas or liquid). Correspondingly, these contributions (from this thesis), as reflected in the appended papers, are briefly highlighted in this chapter. These papers represent a chronological development of the original research questions identified in Chapter 2. Correspondingly, in **Paper A** the fundamentals of the novel multiphase DNS method are established by demonstrating that the Langevin description of the Brownian particle can be combined with a resolved-surface DNS of the Eulerian fluid fields around the particle for a gas-particle system. Subsequently, in **Paper B** the developed framework is extended towards liquid-particle systems, particularly to investigate the hindered diffusion of a spherical particle in arbitrary geometries (including micro-channels and pores). Further, in this paper a directional bias (anisotropy) in the hydrodynamic resistances on the particle is identified, with a pronounced co-axial resistance noted when compared with a wall-normal one. This hydrodynamic bias is further examined in **Paper C** by evaluating the off-axis hindered diffusion dynamics (i.e. at a location displaced from the co-axial axis along the center-line) in micro-channels. Next, in **Paper D** the liquid-particle investigations are extended towards pair-wise transport and diffusion near a soft-boundary (formed at the interface of two liquids), thereby demonstrating the capabilities of $LaIBM$ in handling multi-particle dynamics (in the former) as well as complex diffusive behavior (in the latter), which are beyond the scope of the traditional analytical methods (as discussed in Section 4.1.3). Finally, in **Paper E** the gas-particle system is revisited at a molecular level of abstraction using the DSMC method to better understand the non-equilibrium effects around a symmetric particle in a micro-channel. In summary, the main scientific contributions from this thesis (which are summarized in Table 5.1) address some of the challenges encountered while studying the transport of Brownian nanoparticles (such as a nanocarrier or soot particles) under hydrodynamic confinement and further establishes the foundations for an *in-silico* assessment of such complex transport of nanoparticles. The rest of this chapter contains a summary of each appended paper.

Table 5.1: Key scientific contributions in the appended papers.

	Highlights
Paper A	• Derived and validated a multiphase DNS framework for Brownian motion in a gas-particle system. • Extended the DNS method to include non-equilibrium (rarefied) particle dynamics. • Modeled the diffusion dynamics of a fractal shaped soot particle.
Paper B	• Derived and validated the multiphase DNS framework for Brownian motion in a liquid-particle system. • Extracted the reduction in particle mobility, λ, from the resolved hydrodynamic field around the particle (λ estimation on-the-fly), for a Brownian particle under hydrodynamic confinement (wall-bounded diffusion). • Incorporated the resolved instantaneous hydrodynamics around the Brownian particle (without the need for an *a priori* determination of the relevant mobility tensors) into the particle Langevin equation of motion. • Identified anisotropies in the hydrodynamic resistances on the Brownian particle in the wall-normal and co-axial directions. • Modeled the diffusion dynamics in an arbitrary pore.
Paper C	• Established a hydrodynamic basis for off-axis Brownian diffusion in micro-channels (i.e. at a location off-set from the co-axial axis of the channel). • Identified an enhancement in co-axial diffusivity during off-axis hindered diffusion under intermediate confinements.
Paper D	• Extended the applicability of the validated multiphase DNS framework towards multi-particle systems (i.e. pairwise diffusion) and diffusion near a soft-boundary (a 3-phase system). • Demonstrated that the inter-particle interactions (mediated by the fluid) leads to a correlated motion between the pair of particles as a result of being accelerated by each other's wakes. • Demonstrated that particle mobility is enhanced near a soft-boundary due to a significant reduction in the hydrodynamic resistances near such an interface (accomplished by incorporating the dynamics of the evolving interface with $LaIBM$ through a volume of fluid coupling).
Paper E	• Demonstrated the impact of a particle on the Knudsen paradox in micro-channel Poiseuille flows. • Identified that the Knudsen minimum is shifted towards higher Kn and that the mass-flow rate changes (in the channel) become less pronounced towards the free molecular flow regime (due to a shift towards relatively more ballistic molecular motion at shorter geometrical distances).

Paper A

A. S. Kannan, V. Naserentin, A. Mark, D. Maggiolo, G. Sardina, S. Sasic, and H. Ström. A continuum-based multiphase DNS method for studying the Brownian dynamics of soot particles in a rarefied gas. *Chemical Engineering Science* **210** (2019), 115229. ISSN: 0009-2509. DOI: 10.1016/j.ces.2019.115229

Motivation and division of work

The main objective of this paper is to derive and validate a novel multiphase DNS technique based on the immersed boundary method (that satisfies some of the requirements listed in Section 4.2) to study the diffusion dynamics of a nanoparticle in a gas-particle system. Besides being the main author, my contribution consisted of setting-up/conceptualizing the simulations and post-processing/analyzing the results. The other co-authors supervised, reviewed and provided valuable feedback on the analyzed results and on the drafted manuscript.

Results and discussion

In this paper, the fundamentals of the novel multiphase DNS method are established by showing that the Langevin description of the Brownian particle can be combined with a resolved-surface DNS of the Eulerian fluid fields around the particle. The developed general framework is validated using a gas-particle quiescent aerosol inclusive of non-continuum effects (modeled with the Cunningham correction i.e. Eq. 3.16). It is shown that this framework can capture the diffusion dynamics of a spherical Brownian particle (with a 400 nm diameter) in an unbounded domain, including its transition from a particle-inertia dominated (correlated ballistic regime) to a non-correlated diffusive one. Further, the exponential decay (due to creeping flow conditions) of the velocity auto-correlation function (as given in Eq. 3.11) is also captured. The assessment is carried out over a range of particle-fluid density ratios relevant to soot aerosol applications, mimicking the conditions established in the analytical basis described in Chapter 3. Furthermore, the proposed DNS method is extended to model the diffusion dynamics of a real fractal soot aggregate. The reported results show that the proposed framework can reproduce the meandering motion of soot particles under rarefied conditions.

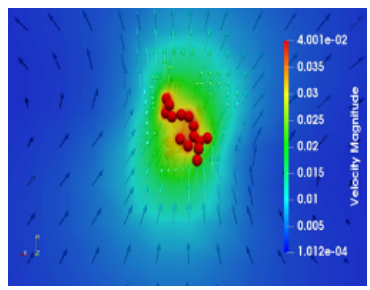

Vectors of velocity magnitude around a fractal aggregate (with diameter 348 nm).

Paper B

A. S. Kannan, A. Mark, D. Maggiolo, G. Sardina, S. Sasic, and H. Ström. Assessment of hindered diffusion in arbitrary geometries using a multiphase DNS framework. *Chemical Engineering Science* **230** (2021), 116074. ISSN: 0009-2509. DOI: 10.1016/j.ces.2020.116074

Motivation and division of work

The main objective of this paper is to extend the applicability of the developed multiphase DNS framework towards liquid-particle systems, particularly to investigate the hindered diffusion of a spherical particle in arbitrary geometries (including micro-channels and pores). Besides being the main author, my contribution consisted of setting-up/conceptualizing the simulations and post-processing/analyzing the results. The other co-authors supervised, reviewed and provided valuable feedback on the analyzed results and on the drafted manuscript.

Results and discussion

In this paper, the hindered diffusion of a spherical particle in arbitrary geometries is investigated. The correction factor for Stokes mobility (given by Eq. 3.3) of the particle, λ (given by Eq. 4.14), is directly estimated from the Eulerian solution of the surrounding fluid. This estimated value is further used to adjust the stochastic forcing (given by Eq. 4.16) on the Brownian particle to accurately represent the relevant diffusive behavior. As a proof-of-concept, the Brownian diffusion of a spherical nanoparticle (with a 400 nm diameter) under creeping flow conditions is assessed at varying degrees of confinement (i.e across progressively narrower micro-channels). Correspondingly, the fundamental form of the Langevin equation (i.e. Eq. 3.6), with the additional correction (λ) for the increased hydrodynamic wall resistances, is employed. The relevant dynamics of the Brownian particle are reproduced including, the transition from a ballistic to a diffusive regime and the exponential decay of the velocity auto-correlation function (due to creeping flow conditions). Further, a directional bias (anisotropy) in the hydrodynamic resistances on the particle is identified, with a pronounced co-axial resistance noted when compared with a wall-normal one. These observations are also corroborated with relevant analytical [195, 196] and experimental [197] studies from literature. Additionally, the qualitative capabilities of the DNS framework in resolving the hydrodynamics around a Brownian particle diffusing in an arbitrary pore are also demonstrated.

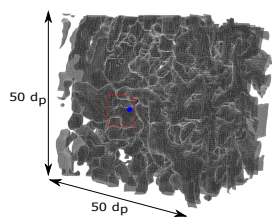

Spherical particle diffusing in an arbitrary pore.

Paper C

A. S. Kannan, A. Mark, D. Maggiolo, G. Sardina, S. Sasic, and H. Ström. A hydrodynamic basis for off-axis Brownian diffusion under intermediate confinements in micro-channels. *International Journal of Multiphase Flow* (Submitted December 2020)

Motivation and division of work

The main objective of this paper is to further examine the hydrodynamic ansiotropies reported in **Paper B** by evaluating off-axis hindered diffusion dynamics (i.e. at a location displaced from the co-axial axis along the center-line) in micro-channels. Besides being the main author, my contribution consisted of setting-up/conceptualizing the simulations and post-processing/analyzing the results. The other co-authors supervised, reviewed and provided valuable feedback on the analyzed results and on the drafted manuscript.

Results and discussion

In this paper, the directionally varying diffusive behavior of a spherical nanoparticle (with a 400 nm diameter) diffusing at a location off-set from the center-line (co-axial axis) of a square micro-channel (over varying degrees of intermediate hydrodynamic confinements) is investigated using the DNS framework proposed in the earlier papers. It is showed that the co-axial diffusivity of a particle diffusing off-axis is enhanced when compared with a corresponding center-line diffusion. Further, this effect is augmented as the particle confinement increases (or as the micro-channel gets narrower). This increased particle diffusivity is attributed to the reduced co-axial fluid resistance on the particle when it is displaced off-center. A hydrodynamic basis is established for the noted anisotropies in the resistances by further supporting the hydrodynamic fields around the diffusing particle with CFD simulations around a similar moving non-Brownian particle (the general hydrodynamic behavior is similar in both cases). More specifically, the direction of fluid motion in the narrow region between the particle and the wall changes with the particle-wall distance at tighter confinements, creating a position of minimum hydrodynamic resistance for co-axial motion at an off-axis location (which in turn is a function of the effective confinement). Such a minimum was noted in both multiphase DNS and steady-state CFD results, as well as in the results reported in literature (the dissipative particle dynamics results of Gubbiotti et al. [123]).

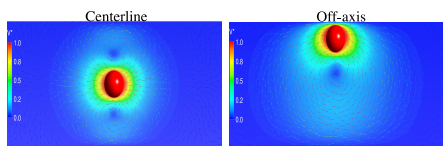

Hydrodynamic fields around a spherical particle: contours of non-dimensional velocity overlaid with flow vectors (from the CFD simulations).

Paper D

A. S. Kannan, A. Mark, D. Maggiolo, G. Sardina, S. Sasic, and H. Ström. Hindered diffusion of nanoparticles in a liquid re-visited with a continuum based direct numerical simulation framework. *To be submitted to a journal* (2021)

Motivation and division of work

The main objective of this paper is to extend the applicability of the validated DNS framework from the earlier papers towards multi-particle systems (i.e. pairwise diffusion) and diffusion near a soft-boundary (a 3-phase system). Besides being the main author, my contribution consisted of setting-up/conceptualizing the simulations and post-processing/analyzing the results. The other co-authors supervised, reviewed and provided valuable feedback on the analyzed results and on the drafted manuscript.

Results and discussion

In this paper, the hindered diffusion problem in a liquid – wherein hydrodynamic interactions mediated by the fluid (such as particle-particle or particle-boundary effects) influence the governing particle dynamics, is revisited using the DNS framework derived in the earlier papers. It is shown that the expected hindered diffusion behavior near a no-slip boundary is captured, with both the directional mean squared displacement and velocity auto-correlation functions reflecting the increased hydrodynamic resistance. This discussion is further extended towards diffusion near a soft-boundary (formed at the interface of two liquids) by incorporating the dynamics of the evolving interface with the motion of the nearby Brownian particle, through a volume of fluid coupling. It is shown that the particle mobility is enhanced near such a soft-boundary due to significant reduction in the hydrodynamic resistances that result from the lowered fluid shear near this interface. Furthermore, the pairwise diffusion of Brownian particles is also assessed in this paper. It is demonstrated that the inter-particle interactions (mediated by the fluid) leads to a correlated motion between the pair of particles as a result of being accelerated by each other's wakes. This discussion further establishes the applicability of the proposed DNS framework in evaluating hindered diffusion phenomena over a wide range of applications including (but not limited to) nano-carrier mediated drug delivery and particulate emission dispersion and mitigation.

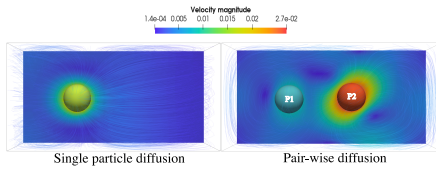

Comparison between single and pair-wise diffusion: contours of velocity magnitude overlayed with flow streamlines around the particle.

Paper E

A. S. Kannan, T. S. B. Narahari, Y. Bharadhwaj, A. Mark, D. Maggiolo, G. Sardina, S. Sasic, and H. Ström. The Knudsen paradox in micro-channel Poiseuille flows with a symmetric particle. *Applied sciences* (Submitted November 2020)

Motivation and division of work

The main objective of this paper is to revisit the gas-particle aerosol at a molecular level of abstraction, by investigating the effects of a stationary particle on a micro-channel Poiseuille flow, using a DSMC framework. Besides being the main author, my contribution consisted of conceptualizing the simulations and post-processing/analyzing the results. Tejas Sharma Bangalore Narahari and Yashas Bharadhwaj set-up the simulations and performed the initial post-processing of the data. The other co-authors supervised, reviewed and provided valuable feedback on the analyzed results and on the drafted manuscript.

Results and discussion

In this paper, the effects of a stationary particle on a micro-channel Poiseuille flow (from continuum to free-molecular conditions) are investigated using the DSMC method. Correspondingly, the non-equilibrium Knudsen paradox (a unique and well-established signature of micro-channel rarefied flows), which is the non-monotonous variation of channel mass-flow rate with the Kn, is evaluated in such micro-channel rarefied flows. These assessments show that with the presence of a particle, the Knudsen minimum is shifted towards higher Kn and the accompanying mass-flow rate changes becomes less pronounced towards the free molecular flow regime. This effect is more significant as the particle becomes large (in relation to the channel) and results from a shift towards relatively more ballistic molecular motion at shorter geometrical distances. Further, an increase in the local hydrodynamic resistances in the flow (due to the presence of the particle), leads to noticeable deviations from the numerical basis derived for straight micro-channel Poiseuille flows by Cercignani et al. [198]. Thus, this paper addresses a perceived knowledge gap in rarefied flows, along with a relevant challenge while modeling reactive gas-solid flows in confined geometries at the nanoscale, where simultaneous handling of local and non-local transport mechanisms over the particle surfaces must be realized.

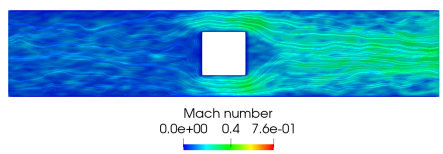

Contours of Mach number (Ma) around a square nanoparticle (in the transition regime), overlaid with velocity streamlines along an xy plane.

6

Final word

Conclusion and future outlook

The primary objective of this thesis was to facilitate an *in-silico* evaluation of nanoparticle transport in a confined environment (such as a micro-channel or a blood vessel), by developing novel strategies to study these complex phenomena at both molecular and continuum scales of abstraction. In this process, the existing collection of numerical tools (routinely used for this purpose) are improved and further extended, thereby complementing and in some cases replacing experimental based efforts. This is increasingly the trend, as assessments in such highly confined Brownian systems are challenging to undertake due to the inherent difficulties with accurate measurements at these scales. Furthermore, there are additional difficulties in ensuring proper access for the measurement techniques under such confinements as well. Thus, the next generation of technologies which are needed to tackle some of the common problems that plague our society today (as highlighted in Chapter 1) can be developed and optimized by employing the novel *in-silico* based strategies discussed (see Section 4.1) and developed (see Section 4.3) in this thesis.

Consequently, the two over-arching objectives of this thesis (as listed in Chapter 2), which were:

1. To develop a general numerical method that can handle nanoparticle dynamics in a fluid, including the accompanying macro-scale and micro-scale effects, using a continuum based framework (multiphase direct numerical simulation) i.e. projecting down from the continuum to the molecular scales and,

2. To establish a hydrodynamic basis, using numerical simulations for diffusive transport of nanoparticles, within the context of the two use cases briefly described in Chapter 1 (i.e. hindered diffusion),

have been achieved. This was accomplished by developing a DNS framework ($LaIBM$) that leverages a resolved solution of the hydrodynamics around the Brownian particle and couples this with a Lagrangian Langevin description. This approach is preferred over the alternative fluctuating hydrodynamics based method [43, 142–144, 148, 151–153], due

to the relative ease of implementation and the accompanying avoidance of the issues related to the discretization of the LLNS equations (see Eq. 4.6). To our best knowledge, this is the first continuum-based framework that directly includes the resolved instantaneous hydrodynamics around the Brownian particle into the particle Langevin equation of motion. Consequently, the framework is used to evaluate both gas-particle and liquid-particle systems, probing certain aspects of the Brownian transport problem relevant to the use cases introduced in Chapter 1 (i.e. soot aerosols and nanocarrier mediated drug delivery). In addition, a molecular DSMC method is also used to further probe the non-continuum phenomena (such as the Knudsen paradox) around a symmetrical particle in a rarefied gas (i.e. under conditions where continuum based methods fail). All these assessments combined provide a description that spans across molecular and continuum scales, thereby resolving the Brownian transport problem from two opposing perspectives i.e. building up from kinetic theory or alternately projecting down from continuum theory. The results achieved during the course of this thesis are still in their nascent stages as evidenced by the limitations of the current iteration of the method (as listed in Section 4.3.4). However, a lot of the future potential is already built into the framework, which makes it equipped to handle the complex transport phenomena encountered in both aerosols and colloids.

Future outlook

This thesis is primarily positioned to encourage a multiphase DNS based assessment of nanoparticle transport, hence, much of the future outlook will be focused on this aspect. Further, although the current form of the framework is based on the steady Langevin equation (see Eq. 3.6), it could be extended towards the generalized Langevin equation [32, 199] including unsteady effects (such as Basset history, added mass force etc), provided the stochastic forcing has the right form (the Gaussian noise is replaced by a colored noise instead). As stated earlier, the developed $LaIBM$ framework has the in-built capability to account for multi-particle dynamics including collisions. Moreover, as an IB method is used, complex fractal-shapes as well as any other type of particle including (but not limited to) nanofibers or droplets can be included. Since the framework relies on a continuum-based solution to the surrounding flow field, additional transport of temperature and/or species can be directly incorporated by solving the relevant transport equations. Hence, it has the inherent capability to provide a detailed insight into reactive pore-scale phenomena as well. Furthermore, this framework can also resolve particle deformation if needed (coupling between hydrodynamics and structural mechanics), which is very useful while evaluating the interactions of a nanocarrier with the constituent entities (such as red blood corpuscles) in blood. More recently, the IBM method has also been demonstrated to handle non-Newtonian fluids [173, 174], another feature that can support the *in-silico* modeling of nanocarrier transport. In summary, this framework has the necessary infrastructure to simulate the complex Brownian phenomena of nanoparticles in a fluid by taking into account both the hydrodynamic and molecular interactions that govern such flows.

7

Appendix

7.1 Derivation of the Stokes-Einstein relation

A detailed derivation of the closed-form expression for the diffusion coefficient D_∞ in Eq. (3.2). This derivation is done in accordance to Peskir's [200] ideas, by establishing a dynamic equilibrium between the pressure and viscous forces acting on the particle, thereby aiding in a simplified representation of Einstein's [14] original derivation.

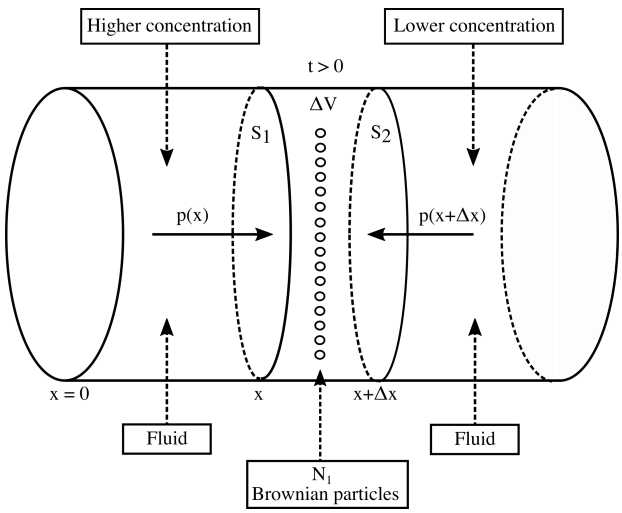

Figure 7.1: *A schematic of a cylindrical vessel filled with a fluid, containing N suspended Brownian particles.Due to the impacts by fluid molecules, Brownian particles will begin the process of diffusion.*

Consider a cylindrical vessel as shown in Fig. 7.1 filled with a fluid containing N suspended Brownian particles at $t = 0$. The diffusion of the Brownian particles is initiated from $x = 0$ due to collisions with the fluid molecules. Thus, at an instant $t > 0$, a concentration gradient for the Brownian particles is established across the cylinder, with a higher number of particles on the left side as opposed to the right (assuming diffusion

is from left to right), as shown in the Fig. 7.1. Consequently, the pressure on imaginary cross-sections S_1 and S_2 (with area A) of a fluid control volume, at locations x and $x+\Delta x$ is:

$$\frac{p(x) - p(x+\Delta x)}{\Delta x} = \frac{F(x) - F(x+\Delta x)}{A\Delta x} = \frac{N_1 F_p}{A\Delta x}, \tag{7.1}$$

where $p(x) > p(x+\Delta x)$ and N_1 is the number of Brownian particles in the fluid element with volume ΔV. F_p is the force exerted on every Brownian particle that passes through this control volume. Taking $\lim_{\Delta x \to 0}$ in Eq. (7.1):

$$\frac{\partial p}{\partial x} = -\nu F_p, \tag{7.2}$$

where, $\nu = \nu(t, x)$ is the average number of Brownian particles in the control volume. This force on the particle will impose a velocity on each particle given as:

$$F_p = \frac{v_p}{\beta_{St}} = -F_f, \tag{7.3}$$

with $1/\beta_{St}$ as the fluid friction. This equation demonstrates a dynamic equilibrium between the forces of pressure and friction i.e. F_p is retarded by the fluid force F_f. Further, Einstein concluded with statistical mechanical arguments that N Brownian particles suspended in a liquid satisfy the equation of state given by:

$$pV = nRT, \tag{7.4}$$

where, n is the number of moles and R is the gas constant (one mole of the gas contains N_{av} molecules). Thus, with $N_1 = nN_{av}$:

$$p = \frac{nN_{av}}{\Delta V}\frac{R}{N_{av}}T = \nu k_B T. \tag{7.5}$$

Differentiating Eq. (7.5) and using Eqs. (7.2) and (7.3), we get:

$$\frac{\partial p}{\partial x} = k_B T \frac{\partial \nu}{\partial x} = -\nu F_p = -\frac{v_p \nu}{\beta_{St}}. \tag{7.6}$$

The number of Brownian particles (ΔN) passing through an area ΔA under an interval Δt is given by Fick's law as:

$$\Delta N = -D_\infty \frac{\partial \nu}{\partial n} \Delta A \Delta t. \tag{7.7}$$

Thus, it follows that:

$$\nu v = \frac{N_1}{A\Delta x}\frac{\Delta x}{\Delta t} = \frac{N_1}{A\Delta t} = -D_\infty \frac{\partial \nu}{\partial x} \tag{7.8}$$

Inserting Eq. (7.8) into Eq. (7.6), we get the Stokes-Einstein relation:

$$D_\infty = \frac{k_B T}{6\pi \mu_f r_p} \tag{7.9}$$

when, the Stokes mobility of the particle is:

$$\beta_{St} = \frac{1}{6\pi \mu_f r_p}. \tag{7.10}$$

7.2 Derivation of the MSD, VACF and fluctuation-dissipation relation from the Langevin equation

The equation of motion for a Brownian particle, with mass m_p, is formally based on Newton's second law as:

$$m_p \frac{\mathrm{d}u_p}{\mathrm{d}t} = -\gamma_{St} u_p + \chi(t), \tag{7.1}$$

The fluctuating component $\chi(t)$ is assumed to be independent of the velocity u_p and further fluctuate rapidly in comparison with variations in velocity. Consequently, in this description, the particle velocity is well defined and is subject to both the viscous dissipation (friction force) from the fluid and the random stochastic forcing. Uhlenbeck [31] further showed that Eq. (7.1) is constrained by certain restrictions on the fluctuating component $\chi(t)$, i.e. it follows a Gaussian white noise process. Hence, the stochastic forcing (with an intensity S_{uu}) satisfies:

$$\begin{gathered} \langle \chi(t) \rangle = 0, \quad \langle \chi(t) \chi(t') \rangle = S_{uu} \delta(t - t') \\ \langle \chi(t) x(t') \rangle = 0, \quad \langle \chi(t) u_p(t') \rangle = 0. \end{gathered} \tag{7.2}$$

The MSD can be derived by re-writing Eq. (7.1) in terms of the position $x(t)$ as:

$$m_p \frac{\mathrm{d}^2 x}{\mathrm{d}t^2} = -\gamma_{St} \frac{\mathrm{d}x}{\mathrm{d}t} + \chi(t), \tag{7.3}$$

Multiplying Eq. (7.3) with x and by further using:

$$\begin{gathered} \frac{\mathrm{d}x^2}{\mathrm{d}t} = 2x \frac{\mathrm{d}x}{\mathrm{d}t} \quad \text{and} \\ \frac{\mathrm{d}^2 x^2}{\mathrm{d}t^2} = 2(\frac{\mathrm{d}x}{\mathrm{d}t})^2 + 2x \frac{\mathrm{d}^2 x}{\mathrm{d}t^2}, \end{gathered} \tag{7.4}$$

we get:

$$\frac{m_p}{2} \frac{\mathrm{d}^2 x^2}{\mathrm{d}t^2} - m_p u_p^2 = -\frac{\gamma_{St}}{2} \frac{\mathrm{d}x^2}{\mathrm{d}t} + x\chi(t). \tag{7.5}$$

Averaging Eq. (7.5) (or using the $\langle ... \rangle$ operator) under the constraints presented in Eq. (7.2) and by applying the equipartition theorem $m_p \langle u_p^2 \rangle = k_B T$ [‡], we obtain the differential equation:

$$\frac{m_p}{2}\frac{\mathrm{d}\mathbf{z}}{\mathrm{d}t} + \frac{\gamma_{St}}{2}\mathbf{z} = k_B T, \tag{7.6}$$

where, $\mathbf{z} = \frac{d}{dt}\langle x^2 \rangle$.

Since $\langle \mathbf{z} \rangle = 2\langle x(0) u_p(0) \rangle = 0$, the solution of Eq. (7.6) is given as:

$$\mathbf{z}(t) = \frac{2k_B T}{\gamma_{St}}(1 - \mathrm{e}^{\frac{-\gamma_{St} t}{m_p}}). \tag{7.7}$$

Eq. (7.7) is integrated to yield the expression for MSD at all time scales as:

$$\langle \Delta x^2(t) \rangle = \frac{2k_B T}{\gamma_{St}} \left(t - \frac{m_p}{\gamma_{St}} + \frac{m_p}{\gamma_{St}} \mathrm{e}^{\frac{-\gamma_{St} t}{m_p}} \right). \tag{7.8}$$

In Eq. (7.8), when $t \gg \tau_B$, the exponential term is negligible, leading to the Einstein's result for long-term or over-damped behavior in 1D. Correspondingly, the MSD of the particle increases linearly in time as:

$$< \Delta x(t)^2 >= 2Dt. \tag{7.9}$$

When $t \ll \tau_B$ or as $t \to 0$, the ballistic or under-damped result can be obtained. This is done by using the power series:

$$\mathrm{e}^{-t} = 1 - t + \frac{t^2}{2!} + O(t^3), \tag{7.10}$$

in Eq. (7.8). We then obtain the result (consistent with the equipartition theorem):

$$< \Delta x(t)^2 >= \frac{k_B T}{m_p} t^2 = u_{rms}^2 t^2. \tag{7.11}$$

Here, u_{rms} is the root-mean-squared velocity of the particle. The corresponding time scale (i.e. the relaxation time for the Brownian particle) in the ballistic regime, τ_B, is given as:

[‡]A colloidal particle suspended in a liquid at temperature T is assimilated to a particle of the liquid, so that it possesses an average kinetic energy $\frac{2RT}{N_{av}}$. Accordingly we get: $\frac{1}{2} m_p \langle u_p^2 \rangle = \frac{2RT}{N_{av}}$

$$\tau_B = \frac{m_p}{\gamma_{St}}. \tag{7.12}$$

The VACF of the Brownian particle can be derived by evaluating the solution of the first-order inhomogeneous stochastic differential equation i.e. Eq. (7.1). Ornstein-Uhlenbeck showed that a formal solution to this equation is:

$$u_p(t) = u_p(0)\mathrm{e}^{\frac{-\gamma_{St}t}{m_p}} + \frac{1}{m_p}\int_0^t \mathrm{e}^{\frac{-\gamma_{St}(t-\xi)}{m_p}}\chi(\xi)\mathrm{d}\xi. \tag{7.13}$$

Using the $\langle ... \rangle$ operator in Eq. (7.13), under the constraints in Eq. (7.2) and assuming that all particles start at $t = 0$ with the same velocity $u_p(0)$, we get:

$$\langle u_p \rangle = u_p(0)\mathrm{e}^{\frac{-\gamma_{St}t}{m_p}}. \tag{7.14}$$

This equation shows that velocity goes down exponentially due to the fluid friction. This exponential decay is further visible in the VACF, which is obtained by multiplying Eq. (7.13) with $u_p(0)$ and using the $\langle ... \rangle$ operator under the corresponding constraints. This simplification leads to:

$$C(t) \equiv \langle u_p(0)u_p(t) \rangle = \left\langle u_p^2(0) \right\rangle \mathrm{e}^{\frac{-\gamma_{St}t}{m_p}} = \frac{k_B T}{m_p}\mathrm{e}^{\frac{-\gamma_{St}t}{m_p}}. \tag{7.15}$$

Fluctuation-dissipation theorem

Furthermore, squaring Eq. (7.14) and using the $\langle ... \rangle$ operator again, we obtain:

$$\langle u_p^2 \rangle = \langle u_p^2(0) \rangle \mathrm{e}^{\frac{-2\gamma_{St}t}{m_p}} + \mathrm{e}^{\frac{-2\gamma_{St}t}{m_p}} \int_0^t \int_0^t \mathrm{e}^{\frac{t(\xi+\eta)}{m_p}} \langle \chi(\xi)\chi(\eta) \rangle d\xi d\eta. \tag{7.16}$$

Ornstein-Uhlenbeck further showed that the integral in Eq. (7.16) can be written as:

$$\int_0^t \int_0^t \mathrm{e}^{\frac{t(\xi+\eta)}{m_p}} \langle \chi(\xi)\chi(\eta) \rangle d\xi d\eta = \frac{\zeta}{2\gamma_{St}m_p}(1 - \mathrm{e}^{\frac{-2\gamma_{St}t}{m_p}}). \tag{7.17}$$

Hence, the mean-squared velocity is given as:

$$\langle u_p^2 \rangle = \langle u_p^2(0) \rangle \mathrm{e}^{\frac{-2\gamma_{St}t}{m_p}} + \frac{\zeta}{2\gamma_{St}m_p}(1 - \mathrm{e}^{\frac{-2\gamma_{St}t}{m_p}}). \tag{7.18}$$

Over long times, the equipartition theorem is valid, meaning:

$$\zeta = 2\gamma_{St}k_B T. \tag{7.19}$$

This represents a fundamental relation named as the fluctuation-dissipation theorem, which shows that the magnitude of the fluctuation ζ must be balanced by the strength of the dissipation γ_{St} so that the temperature is well defined in Langevin's model. Therefore, the pair of friction and random forces acts as a thermostat for a Langevin system. This relationship between the friction and random forcing on the particle is physically reasonable since they have a common origin i.e. interactions between the particle and the surrounding fluid molecules.

Additionally, by taking the integral of the VACF of the Brownian particle i.e. Eq. (7.15), we can observe that:

$$\int_0^\infty \langle u_p(0)u_p(t) \rangle \mathrm{d}t = \frac{k_\mathrm{B}T}{m_p} \int_0^\infty \mathrm{e}^{\frac{-\gamma_{St}t}{m_p}} \mathrm{d}t = \frac{k_\mathrm{B}T}{\gamma_{St}} = D_\infty, \tag{7.20}$$

which is the Stoke-Einstein relation for a free particle. This Eq. (7.20) is a fundamental relation, known in statistical mechanics as the Green-Kubo relation [32], that relates the macroscopic transport coefficients to the correlation functions of the variables fluctuating due to said microscopic processes. Similarly, the time-dependent diffusion co-efficient is obtained from the VACF as:

$$D_\infty(t) \equiv \int_0^t \langle u_p(0)u_p(t) \rangle \mathrm{d}\tau = \frac{1}{2}\frac{d}{dt}\langle \Delta x^2(t) \rangle = \frac{k_B T}{\gamma_{St}}(1 - \mathrm{e}^{\frac{-\gamma_{St}t}{m_p}}). \tag{7.21}$$

This equivalence of the two definitions for the VACF and the MSD is because the VACF can be calculated from the second derivative of the MSD[§].

[§] $\frac{d}{dt}\langle \Delta x^2(t) \rangle = 2\int_0^t C(\tau)d\tau$

7.3 Power spectrum of an Ornstein-Uhlenback process

The correlation functions, derived previously (Eq. (3.11)) represents the stochastic processes in the time domain, provided it is stationary [¶] and the Wiener-Khinchin theorem [‖] is satisfied. It follows that, such time signals can be represented in the frequency space using the corresponding Fourier transforms. The output, $y(t)$ of a LTI system can be obtained by the convolution of the input signal ($x(t)$) and its impulse response ($r(t)$), as:

$$y(t) = \int_{-\infty}^{\infty} x(\tau) r(t-\tau) d\tau. \tag{7.1}$$

The corresponding output, $Y(\omega)$, in the frequency domain can be written based on the convolution theorem [**] as:

$$Y(\omega) = X(\omega) R(\omega), \tag{7.2}$$

where, $R(\omega)$ and $X(\omega)$ are the Fourier transform of the impulse response $r(t)$ and the time domain input $x(t)$, respectively. In the context of a Brownian particle being excited by a stochastic noise, this response, $R(\omega)$, is nothing but the mobility (Eq. (3.3)) of the particle. The fluctuation-dissipation relation or Green-Kubo formula (see Eq. (7.20) in Appendix 7.2) has a corresponding form in the frequency space by relating the mobility $R(\omega)$ to the Fourier-Laplace transform of the velocity auto-correlation, as:

$$Y(\omega) = \frac{1}{k_B T} \int_0^{\infty} \mathrm{e}^{i\omega t} C(t) dt. \tag{7.3}$$

Correspondingly, the Fourier transform of the Langevin equation (see Eq. (3.6)) is given as:

$$-i\omega m_p u_p(\omega) + \gamma_{St} u_p(\omega) = S(\omega). \tag{7.4}$$

[¶] A continuous-time random process, $X(t), t \in \mathbb{R}$ is wide sense stationary if:

1. $\mu_X(t) = \mu_X$, for all $t \in \mathbb{R}$, where μ_X is the mean.
2. $C_X(t_1, t_2) = C_X(t_1 - t_2)$, for all $t_1, t_2 \in \mathbb{R}$, where C_X is the correlation function.

[‖] The power spectrum $S(\omega)$ of a stationary random process and its auto-correlation function are Fourier transform pairs

[**] The Fourier transform of a convolution in the time domain equals the product of the Fourier transforms of each function in the frequency domain

The response $R(\omega)$, of the system (based on Eq. (7.2)) can be written as:

$$R(\omega) = \frac{1}{-i\omega m_p + \gamma_{St}}. \tag{7.5}$$

Thus, the power spectrum density, $\tilde{S}_u(\omega)$, of the random process output (based on the velocity), which is needed in order to describe the Gaussian white noise signal, can be deduced using the Wiener-Kinchin theorem as:

$$\tilde{S}_{uu}(\omega) = \int_{-\infty}^{\infty} \mathrm{e}^{i\omega t} \langle u_p(0) u_p(t) \rangle dt. \tag{7.6}$$

Using Eq. (7.3) in Eq. (7.6), we obtain:

$$\tilde{S}_{uu}(\omega) = 2k_B T \mathbb{R}[R(\omega)] = \frac{k_B T \gamma_{St}}{\pi m_p} = \frac{2{\gamma_{St}}^2}{\pi} D_\infty, \tag{7.7}$$

where, $\mathbb{R}[R(\omega)$ is the real part of the mobility given in Eq. (7.4). This is obtained by summing Eq. (7.3) and its complex conjugate and use the fact that the VACF is an even function. The position power spectrum density is obtained from Eq. (7.7) as:

$$\tilde{S}_x(\omega) = \frac{\tilde{S}_u(\omega)}{\omega^2} = \frac{2k_B T \mathbb{R}[R(\omega)]}{\omega^2}. \tag{7.8}$$

Thus, the stochastic forcing term, $\chi(t)$, in the Langevin equation (see Eq. (7.1)) is modeled as a Gaussian white noise process with the vector of spectral intensity S_{ij}^n given as:

$$S_{ij}^n = \tilde{S}_{uu}(\omega) \delta_{ij}. \tag{7.9}$$

References

[1] A. S. Kannan, V. Naserentin, A. Mark, D. Maggiolo, G. Sardina, S. Sasic, and H. Ström. A continuum-based multiphase DNS method for studying the Brownian dynamics of soot particles in a rarefied gas. *Chemical Engineering Science* **210** (2019), 115229. ISSN: 0009-2509. DOI: 10.1016/j.ces.2019.115229.

[2] A. S. Kannan, A. Mark, D. Maggiolo, G. Sardina, S. Sasic, and H. Ström. Assessment of hindered diffusion in arbitrary geometries using a multiphase DNS framework. *Chemical Engineering Science* **230** (2021), 116074. ISSN: 0009-2509. DOI: 10.1016/j.ces.2020.116074.

[3] A. S. Kannan, A. Mark, D. Maggiolo, G. Sardina, S. Sasic, and H. Ström. A hydrodynamic basis for off-axis Brownian diffusion under intermediate confinements in micro-channels. *International Journal of Multiphase Flow* (Submitted December 2020).

[4] A. S. Kannan, A. Mark, D. Maggiolo, G. Sardina, S. Sasic, and H. Ström. Hindered diffusion of nanoparticles in a liquid re-visited with a continuum based direct numerical simulation framework. *To be submitted to a journal* (2021).

[5] A. S. Kannan, T. S. B. Narahari, Y. Bharadhwaj, A. Mark, D. Maggiolo, G. Sardina, S. Sasic, and H. Ström. The Knudsen paradox in micro-channel Poiseuille flows with a symmetric particle. *Applied sciences* (Submitted November 2020).

[6] A. S. Kannan, A. Mark, D. Maggiolo, G. Sardina, S. Sasic, and H. Ström. "A novel multiphase DNS method for the resolution of Brownian motion in a weakly rarefied gas using a continuum framework". *Proceedings of the 10th International Conference on Multiphase Flow (ICMF19)*. Rio de Janeiro, Brazil, May 2019.

[7] H. Ström, J. Sjöblom, A. S. Kannan, H. Ojagh, O. Sundborg, and J. Koegler. Near-wall dispersion, deposition and transformation of particles in automotive exhaust gas aftertreatment systems. *International Journal of Heat and Fluid Flow* **70** (2018), 171–180. ISSN: 0142-727X. DOI: 10.1016/j.ijheatfluidflow.2018.02.013.

[8] A. S. Kannan, A. Mark, D. Maggiolo, G. Sardina, S. Sasic, and H. Ström. "Assessment of pore diffusion in a micro-channel using an immersed boundary method". *Proceedings of the 14th International Conference on Multiphase Flow in Industrial Plant (MFIP17)*. Desenzano del Garda, Italy, 2017.

[9] A. S. Kannan, K. Jareteg, N. C. K. Lassen, J. M. Carstensen, M. A. E. Hansen, F. Dam, and S. Sasic. Design and performance optimization of gravity tables using a combined CFD-DEM framework. *Powder Technology* **318** (2017), 423–440. ISSN: 0032-5910. DOI: 10.1016/j.powtec.2017.05.046.

[10] A. S. Kannan, N. C. K. Lassen, J. M. Carstensen, J. Lund, and S. Sasic. Segregation phenomena in gravity separators: A combined numerical and experimental study. *Powder Technology* **301** (2016), 679–693. ISSN: 0032-5910. DOI: 10.1016/j.powtec.2016.07.003.

[11] J. Sjöblom, H. Ström, A. S. Kannan, and H. Ojagh. Experimental Validation of Particulate Matter (PM) Capture in Open Substrates. *Industrial & Engineering Chemistry Research* **53**.9 (2014), 3749–3752. DOI: 10.1021/ie404046y.

[12] J. Sjöblom, A. S. Kannan, H. Ojagh, and H. Ström. Modelling of particulate matter transformations and capture efficiency. *The Canadian Journal of Chemical Engineering* **92**.9 (2014), 1542–1551. DOI: 10.1002/cjce.22004.

[13] J. Renn. Einstein's invention of Brownian motion. *Annalen der Physik* **14**.S1 (2005), 23–37. DOI: 10.1002/andp.200410131.

[14] A. Einstein. Über die von der molekularkinetischen Theorie der Wärme geforderte Bewegung von in ruhenden Flüssigkeiten suspendierten Teilchen. *Annalen der Physik* **322**.8 (1905), 549–560. DOI: 10.1002/andp.19053220806.

[15] IQAir. *2019 World Air Quality Report*. Report. 2020. URL: https://www.iqair.com/world-most-polluted-cities/world-air-quality-report-2019-vi.pdf.

[16] N. Osseiran and K. Chriscaden. Press Release. 2016. URL: http://www.who.int/news-room/detail/12-05-2016-air-pollution-levels-rising-in-many-of-the-world-s-poorest-cities.

[17] Directive 2008/50/EC of the European Parliament and of the Council of 21 May 2008 on ambient air quality and cleaner air for Europe. *OJ* **L 152** (2008), 1–44.

[18] J. Matthey. *Diesel particulate filter*. 2020. URL: http://www.jmdpf.com/diesel-particulate-filter-DPF-passive-systems-johnson-matthey.

[19] K. Bourzac. Nanotechnology: Carrying drugs. *Nature* 7425 (2012), S58–S60. DOI: 10.1038/491S58a.

[20] C. Wild, E. Weiderpass, and B. Stewart. *World Cancer Report: Cancer Research for Cancer Prevention*. Report. 2020. URL: http://publications.iarc.fr/586.

[21] D. Peer, J. M. Karp, S. Hong, O. C. Farokhzad, R. Margalit, and R. Langer. Nanocarriers as an emerging platform for cancer therapy. *Nature Nanotechnology* **2**.12 (2007), 751–760. DOI: 10.1038/nnano.2007.387.

[22] J. Fu and H. Yan. Controlled drug release by a nanorobot. *Nature Biotechnology* **30**.5 (2012), 407–408. DOI: 10.1038/nbt.2206.

[23] J. Hrkach, D. Von Hoff, M. M. Ali, E. Andrianova, J. Auer, T. Campbell, D. De Witt, M. Figa, et al. Preclinical Development and Clinical Translation of a PSMA-Targeted Docetaxel Nanoparticle with a Differentiated Pharmacological Profile. *Science Translational Medicine* **4**.128 (2012), 128ra39–128ra39. DOI: 10.1126/scitranslmed.3003651.

[24] W. Sutherland. LXXV. A dynamical theory of diffusion for non-electrolytes and the molecular mass of albumin. *The London, Edinburgh, and Dublin Philosophical Magazine and Journal of Science* **9**.54 (1905), 781–785. DOI: 10.1080/14786440509463331.

[25] M. von Smoluchowski. Zur kinetischen Theorie der Brownschen Molekularbewegung und der Suspensionen. *Annalen der Physik* **326**.14 (1906), 756–780. ISSN: 0003-3804. DOI: 10.1002/andp.19063261405.

[26] P. Langevin. Sur la théorie du mouvement brownien. *C. R. Acad. Sci. (Paris)* **146** (1908), 530–533. DOI: 10.1119/1.18725.

[27] S. G. Brush. A History of Random Processes: I. Brownian Movement from Brown to Perrin. *Archive for History of Exact Sciences* **5**.1 (1968), 1–36. ISSN: 00039519, 14320657. DOI: 10.2307/41133279.

[28] G. G. Stokes. "On the Effect of the Internal Friction of Fluids on the Motion of Pendulums". *Mathematical and Physical Papers*. Vol. 3. Cambridge Library Collection - Mathematics. Cambridge University Press, 1901, pp. 1–10. DOI: 10.1017/CBO9780511702266.002.

[29] D. S. Lemons and A. Gythiel. Paul Langevins 1908 paper On the Theory of Brownian Motion [Sur la théorie du mouvement brownien, C. R. Acad. Sci. (Paris) 146, 530533 (1908)]. *American Journal of Physics* **65**.11 (1997), 1079–1081. DOI: 10.1119/1.18725.

[30] Perrin, jean. Mouvement brownien et grandeurs moléculaires. *Radium (Paris)* **6**.12 (1909), 353–360. DOI: 10.1051/radium:01909006012035300.

[31] G. E. Uhlenbeck and L. S. Ornstein. On the Theory of the Brownian Motion. *Physical Review* **36**.5 (1930), 823–841. DOI: 10.1103/PhysRev.36.823.

[32] R. Kubo. The fluctuation-dissipation theorem. *Reports on Progress in Physics* **29**.1 (Jan. 1966), 255–284. DOI: 10.1088/0034-4885/29/1/306.

[33] A. Rahman. Correlations in the Motion of Atoms in Liquid Argon. *Phys. Rev.* **136** (2A Oct. 1964), A405–A411. DOI: 10.1103/PhysRev.136.A405.

[34] B. J. Alder and T. E. Wainwright. Decay of the Velocity Autocorrelation Function. *Phys. Rev. A* **1** (1 Jan. 1970), 18–21. DOI: 10.1103/PhysRevA.1.18.

[35] R. Zwanzig and M. Bixon. Hydrodynamic Theory of the Velocity Correlation Function. *Phys. Rev. A* **2** (5 Nov. 1970), 2005–2012. DOI: 10.1103/PhysRevA.2.2005.

[36] A. Widom. Velocity Fluctuations of a Hard-Core Brownian Particle. *Phys. Rev. A* **3** (4 Apr. 1971), 1394–1396. DOI: 10.1103/PhysRevA.3.1394.

[37] E. J. Hinch. Application of the Langevin equation to fluid suspensions. *Journal of Fluid Mechanics* **72**.3 (1975), 499–511. DOI: 10.1017/S0022112075003102.

[38] J. Blum, S. Bruns, D. Rademacher, A. Voss, B. Willenberg, and M. Krause. Measurement of the Translational and Rotational Brownian Motion of Individual Particles in a Rarefied Gas. *Phys. Rev. Lett.* **97** (23 Dec. 2006), 230601. DOI: 10.1103/PhysRevLett.97.230601.

[39] R. Huang, I. Chavez, K. M. Taute, B. Luki, S. Jeney, M. G. Raizen, and E.-L. Florin. Direct observation of the full transition from ballistic to diffusive Brownian motion in a liquid. *Nature Physics* **7** (2011), 576. DOI: 10.1038/nphys1953.

[40] S. Kheifets, A. Simha, K. Melin, T. Li, and M. G. Raizen. Observation of Brownian Motion in Liquids at Short Times: Instantaneous Velocity and Memory Loss. *Science* **343**.6178 (2014), 1493–1496. ISSN: 0036-8075. DOI: 10.1126/science.1248091.

[41] S. Chandrasekhar. Stochastic Problems in Physics and Astronomy. *Reviews of Modern Physics* **15**.1 (1943), 1–89. DOI: 10.1103/RevModPhys.15.1.

[42] X. Bian, C. Kim, and G. E. Karniadakis. 111 years of Brownian motion. *Soft Matter* **12**.30 (2016), 6331–6346. DOI: 10.1039/c6sm01153e.

[43] R. Radhakrishnan, S. Farokhirad, D. M. Eckmann, and P. S. Ayyaswamy. "Chapter Two - Nanoparticle transport phenomena in confined flows". *Advances in*

Heat Transfer. Ed. by E. M. Sparrow, J. P. Abraham, J. M. Gorman, and W. Minkowycz. Vol. 51. Advances in Heat Transfer. Elsevier, 2019, pp. 55–129. DOI: 10.1016/bs.aiht.2019.08.002.

[44] J. Mo and M. G. Raizen. Highly Resolved Brownian Motion in Space and in Time. *Annual Review of Fluid Mechanics* **51**.1 (2019), 403–428. DOI: 10.1146/annurev-fluid-010518-040527.

[45] C. Truesdell. *A First Course in Rational Continuum Mechanics: General concepts*. A First Course in Rational Continuum Mechanics. Academic Press, 1977. ISBN: 9780127013015.

[46] S. Colin. "Chapter 2 - Single-Phase Gas Flow in Microchannels". *Heat Transfer and Fluid Flow in Minichannels and Microchannels (Second Edition)*. Ed. by S. G. Kandlikar, S. Garimella, D. Li, S. Colin, and M. R. King. Second Edition. Oxford: Butterworth-Heinemann, 2014, pp. 11–102. ISBN: 978-0-08-098346-2. DOI: 10.1016/B978-0-08-098346-2.00002-8.

[47] G. G. Stokes. On the Steady Motion of Incompressible Fluids. *Transactions of the Cambridge Philosophical Society* **7** (1848), 439. DOI: 10.1017/CBO9780511702242.002.

[48] I. Karatzas and S. E. Shreve. *Brownian Motion and Stochastic Calculus*. Graduate Texts in Mathematics (113). Springer New York, 1991. ISBN: 9780387976556. DOI: 10.1007/978-1-4612-0949-2.

[49] F. Balboa Usabiaga, X. Xie, R. Delgado-Buscalioni, and A. Donev. The Stokes-Einstein relation at moderate Schmidt number. *The Journal of Chemical Physics* **139**.21 (2013), 214113. DOI: 10.1063/1.4834696.

[50] P. Huang and K. S. Breuer. Direct measurement of anisotropic near-wall hindered diffusion using total internal reflection velocimetry. *Physical Review E - Statistical, Nonlinear, and Soft Matter Physics* **76**.4 (2007), 1–4. ISSN: 15393755. DOI: 10.1103/PhysRevE.76.046307.

[51] H. Ounis and G. Ahmadi. Analysis of Dispersion of Small Spherical Particles in a Random Velocity Field. *Journal of Fluids Engineering* **112**.1 (1990), 114–120. ISSN: 0098-2202. DOI: 10.1115/1.2909358.

[52] H. Ounis and G. Ahmadi. A Comparison of Brownian and Turbulent Diffusion. *Aerosol Science and Technology* **13**.1 (1990), 47–53. ISSN: 0278-6826. DOI: 10.1080/02786829008959423.

[53] A. Li and G. Ahmadi. Dispersion and Deposition of Spherical Particles from Point Sources in a Turbulent Channel Flow. *Aerosol Science and Technology* **16**.4 (1992), 209–226. DOI: 10.1080/02786829208959550.

[54] G. D. M. MacKay and S. G. Mason. Approach of a solid sphere to a rigid plane interface. *Journal of Colloid Science* **16**.6 (1961), 632–635. ISSN: 0095-8522. DOI: https://doi.org/10.1016/0095-8522(61)90049-6.

[55] S. A. Biondi and J. A. Quinn. Direct observation of hindered brownian motion. *AIChE Journal* **41**.5 (1995), 1324–1328. ISSN: 15475905. DOI: 10.1002/aic.690410528.

[56] L. Lobry and N. Ostrowsky. Diffusion of Brownian particles trapped between two walls: Theory and dynamic-light-scattering measurements. *Physical Review*

B - Condensed Matter and Materials Physics **53**.18 (1996), 12050–12056. ISSN: 1550235X. DOI: 10.1103/PhysRevB.53.12050.

[57] M. A. Bevan and D. C. Prieve. Hindered diffusion of colloidal particles very near to a wall: revisited. *Journal of Chemical Physics* **113**.3 (2000), 1228–1236. ISSN: 00219606. DOI: 10.1063/1.481900.

[58] E. R. Dufresne, T. M. Squires, M. P. Brenner, and D. G. Grier. Hydrodynamic Coupling of Two Brownian Spheres to a Planar Surface. *Phys. Rev. Lett.* **85** (15 Oct. 2000), 3317–3320. DOI: 10.1103/PhysRevLett.85.3317.

[59] B. Lin, J. Yu, and S. A. Rice. Direct measurements of constrained Brownian motion of an isolated sphere between two walls. *Phys. Rev. E* **62** (3 Sept. 2000), 3909–3919. DOI: 10.1103/PhysRevE.62.3909.

[60] J. C. Crocker. Measurement of the hydrodynamic corrections to the Brownian motion of two colloidal spheres. *The Journal of Chemical Physics* **106**.7 (1997), 2837–2840. DOI: 10.1063/1.473381.

[61] A. Banerjee and K. D. Kihm. Experimental verification of near-wall hindered diffusion for the Brownian motion of nanoparticles using evanescent wave microscopy. *Physical Review E - Statistical, Nonlinear, and Soft Matter Physics* **72**.4 (2005), 1–4. ISSN: 15393755. DOI: 10.1103/PhysRevE.72.042101.

[62] P. Holmqvist, J. K. G. Dhont, and P. R. Lang. Colloidal dynamics near a wall studied by evanescent wave light scattering: Experimental and theoretical improvements and methodological limitations. *The Journal of Chemical Physics* **126**.4 (2007), 044707. DOI: 10.1063/1.2431175.

[63] C. K. Choi, C. H. Margraves, and K. D. Kihm. Examination of near-wall hindered Brownian diffusion of nanoparticles: Experimental comparison to theories by Brenner (1961) and Goldman et al. (1967). *Physics of Fluids* **19**.10 (2007). ISSN: 10706631. DOI: 10.1063/1.2798811.

[64] A high-precision study of hindered diffusion near a wall. *Applied Physics Letters* **97**.10 (2010), 1–4. ISSN: 00036951. DOI: 10.1063/1.3486123.

[65] H. B. Eral, J. M. Oh, D. Van Den Ende, F. Mugele, and M. H. Duits. Anisotropic and hindered diffusion of colloidal particles in a closed cylinder. *Langmuir* **26**.22 (2010), 16722–16729. ISSN: 07437463. DOI: 10.1021/la102273n.

[66] K. Ishii, T. Iwai, and H. Xia. Hydrodynamic measurement of Brownian particles at a liquid-solid interface by low-coherence dynamic light scattering. *Optics Express* **18**.7 (Mar. 2010), 7390–7396. DOI: 10.1364/OE.18.007390.

[67] C. Ha, H. Ou-Yang, and H. K. Pak. Direct measurements of colloidal hydrodynamics near flat boundaries using oscillating optical tweezers. *Physica A: Statistical Mechanics and its Applications* **392**.17 (2013), 3497–3504. ISSN: 0378-4371. DOI: https://doi.org/10.1016/j.physa.2013.04.014. URL: http://www.sciencedirect.com/science/article/pii/S0378437113003270.

[68] J. Mo, A. Simha, and M. G. Raizen. Broadband boundary effects on Brownian motion. *Phys. Rev. E* **92** (6 Dec. 2015), 062106. DOI: 10.1103/PhysRevE.92.062106.

[69] M. J. Skaug, L. Wang, Y. Ding, and D. K. Schwartz. Hindered Nanoparticle Diffusion and Void Accessibility in a Three-Dimensional Porous Medium. *ACS Nano* **9**.2 (2015), 2148–2156. DOI: 10.1021/acsnano.5b00019.

[70] K. Misiunas, S. Pagliara, E. Lauga, J. R. Lister, and U. F. Keyser. Nondecaying Hydrodynamic Interactions along Narrow Channels. *Phys. Rev. Lett.* **115** (3 July 2015), 038301. DOI: 10.1103/PhysRevLett.115.038301.

[71] W. M. Deen. Hindered transport of large molecules in liquidfilled pores. *AIChE Journal* **33**.9 (1987), 1409–1425. ISSN: 15475905. DOI: 10.1002/aic.690330902.

[72] P. S. Burada, P. Hänggi, F. Marchesoni, G. Schmid, and P. Talkner. Diffusion in confined geometries. *ChemPhysChem* **10**.1 (2009), 45–54. ISSN: 14397641. DOI: 10.1002/cphc.200800526. eprint: 0808.2345.

[73] P. S. Epstein. On the Resistance Experienced by Spheres in their Motion through Gases. *Phys. Rev.* **23** (6 June 1924), 710–733. DOI: 10.1103/PhysRev.23.710.

[74] C. Cercignani and C. D. Pagani. Flow of a Rarefied Gas past an Axisymmetric Body. I. General Remarks. *The Physics of Fluids* **11**.7 (1968), 1395–1399. DOI: 10.1063/1.1692120.

[75] C. Cercignani, C. D. Pagani, and P. Bassanini. Flow of a Rarefied Gas past an Axisymmetric Body. II. Case of a Sphere. *The Physics of Fluids* **11**.7 (1968), 1399–1403. DOI: 10.1063/1.1692121.

[76] N. A. Frej and D. C. Prieve. Hindered diffusion of a single sphere very near a wall in a nonuniform force field. *The Journal of Chemical Physics* **98**.9 (1993), 7552–7564. DOI: 10.1063/1.464695.

[77] E. S. Pagac, R. D. Tilton, and D. C. Prieve. Hindered mobility of a rigid sphere near a wall. *Chemical Engineering Communications* **148-50**.May (1996), 105–122. ISSN: 00986445. DOI: 10.1080/00986449608936511.

[78] H. Brenner. The slow motion of a sphere through a viscous fluid towards a plane surface. *Chemical Engineering Science* **16**.3-4 (1961), 242–251. ISSN: 00092509. DOI: 10.1016/0009-2509(61)80035-3.

[79] A. J. Goldman, R. G. Cox, and H. Brenner. Slow viscous motion of a sphere parallel to a plane wall-I Motion through a quiescent fluid. *Chemical Engineering Science* **22**.4 (1967), 637–651. ISSN: 00092509. DOI: 10.1016/0009-2509(67)80047-2.

[80] K. D. Kihm, A. Banerjee, C. K. Choi, and T. Takagi. Near-wall hindered Brownian diffusion of nanoparticles examined by three-dimensional ratiometric total internal reflection fluorescence microscopy (3-D R-TIRFM). *Experiments in Fluids* **37**.6 (2004), 811–824. ISSN: 07234864. DOI: 10.1007/s00348-004-0865-4.

[81] E. Lauga, M. Brenner, and H. A. Stone. "Chapter - Microfluidics: The No-Slip Boundary Condition". *Handbook of experimental fluid dynamics*. Ed. by C. Tropea, J. Foss, and A. Yarin. Springer Handbooks. Springer, Berlin, Heidelberg, 2007, pp. 1219–1235. DOI: 10.1007/978-3-540-30299-5_19.

[82] E. Bonaccurso, H.-J. Butt, and V. S. J. Craig. Surface Roughness and Hydrodynamic Boundary Slip of a Newtonian Fluid in a Completely Wetting System. *Phys. Rev. Lett.* **90** (14 Apr. 2003), 144501. DOI: 10.1103/PhysRevLett.90.144501.

[83] M. Stimson, G. B. Jeffery, and L. N. G. Filon. The motion of two spheres in a viscous fluid. *Proceedings of the Royal Society of London. Series A, Containing Papers of a Mathematical and Physical Character* **111**.757 (1926), 110–116. DOI: 10.1098/rspa.1926.0053.

[84] G. K. Batchelor. Brownian diffusion of particles with hydrodynamic interaction. *Journal of Fluid Mechanics* **74**.1 (1976), 1–29. DOI: 10.1017/S0022112076001663.

[85] J. Happel and H. Brenner. *Low Reynolds number hydrodynamics*. Martinus Nijhoff publishers, 1983. ISBN: 13: 978-90-247-2877-0. DOI: 10.1007/978-94-009-8352-6.

[86] S. Kim and S. J. Karrila. *Microhydrodynamics: principles and selected applications*. Butterworth-Heinemann, 1991. ISBN: 9781483161242.

[87] R. W. Barber and D. R. Emerson. Challenges in Modeling Gas-Phase Flow in Microchannels: From Slip to Transition. *Heat Transfer Engineering* **27**.4 (2006), 3–12. DOI: 10.1080/01457630500522271.

[88] G. A. Bird. Monte Carlo Simulation of Gas Flows. *Annual Review of Fluid Mechanics* **10**.1 (1978), 11–31. DOI: 10.1146/annurev.fl.10.010178.000303.

[89] A. Beskok, G. E. Karniadakis, and W. Trimmer. Rarefaction and Compressibility Effects in Gas Microflows. *Journal of Fluids Engineering* **118**.3 (1996), 448–456. DOI: 10.1115/1.2817779.

[90] E. S. Piekos and K. S. Breuer. Numerical Modeling of Micromechanical Devices Using the Direct Simulation Monte Carlo Method. *Journal of Fluids Engineering* **118**.3 (1996), 464–469. ISSN: 0098-2202. DOI: 10.1115/1.2817781.

[91] E. B. Arkilic, M. A. Schmidt, and K. S. Breuer. Gaseous slip flow in long microchannels. *Journal of Microelectromechanical Systems* **6**.2 (1997), 167–178. DOI: https://doi.org/10.1109/84.585795.

[92] E. Oran, C. Oh, and B. Cybyk. DIRECT SIMULATION MONTE CARLO: Recent Advances and Applications. *Annual Review of Fluid Mechanics* **30**.1 (1998), 403–441. DOI: 10.1146/annurev.fluid.30.1.403.

[93] G. E. K. Ali Beskok. Report: A model for flows in channels, pipes, and ducts at micro and nano scales. *Microscale Thermophysical Engineering* **3**.1 (1999), 43–77. DOI: 10.1080/108939599199864.

[94] A. Agrawal. A Comprehensive Review on Gas Flow in Microchannels. *International Journal of Micro-Nano Scale Transport* **2**.17 (1 2007), 3411–3421. ISSN: 0017-9310. DOI: https://doi.org/10.1260/1759-3093.2.1.1.

[95] J. C. Maxwell. On Stresses in Rarefied Gases Arising from Inequalities of Temperature. *Philosophical Transactions of the Royal Society of London* **170** (1879), 231–256. DOI: 10.1098/rspl.1878.0052.

[96] E. Cunningham. On the Velocity of Steady Fall of Spherical Particles through Fluid Medium. *Proceedings of the Royal Society of London Series A* **83**.563 (1910), 357–365. DOI: 10.1098/rspa.1910.0024.

[97] R. A. Millikan. The Isolation of an Ion, a Precision Measurement of its Charge, and the Correction of Stokes's Law. *Phys. Rev. (Series I)* **32** (4 Apr. 1911), 349–397. DOI: 10.1103/PhysRevSeriesI.32.349.

[98] M. D. Allen and O. G. Raabe. Slip Correction Measurements of Spherical Solid Aerosol Particles in an Improved Millikan Apparatus. *Aerosol Science and Technology* **4**.3 (1985), 269–286. ISSN: 0278-6826. DOI: 10.1080/02786828508959055.

[99] A. Moshfegh, M. Shams, G. Ahmadi, and R. Ebrahimi. A new expression for spherical aerosol drag in slip flow regime. *Journal of Aerosol Science* **41**.4 (2010), 384–400. ISSN: 0021-8502. DOI: https://doi.org/10.1016/j.jaerosci.2010.01.010.

[100] C. N. Davies. Definitive equations for the fluid resistance of spheres. *Proceedings of the Physical Society* **57**.4 (1945), 259. DOI: 10.1088/0959-5309/57/4/301.

[101] C. Cercignani. *Rarefied gas dynamics: From basic concepts to actual calculations.* Cambridge university press, 2000. ISBN: 9780521659925.

[102] S. Colin. Rarefaction and compressibility effects on steady and transient gas flows in microchannels. *Microfluidics and Nanofluidics* **1**.3 (July 2005), 268–279. ISSN: 1613-4990. DOI: 10.1007/s10404-004-0002-y.

[103] E. Karniadakis George, A. Beskok, and N. Aluru. *Microflows and Nanoflows: Fundamentals and Simulation.* Vol. 23. Springer-Verlag New York, 2005. DOI: 10.1007/0-387-28676-4.

[104] H. Brenner and L. J. Gaydos. The constrained brownian movement of spherical particles in cylindrical pores of comparable radius. Models of the diffusive and convective transport of solute molecules in membranes and porous media. *Journal of Colloid And Interface Science* **58**.2 (1977), 312–356. ISSN: 00219797. DOI: 10.1016/0021-9797(77)90147-3.

[105] B. J. Alder and T. E. Wainwright. Studies in Molecular Dynamics. I. General Method. *The Journal of Chemical Physics* **31**.2 (1959), 459–466. DOI: 10.1063/1.1730376.

[106] D. Hamelberg, J. Mongan, and J. A. McCammon. Accelerated molecular dynamics: A promising and efficient simulation method for biomolecules. *The Journal of Chemical Physics* **120**.24 (2004), 11919–11929. DOI: 10.1063/1.1755656.

[107] G. A. Bird. *Molecular Gas Dynamics and Direct Simulation of Gas Flow.* Oxford University Press, London, 1994.

[108] W. Wagner. A convergence proof for Bird's direct simulation Monte Carlo method for the Boltzmann equation. *Journal of Statistical Physics* **66**.3 (1992), 1011–1044. DOI: 10.1007/BF01055714.

[109] E. E. Michaelides. Nanoparticle diffusivity in narrow cylindrical pores. *International Journal of Heat and Mass Transfer* **114** (2017), 607–612. ISSN: 0017-9310. DOI: 10.1016/j.ijheatmasstransfer.2017.06.098.

[110] L. Kadanoff. "On Two Levels". Physics Today, 1986. DOI: 10.1063/1.2815134.

[111] J. E. Broadwell. Shock Structure in a Simple Discrete Velocity Gas. *The Physics of Fluids* **7**.8 (1964), 1243–1247. DOI: 10.1063/1.1711368.

[112] U. Frisch, B. Hasslacher, and Y. Pomeau. Lattice-Gas Automata for the Navier-Stokes Equation. *Phys. Rev. Lett.* **56** (14 Apr. 1986), 1505–1508. DOI: 10.1103/PhysRevLett.56.1505.

[113] D. D'humières and P. Lallemand. Lattice gas automata for fluid mechanics. *Physica A: Statistical Mechanics and its Applications* **140**.1 (1986), 326–335. ISSN: 0378-4371. DOI: 10.1016/0378-4371(86)90239-6.

[114] S. Chen and G. D. Doolen. Lattice Boltzmann method for fluid flows. *Annual Review of Fluid Mechanics* **30**.1 (1998), 329–364. DOI: 10.1146/annurev.fluid.30.1.329.

[115] T. Krüger, H. Kusumaatmaja, A. Kuzmin, O. Shardt, G. Silva, and E. M. Viggen. *The Lattice Boltzmann Method: Principles and Practice.* Graduate Texts in Physics series (GTP). Springer, Cham, 2017. DOI: 10.1007/978-3-319-44649-3.

[116] A. J. C. Ladd. Numerical simulations of particulate suspensions via a discretized Boltzmann equation. Part 1. Theoretical foundation. *Journal of Fluid Mechanics* **271** (1994), 285–309. DOI: 10.1017/S0022112094001771.

[117] A. J. C. Ladd. Numerical simulations of particulate suspensions via a discretized Boltzmann equation. Part 2. Numerical results. *Journal of Fluid Mechanics* **271** (1994), 311–339. DOI: 10.1017/S0022112094001783.

[118] L. D. Landau and E. M. Lifshitz. "CHAPTER VI - Diffusion". *Fluid Mechanics (Second Edition)*. Pergamon, 1987, pp. 227–237. ISBN: 978-0-08-033933-7. DOI: 10.1016/B978-0-08-033933-7.50014-3.

[119] P. Ahlrichs and B. Dünweg. Lattice-Boltzmann Simulation of Polymer-Solvent Systems. *International Journal of Modern Physics C* **09**.08 (1998), 1429–1438. DOI: 10.1142/S0129183198001291.

[120] M. Mynam, P. Sunthar, and S. Ansumali. Efficient lattice Boltzmann algorithm for Brownian suspensions. *Philosophical Transactions of the Royal Society A: Mathematical, Physical and Engineering Sciences* **369**.1944 (2011), 2237–2245. DOI: 10.1098/rsta.2011.0047.

[121] G. De Fabritiis, M. Serrano, R. Delgado-Buscalioni, and P. V. Coveney. Fluctuating hydrodynamic modeling of fluids at the nanoscale. *Physical Review E* **75**.2 (2007), 026307. DOI: 10.1103/PhysRevE.75.026307.

[122] P. Español and P. B. Warren. Perspective: Dissipative particle dynamics. *The Journal of Chemical Physics* **146**.15 (2017), 150901. DOI: 10.1063/1.4979514.

[123] A. Gubbiotti, M. Chinappi, and C. M. Casciola. Confinement effects on the dynamics of a rigid particle in a nanochannel. *Phys. Rev. E* **100** (5 Nov. 2019), 053307. DOI: 10.1103/PhysRevE.100.053307.

[124] G. Stokes. On the theories of internal friction of fluids in motion and of the equilibrium and motion of elastic solids. *Trans. Camb. Phil. Soc.* **8** (Jan. 1845), 24–40.

[125] O. Darrigol. Between Hydrodynamics and Elasticity Theory: The First Five Births of the Navier-Stokes Equation. *Archive for History of Exact Sciences* **56**.2 (2002), 95–150. ISSN: 00039519, 14320657. DOI: 10.2307/41134138.

[126] D. L. Ermak and J. A. McCammon. Brownian dynamics with hydrodynamic interactions. *The Journal of Chemical Physics* **69**.4 (1978), 1352–1360. ISSN: 0021-9606. DOI: 10.1063/1.436761.

[127] J. F. Brady and G. Bossis. Stokesian Dynamics. *Annual Review of Fluid Mechanics* **20**.1 (1988), 111–157. DOI: 10.1146/annurev.fl.20.010188.000551.

[128] A. M. Ardekani and R. H. Rangel. Unsteady motion of two solid spheres in Stokes flow. *Physics of Fluids* **18**.10 (2006), 103306. DOI: 10.1063/1.2363351.

[129] A. Simha, J. Mo, and P. J. Morrison. Unsteady Stokes flow near boundaries: the point-particle approximation and the method of reflections. *Journal of Fluid Mechanics* **841** (2018), 883–924. DOI: 10.1017/jfm.2018.87.

[130] B. U. Felderhof. Effect of the wall on the velocity autocorrelation function and long-time tail of Brownian motion. *Journal of Physical Chemistry B* **109**.45 (2005), 21406–21412. ISSN: 15206106. DOI: 10.1021/jp051335b.

[131] B. U. Felderhof. Diffusion and velocity relaxation of a Brownian particle immersed in a viscous compressible fluid confined between two parallel plane walls. *The Journal of Chemical Physics* **124**.5 (2006), 054111. DOI: 10.1063/1.2165199.

[132] H. K. Versteeg and W. Malalasekera. *An introduction to computational fluid dynamics - the finite volume method.* Addison-Wesley-Longman, 1995, pp. I–X, 1–257. ISBN: 978-0-582-21884-0.

[133] E. Michaelides, C. T. Crowe, and J. D. Schwarzkopf. "Multiphase Flow Handbook". Second. Boca Raton: CRC Press, 2016. ISBN: 9781315371924. DOI: 10.1201/9781315371924.

[134] M. R. Maxey and J. J. Riley. Equation of motion for a small rigid sphere in a nonuniform flow. *The Physics of Fluids* **26**.4 (1983), 883–889. ISSN: 0031-9171. DOI: 10.1063/1.864230.

[135] A. B. Basset. *A treatise on hydrodynamics: with numerous examples.* Vol. 2. Deighton, Bell and Company, 1888.

[136] B. Noetinger. Fluctuating hydrodynamics and Brownian motion. *Physica A: Statistical Mechanics and its Applications* **163**.2 (1990), 545–558. ISSN: 0378-4371. DOI: 10.1016/0378-4371(90)90144-H.

[137] E. H. Hauge and A. Martin-Löf. Fluctuating hydrodynamics and Brownian motion. *Journal of Statistical Physics* **7**.3 (1973), 259–281. ISSN: 1572-9613. DOI: 10.1007/BF01030307.

[138] P. Español. Stochastic differential equations for non-linear hydrodynamics. *Physica A: Statistical Mechanics and its Applications* **248**.1 (1998), 77–96. ISSN: 0378-4371. DOI: https://doi.org/10.1016/S0378-4371(97)00461-5.

[139] M. M. Mansour, A. L. Garcia, G. C. Lie, and E. Clementi. Fluctuating hydrodynamics in a dilute gas. *Physical Review Letters* **58**.9 (1987), 874–877. DOI: 10.1103/PhysRevLett.58.874.

[140] M. Gad-El-Hak. Gas and Liquid Transport at the Microscale. *Heat Transfer Engineering* **27**.4 (2006), 13–29. ISSN: 0145-7632. DOI: 10.1080/01457630500522305.

[141] A. L. Garcia, M. M. Mansour, G. C. Lie, M. Mareschal, and E. Clementi. Hydrodynamic fluctuations in a dilute gas under shear. *Phys. Rev. A* **36** (9 Nov. 1987), 4348–4355. DOI: 10.1103/PhysRevA.36.4348.

[142] B. Uma, T. N. Swaminathan, R. Radhakrishnan, D. M. Eckmann, and P. S. Ayyaswamy. Nanoparticle Brownian motion and hydrodynamic interactions in the presence of flow fields. *Physics of Fluids* **23**.7 (2011), 073602. DOI: 10.1063/1.3611026.

[143] A. Donev, A. Nonaka, Y. Sun, G. Fai Thomas, A. L. Garcia, and J. B. Bell. Low Mach number fluctuating hydrodynamics of diffusively mixing fluids. *Communications in Applied Mathematics and Computational Science* **9**.1 (2014), 47–105. DOI: 10.2140/camcos.2014.9.47.

[144] A. Donev, A. Nonaka, A. K. Bhattacharjee, A. L. Garcia, and J. B. Bell. Low Mach number fluctuating hydrodynamics of multispecies liquid mixtures. *Physics of Fluids* **27**.3 (2015), 037103. DOI: 10.1063/1.4913571.

[145] A. K. Bhattacharjee, K. Balakrishnan, A. L. Garcia, J. B. Bell, and A. Donev. Fluctuating hydrodynamics of multi-species reactive mixtures. *The Journal of Chemical Physics* **142**.22 (2015), 224107. DOI: 10.1063/1.4922308.

[146] N. Sharma and N. A. Patankar. Direct numerical simulation of the Brownian motion of particles by using fluctuating hydrodynamic equations. *Journal of Computational Physics* **201**.2 (2004), 466–486. ISSN: 0021-9991. DOI: 10.1016/j.jcp.2004.06.002.

[147] N. Ramakrishnan, Y. Wang, D. M. Eckmann, P. S. Ayyaswamy, and R. Radhakrishnan. Motion of a nano-spheroid in a cylindrical vessel flow: Brownian and hydrodynamic interactions. *Journal of Fluid Mechanics* **821** (2017), 117–152. DOI: 10.1017/jfm.2017.182.

[148] B. E. Griffith and N. A. Patankar. Immersed Methods for FluidStructure Interaction. *Annual Review of Fluid Mechanics* **52**.1 (2020), 421–448. DOI: 10.1146/annurev-fluid-010719-060228.

[149] B. Delmotte and E. E. Keaveny. Simulating Brownian suspensions with fluctuating hydrodynamics. *The Journal of Chemical Physics* **143**.24 (2015), 244109. DOI: 10.1063/1.4938173.

[150] Spatially adaptive stochastic methods for fluidstructure interactions subject to thermal fluctuations in domains with complex geometries. *Journal of Computational Physics* **277** (2014), 121–137. ISSN: 0021-9991. DOI: 10.1016/j.jcp.2014.07.051.

[151] P. J. Atzberger, P. R. Kramer, and C. S. Peskin. A stochastic immersed boundary method for fluid-structure dynamics at microscopic length scales. *Journal of Computational Physics* **224**.2 (2007), 1255–1292. ISSN: 0021-9991. DOI: 10.1016/j.jcp.2006.11.015.

[152] P. R. Kramer, C. S. Peskin, and P. J. Atzberger. On the foundations of the stochastic immersed boundary method. *Computer Methods in Applied Mechanics and Engineering* **197**.25 (2008). Immersed Boundary Method and Its Extensions, 2232–2249. ISSN: 0045-7825. DOI: 10.1016/j.cma.2007.11.010.

[153] Inertial coupling method for particles in an incompressible fluctuating fluid. *Computer Methods in Applied Mechanics and Engineering* **269** (2014), 139–172. ISSN: 0045-7825. DOI: 10.1016/j.cma.2013.10.029.

[154] Y. Wang, H. Lei, and P. J. Atzberger. Fluctuating hydrodynamic methods for fluid-structure interactions in confined channel geometries. *Applied Mathematics and Mechanics* **39**.1 (2018), 125–152. DOI: 10.1007/s10483-018-2253-8.

[155] J. Vom Scheidt. Kloeden, P. E.; Platen, E., Numerical Solution of Stochastic Differential Equations. Berlin etc., Springer-Verlag 1992. XXXVI, 632 pp., 85 figs., DM 118,OO. ISBN 3-540-54062-8 (Applications of Mathematics 23). *ZAMM - Journal of Applied Mathematics and Mechanics / Zeitschrift für Angewandte Mathematik und Mechanik* **74**.8 (1994), 332–332. ISSN: 0044-2267. DOI: 10.1002/zamm.19940740806.

[156] K. Itô. "Stochastic integration". *Vector and Operator Valued Measures and Applications*. Ed. by D. H. Tucker and H. B. Maynard. Academic Press, 1973, pp. 141–148. ISBN: 978-0-12-702450-9. DOI: 10.1016/B978-0-12-702450-9.50020-8.

[157] C. S. Peskin. The Fluid Dynamics of Heart Valves: Experimental, Theoretical, and Computational Methods. *Annual Review of Fluid Mechanics* **14**.1 (1982), 235–259. DOI: 10.1146/annurev.fl.14.010182.001315.

[158] R. Mittal and G. Iaccarino. Immersed Boundary Methods. *Annual Review of Fluid Mechanics* **37**.1 (2005), 239–261. DOI: 10.1146/annurev.fluid.37.061903.175743.

[159] F. C. Centre. *IPS IBOFLow*. URL: http://www.fcc.chalmers.se/software/ips/iboflow/.

[160] A. Mark, R. Rundqvist, and F. Edelvik. Comparison Between Different Immersed Boundary Conditions for Simulation of Complex Fluid Flows. *Fluid Dynamics and Materials Processing* **7** (Sept. 2011), 241–258. DOI: 10.3970/fdmp.2011.007.241.

[161] A. Mark and B. G. M. van Wachem. Derivation and validation of a novel implicit second-order accurate immersed boundary method. *Journal of Computational Physics* **227**.13 (2008), 6660–6680. ISSN: 0021-9991. DOI: 10.1016/j.jcp.2008.03.031.

[162] A. Mark, E. Svenning, and F. Edelvik. An immersed boundary method for simulation of flow with heat transfer. *International Journal of Heat and Mass Transfer* **56**.1 (2013), 424–435. ISSN: 0017-9310. DOI: 10.1016/j.ijheatmasstransfer.2012.09.010.

[163] J. P. V. Doormaal and G. D. Raithby. Enhancements of the SIMPLE method for predicting incompressible fluid flows. *Numerical Heat Transfer* **7**.2 (1984), 147–163. DOI: 10.1080/01495728408961817.

[164] C. M. Rhie and W. L. Chow. Numerical study of the turbulent flow past an airfoil with trailing edge separation. *AIAA Journal* **21**.11 (1983), 1525–1532. DOI: 10.2514/3.8284.

[165] M. Naumov, M. Arsaev, P. Castonguay, J. Cohen, J. Demouth, J. Eaton, S. Layton, N. Markovskiy, I. Reguly, N. Sakharnykh, V. Sellappan, and R. Strzodka. AmgX: A Library for GPU Accelerated Algebraic Multigrid and Preconditioned Iterative Methods. *SIAM Journal on Scientific Computing* **37**.5 (2015), S602–S626. DOI: 10.1137/140980260.

[166] R. Rundqvist, A. Mark, B. Andersson, A. Ålund, F. Edelvik, S. Tafuri, and J. S. Carlson. "Simulation of Spray Painting in Automotive Industry". *Numerical Mathematics and Advanced Applications 2009*. Ed. by G. Kreiss, P. Lötstedt, A. Målqvist, and M. Neytcheva. Berlin, Heidelberg: Springer Berlin Heidelberg, 2010, pp. 771–779. ISBN: 978-3-642-11795-4. DOI: 10.1007/978-3-642-11795-4_83.

[167] J. Göhl, A. Mark, S. Sasic, and F. Edelvik. An immersed boundary based dynamic contact angle framework for handling complex surfaces of mixed wettabilities. *International Journal of Multiphase Flow* (2018). ISSN: 0301-9322. DOI: 10.1016/j.ijmultiphaseflow.2018.08.001.

[168] J. Göhl, K. Markstedt, A. Mark, K. Håkansson, P. Gatenholm, and F. Edelvik. Simulations of 3D bioprinting: predicting bioprintability of nanofibrillar inks. *Biofabrication* **10**.3 (2018), 034105. URL: http://stacks.iop.org/1758-5090/10/i=3/a=034105.

[169] T. Johnson, S. Jakobsson, B. Wettervik, B. Andersson, A. Mark, and F. Edelvik. A finite volume method for electrostatic three species negative corona discharge simulations with application to externally charged powder bells. *Journal of Electrostatics* **74** (2015), 27–36. ISSN: 0304-3886. DOI: 10.1016/j.elstat.2014.12.009.

[170] B. Wettervik, T. Johnson, S. Jakobsson, A. Mark, and F. Edelvik. A domain decomposition method for three species modeling of multi-electrode negative corona discharge With applications to electrostatic precipitators. *Journal of Electrostatics* **77** (2015), 139–146. ISSN: 0304-3886. DOI: 10.1016/j.elstat.2015.08.004. URL: http://www.sciencedirect.com/science/article/pii/S0304388615300346.

[171] F. Edelvik, A. Mark, N. Karlsson, T. Johnson, and J. S. Carlson. "Math-Based Algorithms and Software for Virtual Product Realization Implemented in Automotive Paint Shops". *Math for the Digital Factory*. Ed. by L. Ghezzi, D. Hömberg, and C. Landry. Cham: Springer International Publishing, 2017, pp. 231–251. ISBN: 978-3-319-63957-4. DOI: 10.1007/978-3-319-63957-4_11.

[172] T. Johnson, P. Röyttä, A. Mark, and F. Edelvik. Simulation of the spherical orientation probability distribution of paper fibers in an entire suspension using immersed boundary methods. *Journal of Non-Newtonian Fluid Mechanics* **229** (2016), 1–7. ISSN: 0377-0257. DOI: 10.1016/j.jnnfm.2016.01.001.

[173] S. Ingelsten, A. Mark, and F. Edelvik. A Lagrangian-Eulerian framework for simulation of transient viscoelastic fluid flow. *Journal of Non-Newtonian Fluid Mechanics* **266** (2019), 20–32. ISSN: 0377-0257. DOI: 10.1016/j.jnnfm.2019.02.005.

[174] S. Ingelsten, A. Mark, K. Jareteg, R. Kádár, and F. Edelvik. Computationally efficient viscoelastic flow simulation using a Lagrangian-Eulerian method and GPU-acceleration. *Journal of Non-Newtonian Fluid Mechanics* **279** (2020), 104264. ISSN: 0377-0257. DOI: 10.1016/j.jnnfm.2020.104264.

[175] H. Brenner. A general theory of Taylor dispersion phenomena IV. Direct Coupling Effects. *Chemical Engineering Communications* **18**.5-6 (1982), 355–379. DOI: 10.1080/00986448208939976.

[176] G. M. Mavrovouniotis and H. Brenner. Hindered sedimentation, diffusion, and dispersion coefficients for brownian spheres in circular cylindrical pores. *Journal of Colloid And Interface Science* **124**.1 (1988), 269–283. ISSN: 00219797. DOI: 10.1016/0021-9797(88)90348-7.

[177] P. Dechadilok and W. M. Deen. Hindrance Factors for Diffusion and Convection in Pores. *Industrial & Engineering Chemistry Research* **45**.21 (2006), 6953–6959. DOI: 10.1021/ie051387n.

[178] N. M. Newmark. A Method of Computation for Structural Dynamics. *Journal of the Engineering Mechanics Division* **85** (3 1959), 67–94.

[179] R. G. Bartle. Return to the Riemann Integral. *The American Mathematical Monthly* **103**.8 (1996), 625–632. ISSN: 00029890, 19300972. DOI: 10.2307/2974874.

[180] J.-P. Minier and E. Peirano. The pdf approach to turbulent polydispersed two-phase flows. *Physics Reports* **352**.1 (2001), 1–214. ISSN: 0370-1573. DOI: https://doi.org/10.1016/S0370-1573(01)00011-4.

[181] B. U. Felderhof. Diffusion of interacting Brownian particles. **11**.5 (May 1978), 929–937. DOI: 10.1088/0305-4470/11/5/022.

[182] G. A. Bird. *The DSMC method*. CreateSpace Independent Publishing Platform, 2013. ISBN: 978-1492112907.

[183] I. D. Boyd and T. E. Schwartzentruber. "Direct Simulation Monte Carlo". *Nonequilibrium Gas Dynamics and Molecular Simulation*. Cambridge Aerospace Series.

Cambridge University Press, 2017, pp. 183–251. DOI: 10.1017/9781139683494.007.

[184] C. White, M. K. Borg, T. J. Scanlon, and J. M. Reese. A DSMC investigation of gas flows in micro-channels with bends. *Computers and Fluids* **71** (2013), 261–271. ISSN: 0045-7930. DOI: 10.1016/j.compfluid.2012.10.023.

[185] C. White, M. Borg, T. Scanlon, S. Longshaw, B. John, D. Emerson, and J. Reese. dsmcFoam+: An OpenFOAM based direct simulation Monte Carlo solver. *Computer Physics Communications* **224** (2018), 22–43. ISSN: 0010-4655. DOI: 10.1016/j.cpc.2017.09.030.

[186] T. J. Scanlon, E. Roohi, C. White, M. Darbandi, and J. M. Reese. An open source, parallel DSMC code for rarefied gas flows in arbitrary geometries. *Computers and Fluids* **39**.10 (2010), 2078–2089. ISSN: 0045-7930. DOI: 10.1016/j.compfluid.2010.07.014.

[187] H. G. Weller, G. Tabor, H. Jasak, and C. Fureby. A tensorial approach to computational continuum mechanics using object-oriented techniques. *Computers in Physics* **12**.6 (1998), 620–631. DOI: 10.1063/1.168744.

[188] C. White, M. Borg, and S. Longshaw. *MicroNanoFlows: OpenFOAM-2.4.0-MNF*. https://github.com/MicroNanoFlows/OpenFOAM-2.4.0-MNF. 2018.

[189] E. Roohi, M. Darbandi, and V. Mirjalili. Direct Simulation Monte Carlo Solution of Subsonic Flow Through Micro/Nanoscale Channels. *Journal of Heat Transfer* **131**.9 (June 2009). DOI: 10.1115/1.3139105.

[190] M. Darbandi and E. Roohi. Study of subsonic–supersonic gas flow through micro/nanoscale nozzles using unstructured DSMC solver. *Microfluidics and Nanofluidics* **10**.2 (2011), 321–335. DOI: 10.1007/s10404-010-0671-7.

[191] R. C. Palharini, C. White, T. J. Scanlon, R. E. Brown, M. K. Borg, and J. M. Reese. Benchmark numerical simulations of rarefied non-reacting gas flows using an open-source DSMC code. *Computers and Fluids* **120** (2015), 140–157. ISSN: 0045-7930. DOI: 10.1016/j.compfluid.2015.07.021.

[192] A. Ebrahimi and E. Roohi. DSMC investigation of rarefied gas flow through diverging micro- and nanochannels. *Microfluidics and Nanofluidics* **21**.2 (2017), 18. DOI: 10.1007/s10404-017-1855-1.

[193] G. Yang and B. Weigand. Investigation of the Klinkenberg effect in a micro/nanoporous medium by direct simulation Monte Carlo method. *Phys. Rev. Fluids* **3** (4 Apr. 2018), 044201. DOI: 10.1103/PhysRevFluids.3.044201.

[194] M. Sabouri and M. Darbandi. Numerical study of species separation in rarefied gas mixture flow through micronozzles using DSMC. *Physics of Fluids* **31**.4 (2019), 042004. DOI: 10.1063/1.5083807.

[195] W. L. Haberman and R. M. Sayre. *Motion of rigid and fluid spheres in stationary and moving liquids inside cylindrical tubes*. Tech. rep. Department of the navy - David Taylor model basin, 1958. URL: http://hdl.handle.net/1721.3/48988.

[196] Y. Chang and H. Keh. Slow motion of a slip spherical particle perpendicular to two plane walls. *Journal of Fluids and Structures* **22**.5 (2006), 647–661. ISSN: 0889-9746. DOI: 10.1016/j.jfluidstructs.2006.02.006.

[197] F. S. Gentile, I. D. Santo, G. D'Avino, L. Rossi, G. Romeo, F. Greco, P. A. Netti, and P. L. Maffettone. Hindered Brownian diffusion in a square-shaped geometry.

Journal of Colloid and Interface Science **447** (2015), 25–32. ISSN: 10957103. DOI: 10.1016/j.jcis.2015.01.055.

[198] C. Cercignani and A. Daneri. Flow of a Rarefied Gas between Two Parallel Plates. *Journal of Applied Physics* **34**.12 (1963), 3509–3513. DOI: 10.1063/1.1729249.

[199] F. Mainardi, A. Mura, and F. Tampieri. Brownian motion and anomalous diffusion revisited via a fractional Langevin equation. *Modern Problems of Statistical Physics* **8** (2009), 3–23. URL: http://arxiv.org/abs/1004.3505.

[200] G. Peskir. On the Diffusion Coefficient: The Einstein Relation and Beyond. *Stochastic Models* **19**.3 (2003), 383–405. DOI: 10.1081/STM-120023566.